Fabrication of Physically Crosslinked Hydrogel Materials with Good Mechanical Properties

Dissertation

zur Erlangung des Grades
des Doktors der Naturwissenschaften
der Naturewissenschaftlich-Technischen Fakultäten
der Universität des Saarlandes

von

Fatih Puza

Saarbrücken

2021

Tag des Kolloquiums: 29.01.2021

Dekan: Prof. Dr. Jörn E. Walter

Berichterstatter: Prof. Dr. Aránzazu del Campo Bécares

Prof. Dr. Guido Kickelbick

Vorsitz: Prof. Dr. -Ing. Markus Gallei

Akademischer Mitarbeiterin: Dr. Lola Gonzales-García

Index

List of Tables

List of Figures

Abstract

Soft gels serve promising features for various applications. For this aim, several strategies to form crosslinked networks have been implemented. Mostly, they suffer from non-dynamicity, which leads to limitations of swelling and good mechanical properties. In this thesis, polymer entanglements are used as the main crosslinking method, and enabled good mechanical properties with high swelling (~98 wt%). Entanglements are weak physical interactions, which are result of arbitrary passing polymer chains. They are believed to be too weak to build networks for hydrogelation. The crosslinking is based on *in-situ* entanglement cluster formation inside polymer nanogels. Following that, stimulus-responsive behavior is supplied into the physical entanglement hydrogels (PEH). When nanogels had been switched to thermoresponsive PNIPAM, sliding of chain entanglements can be regulated. PEH does not undergo clear shrinkage, even it is stiffened. In addition, organohydrogel with anisotropic behaviors is investigated in this study. Anisotropy is common in nature, and provides different features in materials. Organohydrogels are able to consist of binary phases of hydrophilic and oleophilic molecules. Herein, anisotropic organohydrogel fabrication via polymerization induced phase separation is developed. The gel can show different properties, including stiffness, viscoelasticity and surface roughness.

Zusammenfassung

Weiche Gele bieten vielversprechende Eigenschaften für verschiedene Anwendungen. Zu diesem Zweck wurden verschiedene Strategien zur Bildung vernetzter Netzwerke implementiert. Meistens leiden sie unter Nichtdynamik, was zu Einschränkungen der Quellung und guten mechanischen Eigenschaften führt. In dieser Arbeit werden Polymerverschränkungen als Hauptvernetzungsmethode verwendet und ermöglichen gute mechanische Eigenschaften bei hoher Quellung (98 Gew.-%). Verwicklungen sind schwache physikalische Wechselwirkungen, die auf willkürlich vorbeiziehende Polymerketten zurückzuführen sind. Es wird angenommen, dass sie zu schwach sind, um Netzwerke für die Hydrogelierung aufzubauen. Die Vernetzung basiert auf der Bildung von In-situ-Verschränkungsclustern in Polymer-Nanogelen. Anschließend wird den physikalischen Verschränkungshydrogelen (PEH) ein auf Reize ansprechendes Verhalten zugeführt. Wenn Nanogele auf thermoresponsives PNIPAM umgestellt wurden, kann das Gleiten von Kettenverschränkungen reguliert werden. PEH schrumpft nicht deutlich, auch wenn es versteift ist. Zusätzlich wird in dieser Studie Organohydrogel mit anisotropem Verhalten untersucht. Anisotropie ist in der Natur üblich und bietet verschiedene Eigenschaften in Materialien. Organohydrogele können aus binären Phasen hydrophiler und oleophiler Moleküle bestehen. Hierin wird eine anisotrope Organohydrogelherstellung durch polymerisationsinduzierte Phasentrennung entwickelt. Das Gel kann verschiedene Eigenschaften aufweisen, einschließlich Steifheit, Viskoelastizität und Oberflächenrauheit.

Acknowledgements

I would like to thank to Dr. Jiaxi Cui for his expertise, assistance, endless support and helpful guidance to improve my knowledge throughout my study. Without his help this would not have been possible. I would like to thank to Prof. Dr. Aránzazu del Campo Bécares for being my advisor. My sincere thanks also go to my labmates, who always helped me when I needed. I appreciate their kind cooperation, advices and supportive attitudes.

Last but not the least, I would like to thank to my wife, Sevde Puza, for her understanding, encouragement and unlimited support throughout this challenging work. Completing tough steps of PhD would not have been imaginable without her endless support and love. Moreover, I am grateful to my parents, who had provided their best and made sacrifices for me to reach this level.

This thesis is dedicated to my beloved daughter, Defne...

Chapter 1: Basics of Hydrogels

1.1. Introduction to Hydrogels

Polymer hydrogels are unique soft materials that are constituted by crosslinked hydrophilic polymer chains and aqueous solutions can be entrapped in their networks. The high water content is advantageous for applications such as soft actuators (1,2), wearable electronic (3), drug delivery (4,5) and tissue engineering (6,7), etc. Although water uptake ability of hydrogels contributes to unique features, it also leads to several handicaps. Most highly swollen hydrogels lack good mechanical properties (8). In conventional polymeric hydrogel, the network is formed by covalent crosslinks, which are non-dynamic (9). Water absorption is accompanied by a huge volume expansion in polymer networks. As consequence, the constituent polymer chains are highly stretched, and overloaded by swelling induced stress. Re-organization of the polymer network, to be able to dissipate stress, is limited covalently crosslinked hydrogels. The lack of efficient network re-organization leads to easy breaking of swollen hydrogels, even at low mechanical stress (10).

The fragile nature of swollen hydrogels restricts their possible applications. Because of that, highly swollen hydrogels with superior mechanical properties are desired. In the past decades, several promising strategies for dynamic network crosslinking using chemical and physical interactions have been reported (11,12). Although some approaches allow efficient energy dissipation, good mechanical properties in highly swollen state remains challenging. New strategies are required to overcome the highlighted restrictions.

1.2. Formation of Hydrogels

Single hydrophilic polymer chains can be dissolved in aqueous conditions. Therefore, hydrogel formation requires crosslinking of the polymer chains. Covalent crosslinking or physical crosslinking is possible. Each of these categories includes different subtypes. Incorporating different crosslinking mechanisms into the network facilitates tuning of hydrogel physical and chemical properties. The type of crosslinking is able to tune hydrogel features, including stiffness, water absorption, and permeability, etc. (13).

1.2.1. Chemical Crosslinking Approach

Reactive chemical groups, either incorporated in the polymer backbone or supplied as small molecules, can help to build up covalent bonds. For instance, end-functionalized macromolecules (e.g. multiarm PEG with acrylate ends) can be polymerized into a hydrogel network (14). Alternatively, molecules containing reactive vinyl groups can be added to solutions of other polymers to accomplish hydrogelation. *N,N′*-methylenebis(acrylamide) (MBA), ethylene glycol diacrylate (EGDA) and PEG diacrylate (PEGDA) constitute examples of commercially available crosslinker types. They can copolymerize with vinylated monomers and polymers, such as acrylamide, acrylic acid and N-isopropylacrylamide (NIPAm) (13). These crosslinkers provide long-lasting and non-degradable properties to the networks, which can no longer be dissolved by water uptake. On the other hand, the usage of this reaction causes some drawbacks. For instance, the chemistry behind the crosslinking is not able to show a dynamic nature, since de-coupling of covalent bonds is not reversible. Because of the rigid stability and non-dynamicity of bonds, polymer network re-organization is limited. In consequence of the limitation, self-organization and energy dissipation of polymer network becomes restricted. The lack of these self-organizations causes reduction of high amount of water uptake, as well. Moreover, when external stress applied to the polymer networks, hydrogels become easily brittle (9).

As alternatives to vinyl crosslinking, researchers have used Schiff base reactions, hydrazone bond reaction and Michael addition reaction, which form sacrificial bonds (15). The development of these strategies has allowed incorporating dynamicity to polymer network, even if chemical bonds are used. Schiff base reactions mainly occur between functional aldehyde and amine groups (Figure 1). The term Schiff base defines a double bond of carbon-nitrogen, which is generated after reaction of the supplied initial functional associations. The main advantage of Schiff base reaction is the reversibility and dynamic nature, which differs from the conventional chemical crosslinking. It was proved that reversibility of crosslinking helps to improve mechanical properties of hydrogels (16). Moreover, Schiff base reactions can be performed simultaneously under physiological conditions. This nature has allowed it to be used in biological materials, especially, as injectable hydrogels (17). The precise control of the reaction possible with the manipulation of in-situ pH values, even with slight changes, and crosslinked hydrogel become stimulus-responsive, as well (18).

Hydrazone bond reaction is another dynamic chemical crosslinking method, which is also a type of Schiff base reaction, based on the linkage of nucleophilic reactive chemical group and carbonyl group. The mostly used chemistry is the reaction of supplied hydrazide and aldehyde groups (Figure 1). As a side product, water molecules are generated during the addition reaction. Hydrazone bond reactions are performed faster, when compared to Schiff base formation. Because of this, it is preferred for the preparation of injectable hydrogels. The gelation process only takes few seconds after the injection, and can be used for biomedical applications (19).

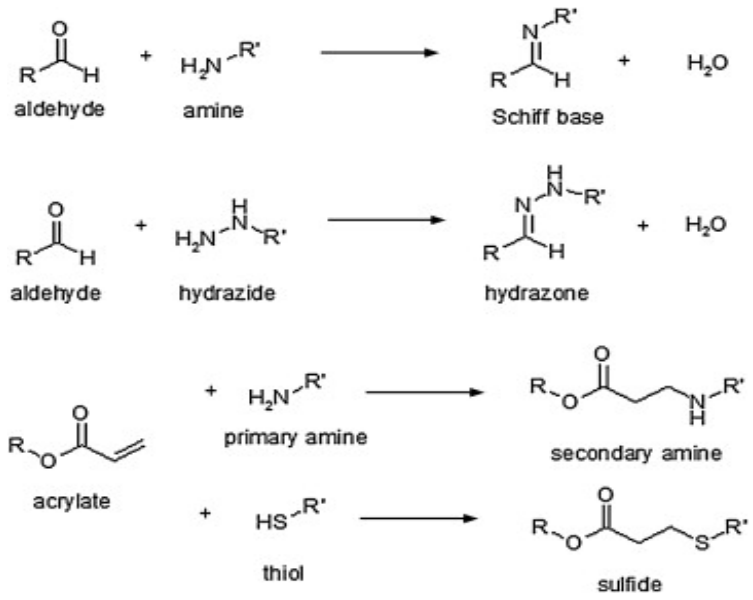

Figure 1. Common functional groups and reactions to form chemically crosslinked hydrogels. a) Schiff base reactions, formed by aldehyde and amine groups. b) Hydrazone structure, obtained from aldehyde and hydrazide groups. c) Michael addition reaction can be performed with acrylate and primary amine or thiol. Reproduced by permission of publisher (5).

Michael addition reactions take into place between electrophile acrylate/vinyl groups and nucleophile amine or thiol functional groups (Figure 1). For instance, PEG, poly (vinyl alcohol), and dextran, etc. functionalized with nucleophilic and electrophilic groups (i.e. PEG-dithiol, PEG-acrylate) have been used for the hydrogel preparation via Michael addition reactions (20). The rapic kinetic of the thiol-ene Michael addition click chemistry is advantageous to form hydrogels within 1 min. Uniform polymer networks have been obtained by this kind of crosslinking (21).

1.2.2. Physical Crosslinking Approach

Physical interactions are dynamic and reversible and can also be used for form functional hydrogels. Physical crosslinking strategy is based on weak interactions. To obtain stable gels, well-optimized synergy between molecules is required (22). Especially, water uptake inside hydrogel easily induces breaking down of physical interactions. The stress in the constituent polymer chains is increased due to the polymer network expansion. When the physical crosslinks cannot be retained anymore the hydrogel becomes dissolved.

Reversible and dynamic crosslinks allow for significant improvements of hydrogel mechanical properties, such as toughness and stretchability (23). Under mechanical stress, the weak crosslinking points can be deformed and even re-formed after the removal of applied force (24). The sacrificial interactions serve a powerful mechanism to improve energy dissipation and overcome brittle hydrogel structure. The incorporation of this molecular instrument significantly enhances toughness. For instance, self-recovery ability is contributed into bulky network, even if high level of strain is exposed to hydrogel (26). Several types of physical interactions can be used to prepare hydrogels and will be described in the following sections.

1.2.2.1. Hydrogen Bonds

Hydrogen bonds are one type of physical interactions, which are abundantly found in nature and have significant roles to keep functional formation and structural integrity of biological molecules such as proteins, DNA, etc. (25). Hydrogen bonds display cooperative forces, and different polymers inside hydrogels can behave as donors and acceptors. The existence of cooperativity induces the improvement of the bond strengths (27). Using this phenomenon, the mechanical properties of hydrogels can be improved. The stronger hydrogen bonds, the better toughness and stretchability that is possible to reach.

In addition to mechanical improvements, one unique functionality, called self-healing, can be achieved by the incorporation of well-arranged hydrogen bond formations. To gather self-healing phenomenon, enhanced cooperative associations are required. For instance, urea isopyrimidone (Upy) contains a functional unit with multiple hydrogen bonds (28, 29). It was shown that hydrogels crosslinked by Upy are able to demonstrate the self-healing property. The presence of such multiple cooperative bonding can be strongly formed between Upy monomers in

damaged areas of hydrogels. Following that, recovery of original bulky structure after the damage becomes possible.

1.2.2.2. Hydrophobic Associations

Hydrophobic interactions have been used in hydrogels to provide properties such as good energy dissipation, stretchability and self-healing ability (30, 31). Hydrophobic monomers or polymers with hydrophobic side groups can be integrated into the hydrophilic hydrogels for this purpose. To design hydrophobic crosslinking domains in hydrogels, the most preferred method is micellar copolymerization (Figure 2) (32). Inherently, surfactants are used to form micelles in aqueous phase. In principle, hydrophobic tails of surfactants generate small-scale hydrophobic domains to dissolve hydrophobic components, which are supplied to the emulsion in the following step. After that, the polymerization process is induced, and copolymerization of hydrophobic monomer in micelles and hydrophilic monomers in aqueous environment is completed at the interface. As a consequence, the unity of crosslinked polymer network is achieved and hydrophobic domains act as crosslinking regions.

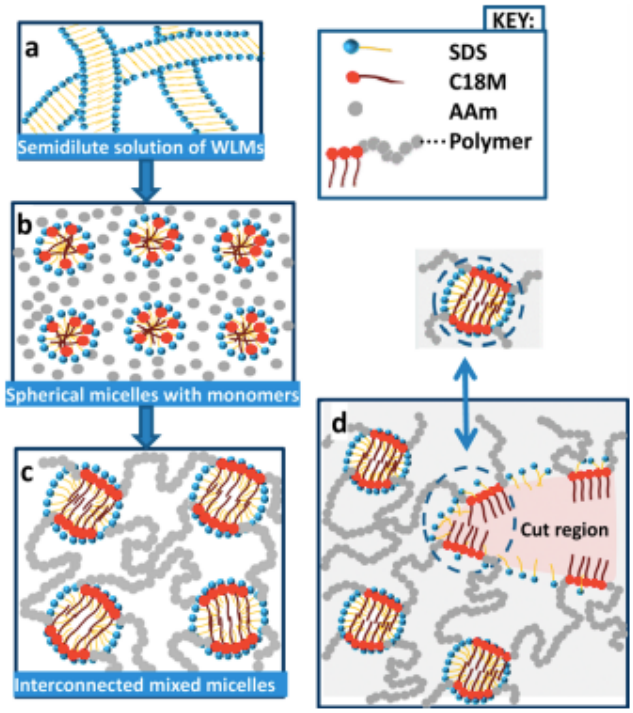

Figure 2. Micellar crosslinking of hydrogel with hydrophobic interactions. Hydrophobic C18 molecules are located inside micelles, and behave as crosslinking points.Reproduced by permission of producer (34).

The hydrophobic crosslinking contributes dynamicity to bulky material. Even though hydrophobic interactions are efficient strong to keep polymer network stable, the application of external forces could vanish the interactions and micelles. After removal of the force, hydrophobic interactions with micelles could mostly be re-formed. By considering this, hydrogels that demonstrate unique characteristics have been developed. For instance, tough and highly stretchable self-healing hydrogel designed by stearyl methacrylate monomers containing a hydrophobic long alkyl chain (33). Furthermore, it was demonstrated that self-healing phenomenon occurs as a consequence of micellar dynamic, and re-formed hydrophobic domains in the micelles achieve the complete self-healing (34).

1.2.2.3. Ionic Interactions

Ionic interaction-based crosslinking strategy is established from the interaction of positive and negative charged polymers. In consequence of opposite electric charges, polymer chains are able to form weak a synergy and polyelectrolyte complexes, which behave as a crosslinking. Ionic crosslinking is a beneficial tool to fabricate hydrogels, since great amount of natural and synthetic ionic polymer chains are available (35).

Charged natural polymers such as alginate, chitosan, and their derivatives are often used as polymeric chains for hydrogels. For hydrogel formation, these polymers require supplementary of divalent cations, such as Mg^{2+}, Ca^{2+}, to induce the crosslinking phenomenon. For instance, guluronate repeating units of alginate polymer can interact with the cations and build up a strong crosslinking, which is efficient to keep gel network in swollen state, as well (36). Chitosan has cationic repeating units in its backbone (37). It can form polyelectrolyte complex with anionic polymers. For instance, the polyelectrolyte complex can be assembled with either with natural polymers like alginate, chondroitin sulfate, pectin, or synthetic polymers, such as polyacrylic acid and polylactic acid.

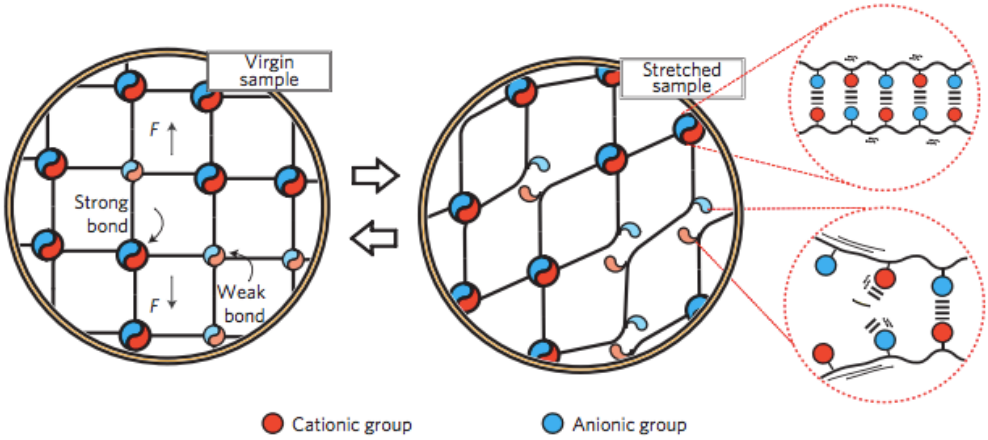

Figure 3. Schematical demonstration of ionically crosslinked hydrogel network, consisting of aionic groups (NaSS and AMPS) and cationic groups (MTPC and DMAEA-Q). Reproduced by permission of publisher (38).

In addition to natural polymers, several hydrogels, which consist of merely synthetic polymers with charged natures, have been reported. It has been demonstrated that incorporation of ionic interactions into the network enhances mechanical properties, such as toughness, stretchability, etc. (38). For instance, hydrogels constituted by anionic (NaSS and AMPS) and cationic synthetic monomers (MTPC and DMAEA-Q) showed toughness, stretchability (up to ~10 times) and self-healing properties (~ 99% efficiency) at the same time (Figure 3) (38, 39). The random presence of ionic bonds creates strong and weak interactions, which are between certain types of monomers, in the bulky material. The strong ionic interactions perform as a permanent crosslinking, while the weak bonds bring a reversibility to dissipate the mechanical energy by destroying and re-forming ionic interactions.

1.2.2.4. Host-Guest Interactions

Host-guest chemistry can be used to prepare dynamic supramolecular hydrogels, crosslinked molecular recognition. The host molecules mostly consist of a "ring-like" structure, and guest molecules could be locked inside them (Figure 4). The backbones of polymer chains can be modified with these special structures to form crosslinking and hydrogels, as well (40). This locking process is ruled by a stoichiometry and equilibrium constant, which means that sufficient enough of host and guest molecules should be supplied during the network formation (41). Furthermore, reversibility is an exciting property of these kinds of locking phenomenon, since it contributes to improving of the mechanical energy dissipation. So far, many types of natural and synthetic host molecules have been reported. The most used ones can be classified as group

of cyclodextrins. Cyclodextrins (CDs) are natural cyclic oligosaccharides, which consist of D-Glucose repeating units. Most commonly used sub-groups are called with α-, β-, γ-CDs. The CDs are very small structures that undergo Angstrom (Å) level size. For instance, the depth of ring is 7.9 Å, and space for fixing the guest molecule is very limited (41). As a result, the presence of multiple guest molecules in one host molecule is not possible, and supply of stoichiometrically well-optimized components is required.

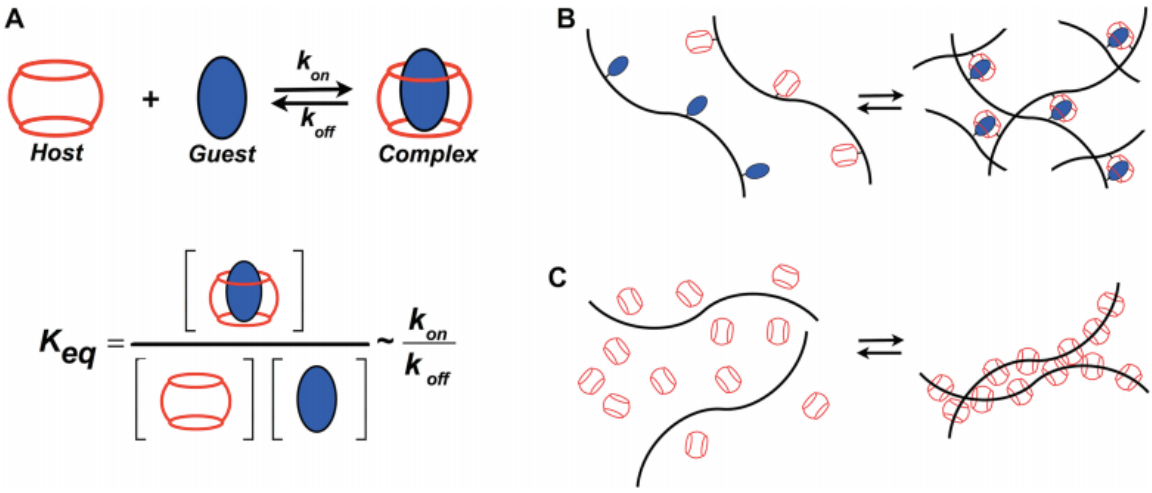

Figure 4. Demonstration of host-guest interactions a) Stoichiometric relationship between host-guest molecules b) Two different polymers can be crosslinked by host-guest interactions c) Polymer chains can pass through ring structures of CDs. Reproduced by permission of publisher (41).

The ring structure of CDs can be used to crosslink polymer chains, as well. It was proved that linear polymer chains can go through the inner side of CDs and create a similar formation like necklace (42). Slide-ring hydrogels are one kind of well-developed systems that demonstrate good mechanical properties. The concept of slide-ring crosslinking arises from reinforcements of CDs and polymer chains that are able to penetrate into cavity of CDs. In terms of mechanical stress exposure, the sliding nature, which comes from non-covalent nature, of polymer chains helps to dissipate energy. At the same time, CD ring structures can interact with other ring structures to optimize releasing of mechanical stress. Ito *et al.* demonstrated slide-ring hydrogels, synthesized by this strategy (43). The polyrotaxane hydrogel, based on α-CDs, was fabricated using PEG chains. The end-capping process was performed to prevent release of polymer chains from the ring structures, and dissolving of hydrogel was overcome. The synthesized hydrogel had indicated high level of water uptake (~90 wt%). Furthermore, this strategy results

in good mechanical properties. For instance, one reported kind of polyrotaxane hydrogel can be approximately stretched for 15 times, and shows a tough nature. On the other hand, the ring structures can be modified with functional groups to manipulate hydrogel (44).

1.3. Mechanical Properties of Hydrogels

The mechanical properties of a hydrogel mainly dependent on the rigidity of the constituting polymer chains, the crosslinking degree and the polymer concentration. In general, if polymer fraction and crosslinking are increased, mechanical strength of hydrogel can be enhanced (45).

Hydrogels suffer from poor mechanical properties, as a result of various factors, like random distribution of crosslinking points and inhomogeneous polymer molecular weight. The inhomogeneity in hydrogel arises from the unequal reactivity of monomers and the crosslinker. During in-situ polymerization, crosslinking process occurs densely in some regions, while other regions are loosely crosslinked (46). Also, significant differences in polymer length could be detected (47). When mechanical stress is applied to hydrogel, the force cannot be distributed in a uniform direction. Due to the network inhomogeneity, the overall mechanical property and strength are reduced (45).

The high content of water is also a key factor for the poor mechanical property of hydrogels. High water uptake lowers the density of crosslinking points and the polymer fraction. Also, stress in polymer chains increases, due to the high volume expansion. In this case, exposure of gentle forces could trigger breaking of stressed polymer chains, and macroscopic fracture could be observed (48). Polymer networks of hydrogels with self re-organization ability can help to overcome swelling induced limitations of mechanical properties. The energy dissipation ability of network is vital to overcome brittleness. If polymer network is able to release the external stress in an efficient way, then the disruption of network unity can be prevented (49). It is well known that incorporated crosslinking strategy has important role on energy dissipation. For instance, dynamic physical interactions provide efficiency for the stress distribution, while traditional covalent crosslinking cannot handle it. Additionally, energy dissipation could be contributed by the incorporation of second polymeric network, such as double network hydrogels, which shows the best way to prepare tough hydrogels up to date (24). All hydrogels, which dissipate the applied energy well, require self re-organization of their networks. For this aim, distinct strategies should be integrated inside polymer network.

1.3.1. Energy Dissipation Mechanisms in Tough Hydrogels

The brittle nature of hydrogels could be overcome by introducing energy dissipation mechanisms into hydrogels to enhance their toughness. In the case of tough hydrogel preparation, the design of network should efficiently dissipate the applied stress. The applied stress is exposed in a perpendicular direction during compression test. To prevent crack formation, principally, the network should serve dynamicity during the deformation of network (49). For this case, multi mechanisms, which adopt particular approaches, have been introduced. These approaches can be mainly categorized as; i) polymer chain fracture by stress ii) reversibility of the incorporated crosslinking iii) conformational change of the constituent chains iv) incorporation of definite fillers (50).

Polymer chain fracture by stress: The constituent polymer chains and crosslinker could be broken with the application of stress. Double network (DN) hydrogels, one of the best ways to prepare tough hydrogels, are based on the breaking of polymer with the exposure of stress. The energy dissipation mechanism relies on breaking of covalently bonded (sacrificial bonded) first network. By fracture of the chains, great amount of energy is dissipated into the disrupted network. In this case, the remaining network could stay without any trigger of fracture, and macroscopic damages of hydrogel are prevented, as well. Many types of tough hydrogels with this principle have been introduced. The main drawback of fracture strategy is the reversibility, since polymer chains are permanently damaged. Mostly, the fractured polymer chains cannot recover back to the initial formation. To overcome this drawback, a novel hydrogel system by using dynamic Alginate-Ca^{2+} network as the first network was developed by Suo *et al.* (51). Recently, JP Gong *et al.* had reported a new strategy, which attributes reversibility to the polymer fracture (52). The reported tough DN hydrogel can recover back, and even increases mechanical properties by fracture that mimic build-up of natural muscle tissue.

Reversibility of crosslinking: The second way of energy dissipation is the incorporation of reversible and dynamic crosslinking. As mentioned in previous sections, some kind of crosslinkers undergoes dynamic nature that can be deformed and reformed under stress apply (16, 23). Especially, physical crosslinking is commonly used to prepare tough hydrogels, due to the weak nature of interactions. They formed associations that can be easily manipulated, re-organized and after that dissipate energy inside hydrogels (24). After removal of the external stress, hydrogels can recover to the initial physical properties by re-organization ability of molecules.

For instance, this behavior could help to prepare hydrogels, which are resistant to cyclic loading and keep initial mechanical features.

Conformational change of constituent chains: Although polymer chains are mostly thought as simple and linear, some kind of polymers could form complex conformational chain structures under certain circumstances. Especially, the complex conformations are obtained in terms of biological polymers, such as fibrin, collagen, and polysaccharides, etc. For instance, collagen consists of a specific tri-helix conformation, which is constructed by a precise arrangement of several amino acids (53). In principle, polymers with complex structures can be embedded into the hydrogels to receive tough nature. In the polymer network of hydrogels, these polymers arrange their chains in a certain conformation, and followed by creation of dense domains (54).

Incorporation of fillers: Reinforcement of fillers, including fibers and inorganic clays, could be an efficient way to prepare tough hydrogels, as well. The reinforced fibers and clays are able to distribute great percentage of the applied energy to bounded polymer chains. In this case, the applied energy is reduced and damages in constituent polymer chains are prevented. It was demonstrated that fibers of polycaprolactone, polyglycolic acid, and fibrin enhanced mechanical properties of hydrogels (50,55). On the other hand, high surface area of clays is beneficial to dissipate the energy. The constituent polymers can interact with the clay surface in many regions, and energy transfer between polymer network and fillers can be succeeded (56).

1.4. Applications of Hydrogels

Hydrogels have many applications in different disciplines, such as material science, pharmaceutical industry, biological and environmental science, etc. The application fields of hydrogels can be classified into sub-groups, and some of them were listed below.

Contact Lenses: Contact lenses are the well-optimized hydrogels systems, which provide real-life solution to overcome visual impairments. The transparency of hydrogels allows light to pass through the material. Therefore, water absorption ability of hydrogels helps to stay moisturizing during the usage, and decreases to harm to the contacted tissue. The first hydrogel-based contact lenses were fabricated by poly-2-hydroxyethylmethacrylate (PHEMA), which is a synthetic polymer with showing great biocompatibility. Following the commercialization

PHEMA lenses, various types of polymers, such as PMMA or N-vinyl-2-pyrrolidone (NVP), have been utilized to be used as contact lenses (57).

Wound Dressing: Skin is a barrier that provides protection from outer environment, and its damage could lead to fatal results. For this reason, the healing of skin wounds is significant to protect overall health conditions. Hydrogels are desired to be used as pastes, moist dressings, in case of wound healing. To heal acute and chronic wounds, hydrogels should meet several requirements. For instance, hydrogel adhesion is one property that provides stable wound dressing during the healing process of the damaged tissues. Therefore, the unique nature of hydrogels allows loading substances, namely drugs or growth factors, in their polymer networks. Subsequently, the controlled release of these kinds substances can increase the healing progress (57).

Tissue Engineering: Millions of people suffer from organ failure, and transplantation is challenging due to the donor compatibility. Hydrogels are biocompatible and thus good candidates to overcome such a problem. It has been realized that hydrogels are great matrices to seed and *in-vitro* cultivate some cells. In addition, biocompatible hydrogels do not result in any immunological responses, when they are applied to *in-vivo* conditions and contract with the surrounding tissues. So far, various biopolymers and synthetic polymers have been used for tissue engineering, including chitosan, hyaluronic acid and alginate, poly(acrylic acid), poly(ethylene oxide) and poly(vinyl alcohol), etc. (6,7).

Superabsorbent Products: Superabsorbent hydrogels with fast and high water uptake is desired for some fields in industry, such as cosmetics, agriculture, and hygiene products (B). For instance, superabsorbent material in diapers can keep an approximate volume of 500 cm^3 liquid. Novel polymer systems, such as sodium carboxymethylcellulose (NaCMC) and hydroxyethylcellulose crosslinked divinyl sulfone (DVS) are commonly used to construct superabsorbent hydrogels (58).

Actuators: Hydrogels can be fabricated with polymer systems that are sensitive to a certain stimulus, such as temperature, pH and light, etc. (59). By changing the environmental conditions, the shape transition of hydrogels can be triggered, and actuating phenomenon is succeeded. Up to date, many hydrogel systems with mimicking natural motions (i.e. muscles) have been reported. For instance, hydrogel bilayers are fabricated by combination of two ther-

moresponsive hydrogels (LCST and UCST), which have constant opposite behaviors with temperature systems. When the temperature is altered, one hydrogel layer starts to shrink, while the other increases its swelling capacity. Subsequently, bending of bilayer hydrogel system is achieved. As a typical example of LCST/UCST bending system, hydrogel bilayer of PNIPAM and poly(acrylic acid-co-acrylamide) was reported by Zheng *et al.* (60). Therefore, the actuating behavior of hydrogels mostly demonstrates reversibility, which allows obtaining initial conditions after the stimulus is removed out. In addition to bilayer hydrogels, the actuation nature of hydrogels can be gained by formation of patterned structures. The swelling and shrinkage of certain regions of hydrogels can be controlled by the patterns. In this case, the exposure of stimulus only triggers particular parts in the polymer network. Following that, bending of hydrogels into specific shapes can be accomplished.

1.5. Motivation

Although many types of physical and chemical crosslinking strategies have been developed so far, it is still challenging to obtain good mechanical properties and high swelling ratio together. The previously reported hydrogel systems mostly require high polymer fractions to sustain their mechanical properties (10). For instance, DN hydrogels are one of the most successful hydrogel systems with showing extreme toughness and stretchability. To succeed these properties, they require high polymer fractions, such as 10 wt% (24). Moreover, their swelling capability is limited after a certain level, and reaching to extreme water uptake (i.e. 2 wt%) is problematic.

This study aimed to development a new type of physical crosslinking with dynamic nature, which overcomes the highlighted limitations. Polymer chain entanglements are kind of physical interaction that is easy to be destroyed in hydrated state. It is known that they contribute to good mechanical properties with energy dissipation in several systems (i.e. DN and ionic-covalent entanglement hydrogels) (51, 52). Up to date, hydrogels crosslinked only by polymer entanglement crosslinking has not been reported, due to their weak hydrated state stability. The entanglement ability of polymers could provide dynamic nature with its sliding nature, which can be incorporated into hydrogels and help to obtain good mechanical properties. Therefore, the dynamic free-sliding behavior would provide efficiency to optimize hydrogel network to reach maximum water uptake. By considering its promising nature, a cluster strategy was designed to succeed crosslinking phenomena with entanglements of long polymer chains. The long pol-

ymer chains could pass through several nanogels to succeed three dimensional crosslinked polymer network. It is considered that the incorporation of nanogels would allow to form entanglements inside their polymeric network. The free-sliding long polymer chains inside nanogels would contribute to mechanical properties, such as toughness and stretchability in highly swollen state. Such strategy contributes to obtain hydrogels with extreme swelling (~98 wt%). Therefore, PEH still shows toughness, resistance to cut and stretching (~6 times), which is challenging for the previous hydrogel systems. Moreover, free-sliding nature of PEH helps to fully recover mechanical properties after lyophilization. With this new kind of crosslinking strategy, limitations of swelling and mechanical properties would be overcome. Moreover, dynamic hydrogel networks could be synthesized for various applications.

In addition, it is proposed that controlling free-sliding nature of PEH would present responsive behavior by a simple modification. The transformation of hydrogels and their mechanical properties by stimulants have been demonstrated in literature, but all reported strategies purpose requirement of dimensional changes (i.e. 5, and 10 times) based on water uptake and release. In this case, polymer fraction in the network is also altered, and followed by change in hydrogel stiffness (60, 61). The shift in hydrogel stiffness without inducing initial dimensions and polymer fraction change is aimed with thermoresponsive PEH. For this aim, PEH crosslinking points/nanogels are thought to be changed to a responsive nanogel system. The thermoresponsive nanogels with polymer entanglements constitute only tiny fraction of the hydrogel network. With the implementation of such strategy, incorporation of thermoresponsive behavior into PEH system is aimed. When shrinkage of nanogels are induced, it is supposed that free-sliding of entangled polymer chains would be limited due to restricted space inside nanogels. At the same time, stiffening without significant water ratio and size change was expected, since only crosslinking points are regulated in the network. Note that main compoment in the polymer network is still constructed by non-responsive polyacrylamide in this strategy. In contrast to common thermoresponsive hydrogels, which need high polymer fractions of thermoresponsive constituent, the PEH system only needs very small percentage of stimulus responsive component (i.e. 1 wt%) to demonstrate thermoresponsiveness. Therefore, different responsive behaviors can be implemented to PEH by a simple change of nanogels to other characteristics.

Physical crosslinking strategies are not only implemented for hydrogel synthesis. They can be used for different gel materials, which are called as organohydrogels, and could provide dynamicity into polymer network. Organohydrogels are kind of soft materials with consisting of

binary phases that helps to combine two nature of hydrophilic and lipophilic constituents into gel. Microemulsions are utilized to fabricate such gel materials. In previous reports, several organohydrogels with showing isotropic properties have been reported. These reports use fast gelation methods with chemical crosslinking that prevent phase separation and dynamic formations during the in-situ synthesis (63, 64). Considering this, fabrication of an anisotropic organohydrogel with showing different characteristics, such as surface, mechanical properties etc., in various regions is aimed. The proposed organohydrogel consists of two different phases of water and silicone oil, and dynamically crosslinked by hydrophobic associations. It is known that microemulsions are very sensitive to composition changes. During in-situ polymerization, slight changes in composition of water and silicone phase could lead to obtain phase separation. In case of phase separation, the polymer network of organohydrogels can be differed and anisotropy could be gained to gel material. In contrast to previous reports, this hydrophobic association crosslinking based approach would provide a useful mechanism to fabricate organohydrogels with altered features.

Chapter 2: Physical Entanglement Hydrogels

2.1. Introduction

Polymer entanglements are non-covalent and dynamic interactions, based on arbitrarily cross and lock of long enough polymer chains (65). The term of chain entanglement was first proposed a century ago. Busse had realized this effect in the phenomenon of recovery of deformation of unvulcanized rubber in a short time scale (66). This behavior was attributed to the sliding of constituent polymers. It was found that polymer chains could form physical interlocking structures and demonstrate temporary network formation, induced by deformation and relaxation. The sliding nature of polymer entanglements was investigated by Edwards and characterized by the definition of Tube model theory (67). The tube theory implements restricted motions of surrounding chains, their movement in tube-like structure and topological fixation in the limited regions. It was mentioned that the topological constrains provide to obtain arbitrarily crosslinked networks. The dynamicity of topological constrains or single chains was shown by de Gennes in 1971, and the phenomenon was called “reptation” (68). The term of reptation remarks the free motion of polymer chains in tube structure. It was suggested that even though topological interlocking of polymer chains is succeeded, the polymer chains are still able to continue to simultaneous sliding and diffusing in the dense bulky matrix. The defined reptation phenomenon clarify the dynamic nature of physical entanglement interactions.

Polymer entanglements are remarkably weak interactions, compared to different kinds of dynamic physical interactions, such as hydrogen bond, host-guest cooperation, etc. The entanglement interaction simply implies a topological restriction of molecular motion of polymer chains (69), which is frequently neglected in hydrogelation, since the polymer chains are highly solvated and normally do not entangle each other. It is accepted that physical entanglement interaction is too weak to form efficient crosslinks to stabilize a hydrogel itself. The ability of entanglement formation is dependent on the length of polymer chains, which appears in the network. In case of short chains, the formation of entanglements is challenging, and polymer chains have tendency to slide on another chain (70). If polymer length is enhanced, the entanglement formation becomes easier and polymer chains build up weak interaction by arbitrary passing within each other. In case of hydrogels, the entangled polymer chains easily become dissolved when they are exposed to dense interaction with water molecules (71). Firstly, the diffusion of external water between polymer chains occurs within time. The initial glassy state of entangled polymer chains turns into the rubbery state. In this state, hydrogel unity can be secured by polymer entanglements up to certain level. If the continuous water uptake is progressed, total

dissolution of polymer entanglements is possible. In this case, a certain minimum time is needed for the total reptating out of entanglement polymer chains. The time scale of total disentanglement directly correlates to the reptation time of the chains, which is relevant to the polymer structure and molecular weight. The mobility of polymer chains in highly swollen state is very high. Subsequently, the disentanglement phenomenon becomes excessively dominant and easier. Following that, the transition to a solution state from gel state is obtained (72). After the complete dissolution, disentangled polymer chains start to float in the solution and show Brownian motion.

Although obtaining hydrogels by entanglement crosslinking appears challenging, the dynamic and unique nature of polymer entanglements is expected to provide several advantages, such as good stress distribution, toughness and stretchability. Good stretchability is based on the extensibility of polymer chains(73). Good stress distribution has been achieved in tough hydrogel systems based on interpenetrating polymer networks (74). Double networks hydrogels with high mechanical strength have been designed to replace load-bearing tissues (75). They consists of two polymer networks which are able to slide on each other by exploiting polymer entanglements. The first (i.e. poly(2-acrylamido-2-methypropanesulfonic acid) crosslinked with *N, N′*-methylenebisacrylamide) has high crosslinking degree and provides rigidity. The second polymer network (i.e. polyacrylamide crosslinked with *N, N′*-methylenebisacrylamide) is softer and contains long polymer chains to create entanglements with the first network (76). The presence of high polymer fraction leads to obtain great amount of polymer entanglements within the chemically crosslinked network. These entanglements demonstrate good stress distribution by sliding, which helps to succeed enhanced mechanical strength of hydrogel (77). By increasing the concentration of the entanglement forming second polymer network, the mechanical strength of hydrogel is improved (78). The higher concentration leads to achieve greater polymer entanglements to slide and dissipate the stress.

Ionic-covalent entanglement hydrogels (ICE) are also one sub-class of IPN hydrogels that can present polymer chain entanglements. ICEs are made up from two separate crosslinked network, and these networks do not interact except for entanglements (79). For example, covalently crosslinked polyacrylamide and ionic bonded alginate ICEs can contain 90% water, and undergo 20 times stretchability with the help of entanglement interactions of the each polymer network. The fracture energy was 9,000 J m^{-2} (51). Moreover, by manipulation of polymer entanglements the strain level can be increased, and higher fracture strengths can be received with

the contribution of denser entanglements (80). Stevens *et al.* reported an entanglement incorporated hydrogel system that associates ionic and covalent bonding at the same time (81). It was exhibited that the reinforcement of dense entanglement interactions into the network significantly helped to promote mechanical properties.

In addition to these strategies, reinforcement of micro and nanoparticles inside the hydrogel contribute to energy dissipation, as well. Although the contribution of reinforced particles is significant, the effect of polymer entanglements shouldn't be depreciated. The entangled polymer chains generate a synergetic impact with the composite forming ingredient on mechanical properties. Grafting polymerization is mainly used to supply polymer chains on the surface of the reinforced particles, which consist of a high surface ratio. In that case, covalent bonding takes into account, and polymer chains propagate from nanoparticle surfaces. The nanoparticles begin to act as a crosslinking spot. The abundant presence of grafted polymer chains could form entanglements in the bulky matrix of hydrogel (82,83, 84). The significance of entanglement presence was shown by researchers with using tensile test. It was found that modulus was boosted with the help of physical entanglements. Moreover, hysteresis during loading-unloading test is created with the existence of entanglements (85). Except for mechanical properties, water uptake capability of composite hydrogel can be altered by the entanglement formation. The increased number of entanglements leads to form stronger physical crosslinking, and limits the absorption capacity (86). Another strategy to form nanocomposite is supplying clays into hydrogels. Clays are inorganic materials, which consist of layered structures, and high surface area (87). The reinforcement of such inorganic compounds is essential, since they give raise to more entanglement entity in polymer network. It was shown that remarkable elongation capacity (~8 times) could be received with this strategy, by inducing increase of entanglement numbers (88). In terms of stretching, the entangled polymer chains are able to organize clays to the elongation direction (89). Furthermore, recovery of the initial network, which is energy-sufficient state, is also possible with the release of stress.

In this study, development of a new type of physical entanglement crosslinking, which can form hydrogel network and provide stability up to high swelling ratio, was aimed. Up to date, hydrogels crosslinked with only entanglement interactions has not been reported, due to the weak swollen state stability. The entanglement ability of polymers could provide dynamic nature with its sliding nature, which can be incorporated into hydrogels and help to obtain good mechanical

properties. By considering this, a cluster strategy was designed to succeed crosslinking phenomenon with polymer entanglements. The obtained hydrogel was able to sustain the network unity, even it had absorbed extreme amount of water, and reached to very low polymer fractions (~2 wt%). In swollen state, good mechanical properties, such as toughness, softness and stretchability, were also gathered.

2.2. Results

2.2.1. Synthesis of Physical Entanglement Hydrogels

The proposed design is based on the formation of a densely entangled hydrogel network that incorporates highly crosslinked nanogels (NG) with the same composition (Figure 5). First clusters of polymer chains are formed in confinemen, and multiple entanglements in the clusters are connected together to achieve a hydrogel. The connected polymer chains with entanglements demonstrate a strong nature to retain the elastic state of the hydrogel. Such entanglements are expected to slide, and the dynamicity of hydrogel is achieved. It should be denoted that entanglement crosslinking has difference from the slide-ring hydrogels. While slide-ring crosslinking has terminal groups that strongly limits the dynamicity, the entanglement crosslinking does not contain any terminalization process.

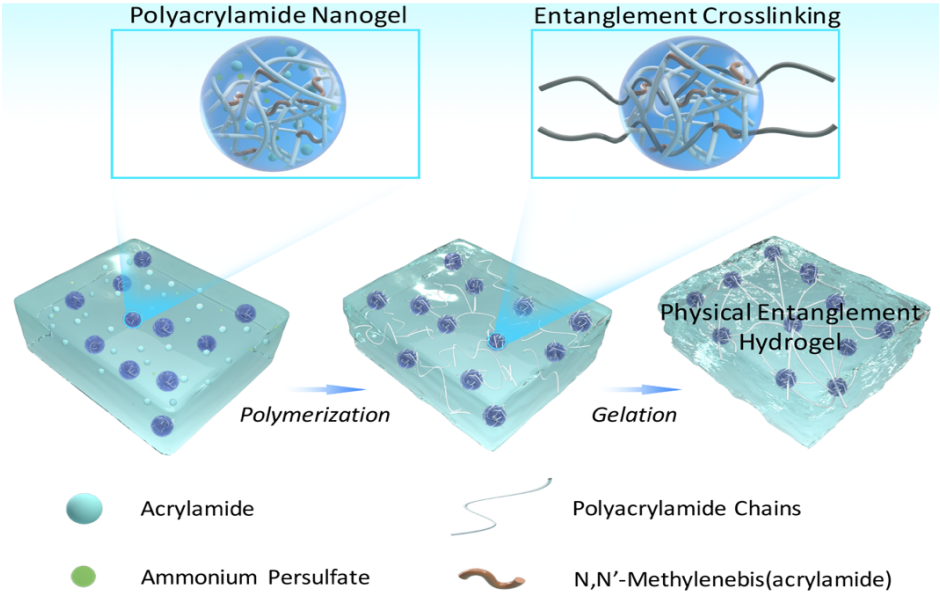

Figure 5. Schematical demonstration of the formation of physical entanglement crosslinking based hydrogel. Highly crosslinked polyacrylamide NG absorbs monomer and initiator that are polymerized in-situ. Entanglement clusters are constituted by polymerization.

To demonstrate the design, polyacrylamide was chosen. Initially, highly crosslinked polyacrylamide NGs were synthesized via microemulsion polymerization. Methylenebisacrylamide (MBA) was used as the crosslinker for the synthesis of NG. All unsaturated vinyl groups are expected to be consumed, and removed for successful formation of entanglements in porous network of NGs. Otherwise, either polymerization on NG surface with unsaturated reactive groups, or unexpected covalent crosslinking during gelation could be gathered. By considering these factors, the removal of unreacted residues was performed by washing with ethanol and centrifugation. The remaining NGs were characterized by analytical methods to monitor possible unsaturated vinyl functional groups before further use. To create entanglement clusters, the synthesized NGs were immersed in an aqueous dense solution of monomer and initiator. Subsequently, the absorption of acrylamide monomer and APS initiator was expected into the NG, and following that in-situ polymerization was started (at room temperature, inert environment).

Table 1. Chemical compositions of fabricated hydrogels.

Sample Code	**Monomer (Acrylamide)**		**NG**		**Initiator (APS)**		**Water**
	Ratio/Amount		**Ratio/Amount**		**Ratio/Amount**		
PEH20-0.75	20 wt%	0.2g	0.75 wt%	0.0015g	3 wt%	0.009g	1ml
PEH30-0.37	30 wt%	0.3g	0.37 wt%	0.0011g	3 wt%	0.009g	1ml
PEH30-0.75	30 wt%	0.3g	0.75 wt%	0.0023g	3 wt%	0.009g	1ml
PEH30-1.5	30 wt%	0.3g	1.5 wt%	0.0046g	3 wt%	0.009g	1ml
PEH40-0.75	40 wt%	0.4g	0.75 wt%	0.003g	3 wt%	0.012g	1ml
AA-MBA	30 wt%	0.3g	0.03 wt% MBA	0.0001g MBA	3 wt%	0.009g	1ml

* The coding of the samples was done considering monomer and NG ratio, respectively.

With the help of in-situ polymerization, polymer chains could be formed and pass through the NGs. Furthermore, very long polymer chains are supposed to be formed, since they should be able to pass through multiple NG. When more than one polymer chains pass through a NG, the polymer network is expected to become crosslinked and stabilized. In this case, hydrogels with good elasticity should be obtained.

2.2.2. Synthesis and characterization of Nanogels

Polyacrylamide NGs were prepared by microemulsion polymerization. Methylenebisacrylamide (MBA) was used as covalent crosslinker to obtain highly crosslinked NGs. Our concept is based on the formation of polymer entanglements, triggered by in-situ polymerization, inside the polymeric network of NGs. At the same time, the polymerized chains can undergo coupling reactions and bind to other chains. These polymer chains start to behave as inter-connective chains, and form crosslinked network.

To achieve in-situ polymerization inside NGs, diffusion and absorption of monomers with initiators inside the NG is necessary. In the normal case such diffusion is when the NG surface contains unsaturated vinyl groups. In this case the monomers would polymerize with the surface reactive groups, and most polymerization would occur on the particle surface.

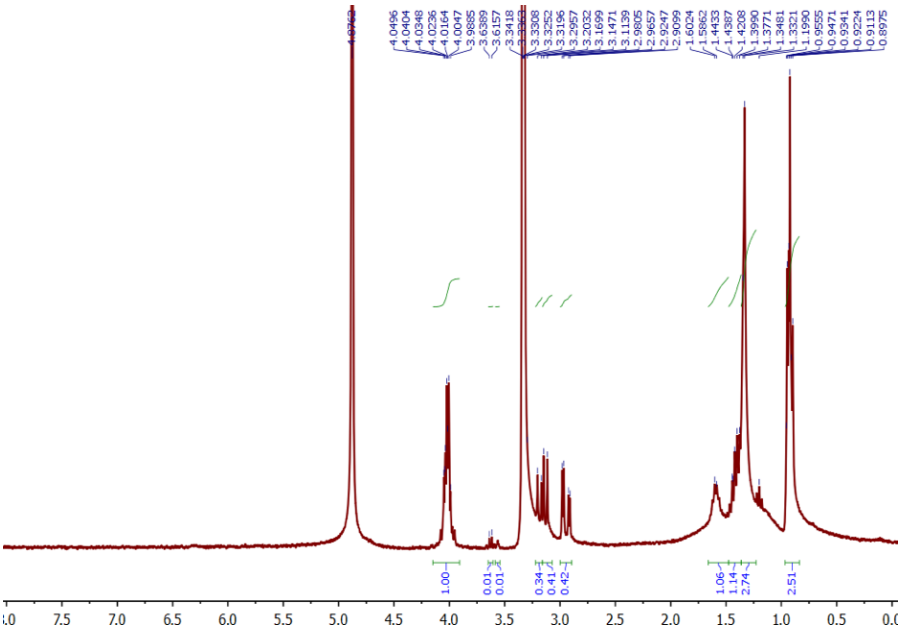

Figure 6. ^{1}H NMR spectrum of synthesized NGs after complete purification.

To avoid surface grafting polymerization, the consumption of all vinyl groups on the surface of the NG was targeted. For this aim, polymerization of nanogels was performed for 2h to consume MBA crosslinker. Following that, washing steps with ethanol were conducted to remove out the unreacted crosslinker residues. The presence of unsaturated vinyl groups, which come from MBA crosslinker, was investigated by ^{1}H NMR. According to the spectra, no clear peak around 6.0-6.5 ppm, which belongs to unsaturated vinyl end of MBA, was detected (Figure 6). It was

concluded that all vinyl groups were consumed and removed out during the synthesis and washing steps. In this way, surface polymerization or covalent crosslinking was prevented. The ^{1}H NMR data indicates that monomers and initiators could easily penetrate into the NG network to perform physical entanglement formation. In the ^{1}H NMR spectra, -CH2-, -CH- groups of polyacrylamide was assigned to the peaks at 1.33 ppm, and 1.42 ppm, respectively. Peaks at 1.58 ppm and 4.01 ppm were contributed from -CH- and -CH2- of MBA crosslinker. Methanol solvent presented two peaks at 3.33 and 4.07 ppm.

Following the chemical characterization, physical properties of NGs were also investigated. The size features of NGs could have a vital role, since absorbed monomer and initiator abundance is dependent on the polymeric network volume. For this reason, the shape and size properties of synthesized NG were investigated. To evaluate size distribution, DLS measurement was performed. Prior to the measurement, the dried NGs were dispersed in water via ultrasonication to obtain homogenous scattering. Following the ultrasonication, the DLS measurement was conducted at room temperature, immediately. Immediate DLS measurement is preferred to understand initial size of the nanogels since polymeric nanogels would undergo continous swelling behavior. In this case, the equilibrium state size and initial size of nanogels is differed. The average size of polyacrylamide NGs was detected as 140±105 nm after being soaked in water. Furthermore, a broad and non-homogenous distribution profile was observed (Figure 7).

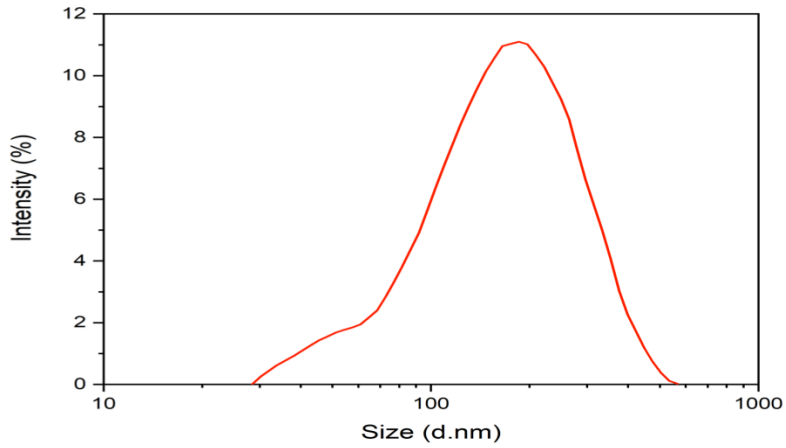

Figure 7. Characterization of NG size distribution, obtained by dynamic light scattering. Nanogels were dispersed in water prior to DLS measurement.

As the next step, the morphology of the synthesized NGs was investigated. For this aim, transmission electron microscopy (TEM) imaging was implemented. The dried polyacrylamide NGs

were dispersed in ethanol before imaging process, since it was aimed not to trigger swelling process via water. In this case, the initial original size and morphology can be kept during the measurements. It is known that swelling process could cause to changes in terms of shape. According to TEM images, synthesized NGs have round shapes (Figure 8). The average size of dried polyacrylamide nanogels were found as 55±12 nm , which is significantly lower than the average size of DLS measurement. The result shows that polyacrylamide nanogels can swell great amount of water inside even after immediate soaking in water. This behavior also suggested that the NGscould absorb significant amount of monomers and initiators together with water into their polymer networks.

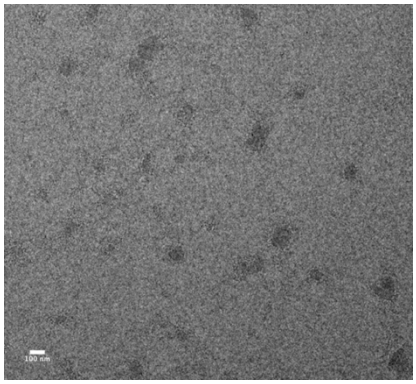

Figure 8. Dry state of NG was investigated by TEM to observe their size and shape.

2.2.3. Swellability of PEH

The presence of weak polymer entanglement crosslinking is expected to allow dynamic network re-arrangements during external water uptake. The reason is that sliding of polymer entanglements and chains could become easier in swollen state, since entanglement strength would significantly decrease. When it is compared to other kinds of dynamic networks, such as slide ring and host-guest interactions, physical entanglement based crosslinking leads to weaker interactions in swollen state. Such a weak crosslinking interaction could help to induce an easier swelling with great amount of water absorption.

The swelling of PEHs was tested by immersing in water at room temperature. The initial and final weights of samples were checked after a certain timespan. First of all, as-prepared and freeze-dried samples were soaked in water for 24h and long term (Figure 9a, and 9b). After 24h swelling, the polymer fraction of most PEHs attained to (~2 wt%), while covalently crosslinked AA-MBA control hydrogel was able to reach to only ~8 wt% (Figure 9a). These findings had shown self-organization ability of PEH network to reach maximal water capture. In contrast,

non-dynamic covalent crosslinking of AA-MBA had resulted to limited water uptake capability. PEH20-0.75 demonstrated slightly lower polymer fraction than the other groups and reached less than 2 wt% polymer fraction (Figure 9a). On the other hand, it was found that higher amount of initial monomer concentration limits the final swelling ratio of hydrogels. PEH40-0.75 had approximately 4 wt% polymer fraction in swollen state. It was attributed to dense formation of entanglements inside NG. The denser entanglement interactions would block self-organization capacity of polymer network during the swelling. Subsequently, water uptake ability is limited (Figure 9a). Interestingly, no direct impact of NG concentration on swelling ratio was identified. PEH30-0.37, PEH30-0.75 and PEH30-1.5 had almost same swelling ratio after 24h (Figure 9a). In case of traditional hydrogels, the change in crosslinking ratio normally leads huge change in water absorption capacity. PEHs had demonstrated a controversy behavior to the well-known crosslinking-swelling relationship. It was attributed to the free-sliding behavior of polymer entanglements and dynamicity of polymer network.

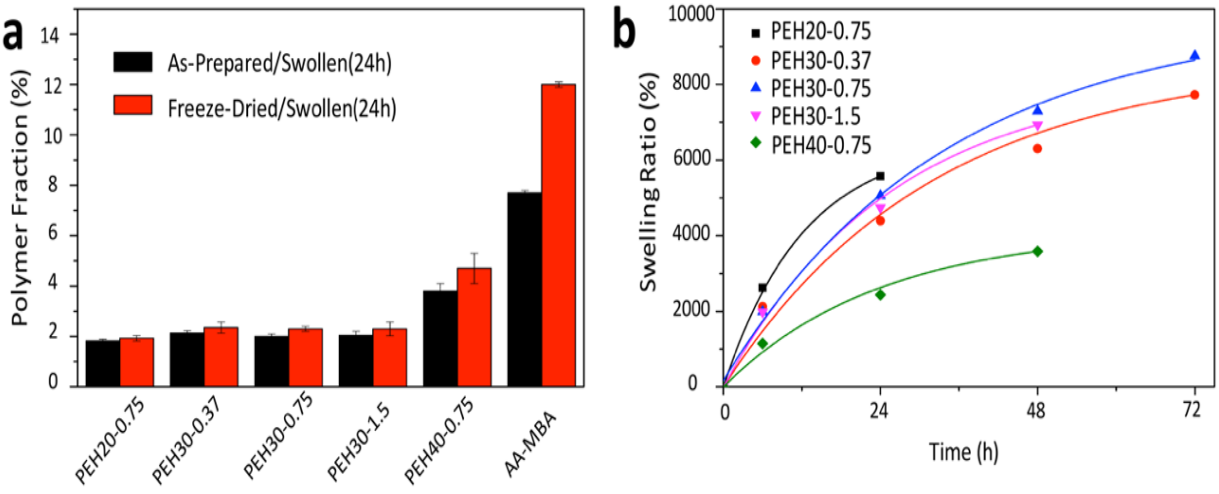

Figure 9. Swelling ability of PEHs a) Polymer fraction of PEHs after 24h water absorption. Black columns show 24h water uptake of as-prepared samples, while red columns belong to swelling of freeze-dried samples. b) Continuous swelling profile of PEHs until complete dissolution is gathered.

Long term swelling test was performed to test the stability of the physical entanglement crosslinking. If continuous water molecule entrapping is induced, the stress in polymer network would be triggered and caused stretch of polymer chains, as well. As discussed before, polymer entanglements are formed by very weak interactions, and tend to be lost in aqueous environment. Without consistence of any covalent bond and terminal group modification, the entangled

polymer chains could escape from NGs within time. The complete dissolution of hydrogels is expected to be observed with long term water absorption. It was observed that all samples with physical entanglements had lost network unity and dissolved after immersion in water for 3 days (Figure 9b). PEH30-0.37 and PEH30-0.75 showed the longest stability (3 days). PEH30-0.75 was able to absorb the highest degree of water, i.e. ~85 times. Changes in the NG (e.g. PEH30-1.5) and feed monomer concentration lead to a decrease in stability. PEH20-0.75 showed the lowest stability with a faster swelling rate, while PEH40-0.75 showed the highest stability. It can be concluded that the optimization of feed monomer ratio and NG amount, likewise PEH30-0.75, are required to achieve high swelling and long term stability. Finally, , entanglements in PEH have led to high stability compared to normal entangled hydrogels, which undergo fast disentanglement process in aqueous conditions.

The presence of long inter-connective polyacrylamide chains was also investigated. To analyze the molecular weight distribution of polyacrylamide chains which form entanglements and interconnectivity, PEH sample was exposed to long term swelling in water and the dissolved polymer solution was collected. Analysis by gel permeation chromatography (GPC) povided quantitative data for the molecular weight (Figure 10). The dissolved sample shows high molecular weights up to 10^7 g/mol (Figure 10a). Although dissolved sample consists of linear polymer chains and nanogels together, the fraction of nanogels is very low (e.g. 2 wt%) and therefore, the high molecular weights were assigned to the linear polymer chains. To confirm this, GPC characterization of NGs was also conducted for the comparison. The nanogels were dispersed in water and measured under the same experimental conditions. In this case, the maximum molar mass of $2x10^6$ g/mol was detected in the spectra (Figure 10b). The NGs had demonstrated clearly lower molecular mass values than PEH. According to these two data, it can be concluded that high molecular weight (10^7 g/mol) after dissolving PEH was obtained from the inter-connective polymer chains. The presence of such extremely long polymer chains would allow forming entanglements inside NG, and pass through several NGs to succeed the cross-linked network.

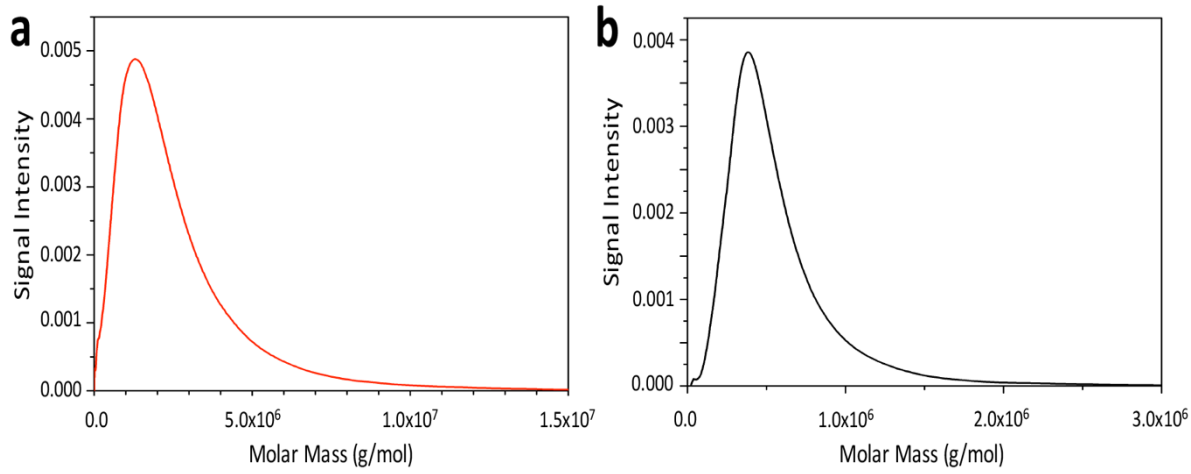

Figure 10. Molecular mass distributions, obtained from GPC a) dissolved PEHs b) NG

The obtained swelling data indicated that dynamic and sliding nature of physical entanglement crosslinking helps to achieve high degree of water presence inside hydrogel. In contrast, AA-MBA had a limited swelling capability. The morphological differences between physical entanglement and covalent crosslinking based hydrogels were also evidenced by scanning electron microscope (SEM) analysis of crossections of the hydrogels (Figure 11). The bulky matrix of hydrogels can be altered by water uptake. If the existence of water becomes great, huge morphological changes could be observed. As-prepared and swollen states of samples were characterized to see transformations with water uptake. In case of as-prepared PEH, the dense matrix with sporadic pores were monitored (Figure 11a). With an external swelling, the initial dense matrix had transformed to highly porous and inter-connective morphology. Moreover, the formation of very thin pore walls was detected (Figure 11b).

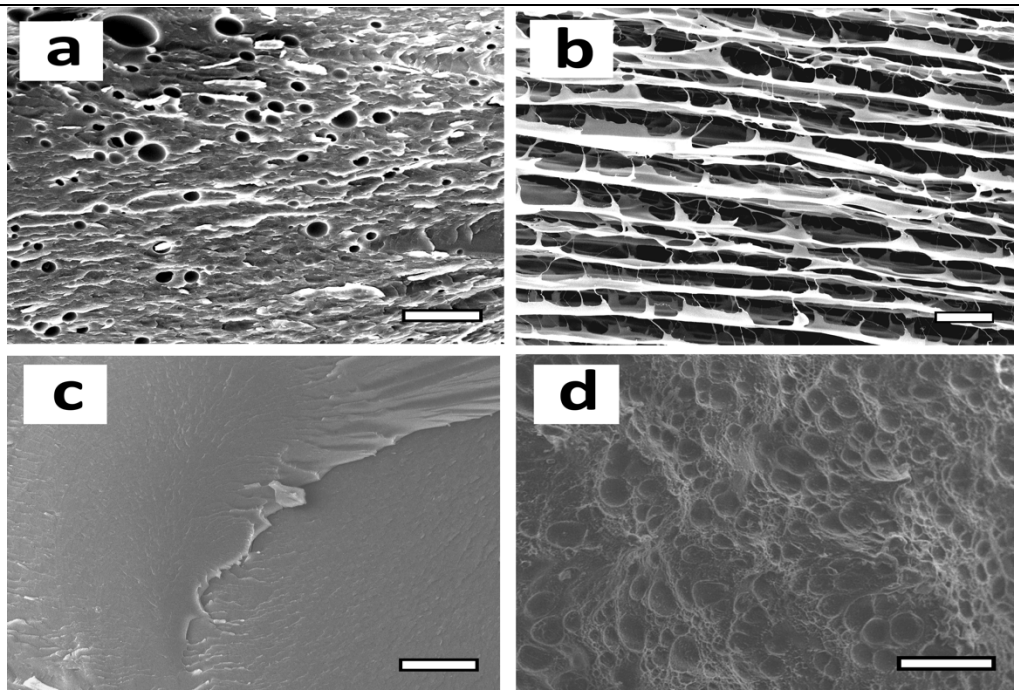

Figure 11. Cross-sectional SEM images of as-prepared and swollen hydrogels a) As-prepared PEH30-0.75 b) Swollen PEH with ~2 wt% polymer fraction c) As-prepared AA-MBA control hydrogel d) 24h swollen AA-MBA, which is only able to attain ~8 wt% polymer fraction. Scale bars are in (a), (c), (d) are 100 μm, that in (b) is 10 μm.

Nonetheless, the swelling induced network alterations of AA-MBA was very limited. In contrast to PEH, AA-MBA hydrogel displayed a dense bulky matrix without any pore formation (Figure 11c). Although external water was soaked in and polymer fraction reached to ~8 wt%, the xerogel morphology still indicated a very dense polymer matrix. Apparently, the non-dynamic covalent crosslinking had limited significant morphological changes (Figure 11d). When PEH and AA-MBA hydrogels were compared, the morphological characterization demonstrated self-optimization ability of PEH, which arise from its dynamic and sliding nature.

2.2.4. Mechanical Properties of Highly Swollen PEH

Firstly, mechanical properties of PEHs in swollen state were tested by simple demonstrations to show natural behavior of designed soft material. Following that, analytic characterization methods, such as rheology and compression tests, were performed. Before testing, PEH samples were immersed in water until reaching ~2 wt% polymer fraction. The comparison tests were

done by using AA-MBA, which contains ~8 wt%. The covalently crosslinked AA-MBA sample was only able to reach to this fraction after soaked in water for 24h.

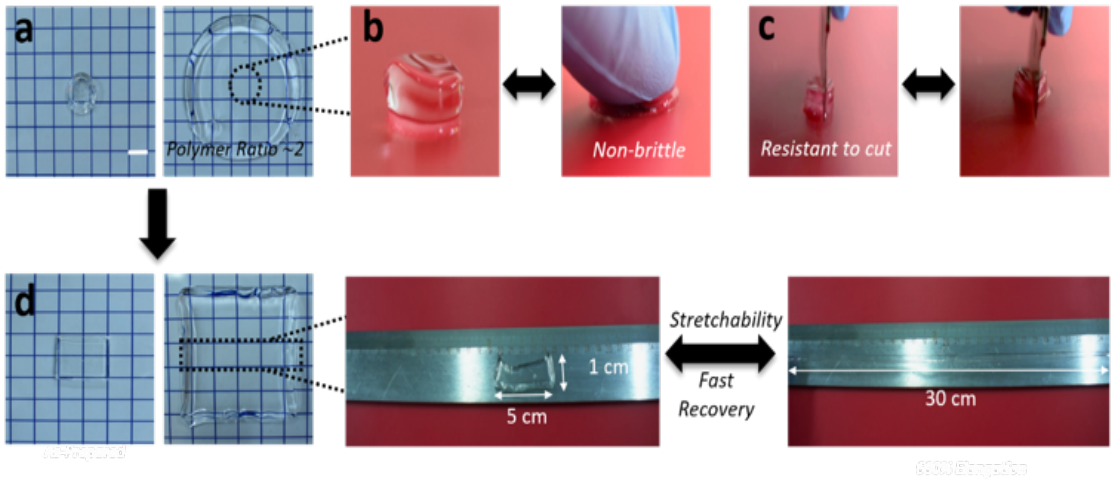

Figure 12. Demonstration of PEH mechanical properties a) Dried and swollen PEH30-0.75 samples. ~2 wt% polymer fraction is reached after 24h swelling. Scale bar is 1 cm b) PEH shows tough nature when compressed, and it can mostly recover initial shape after removal of force. c) Slipper nature of PEH helps to show cutting resistant behavior. d) As-prepared and swollen square shaped PEH. The initial shape is retained, even though very low polymer fraction is obtained. The swollen PEH can be stretched for 600% without showing any fracture. When force is released, initial form of hydrogel can be gathered in seconds.

Typically, achieving very low polymer fractions is challenging for conventional hydrogels. Even after it is succeeded, hydrogels with an excessive water absorbance mostly show brittle nature. The proposed physical entanglement crosslinking helped us to overcome these two limitations. The PEHs exhibited toughness and elasticity in highly swollen state (~98 wt%). They maintained a well-defined shape after swelling (Figure 12a, 12d). To show toughness of PEH, tea manueal compression test was operated by pressing with the finger. The hydrogel did not show any fracture after being compressed, and mostly recovered when the external applied force was released out (Figure 12b). The toughness was attributed to sliding nature of entanglements. The efficient energy dissipation in the network can be succeeded by dynamic movement of crosslinking mechanisms. One of the unique feature of PEH is showing resistance to cut. Highly swollen nature and dynamic network help to provide cutting resistance to normal force applications (Figure 12c).

Moreover, the gels showed high level of stretchability. The demonstration of stretching ability was only performed by a simple demonstration, since the slippery nature of the probe makes normal tensile test impossible. By simple manual stretching, ~6 times elongation was achieved (Figure 12d). Taking into account the low polymer fraction of these hydrogels (2 wt%), this stretchability represents one of the highest in the literature. To this date, one of the best stretchable hydrogel with high water content, which is synthesised by acrylamide and alginate networks, had showed ~21 times strecthing capability with 86 wt% water content (51). Therefore, ~9 times strecthability was obtained with slide-ring polyrotaxane crosslinking strategy. In this case, hydrogel had 78.5 wt% water content in its network (44). After release of stretching force, the elongated PEH recovered its initial length in seconds, indicating a fast recovery rate. The ability of extraordinary elongation and recovery rate was attributed to the lose sliding of entangled polymer chains in the NG. Even though some of polymer chains might be pulled out from the NGs by stretching, most polymers chains seem to remain entangled and maintain a crosslinked network during the stretching. The remaining entangled chains, which pass through several NGs, slide during deformation. The sliding of entanglements can re-organize the network when the stress is applied, and turn back to the original minimal energy state after withdrawal of the force. Polymer slidingafter releasing of the applied stress occurred in seconds time scale and, therefore, the energy favor state can be restored fast.

The rheological properties of hydrogels were characterized by frequency and strain sweeps. First of all, as-prepared hydrogels were subjected to the frequency sweep. In each sample, G' was greatly bigger than G'', which indicates well crosslinked network structure. Chnges in the NG concentration had a limited effect in the rheological properties of non-swollen samples (Figure 13a).

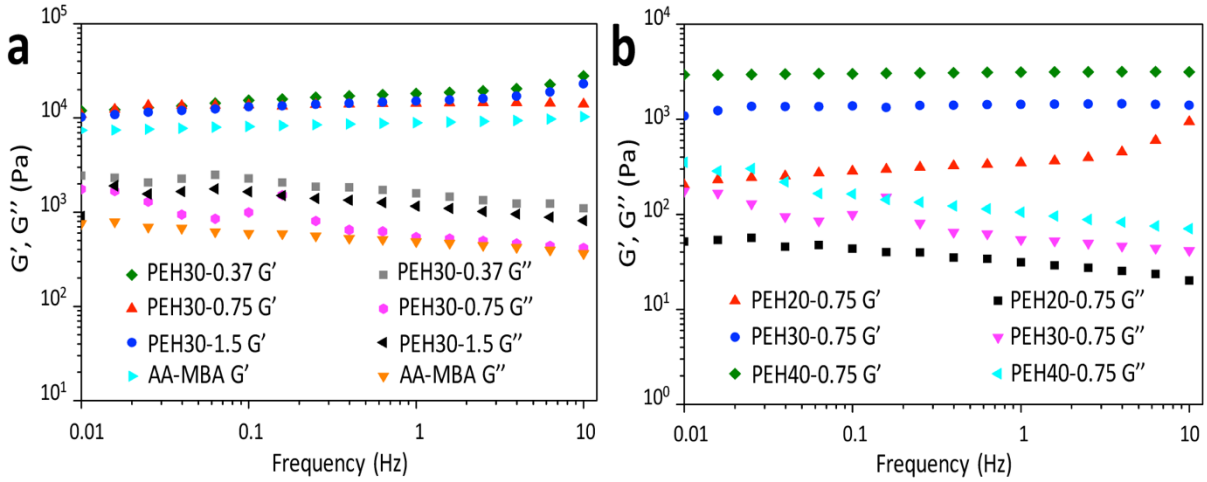

Figure 13. Frequency sweep of as-prepared hydrogels. a) NG concentration influence of rheological properties. b) Effect of initial monomer ratio on G' and G'' values.

In contrast, changes in the initial monomer amount lead to significant shifts in G' (Figure 13b). The highest G' value was shown by PEH40-0.75, with the highest monomer ratio. A dependency between the shear modulus and the monomer ratio was observed, with G' values of PEH20-0.75 being the lowest (Figure 13b). The swollen hydrogels (set to 2wt% polymer fraction) were also characterized by using a dynamic rheometer. The swollen PEHs exhibited storage modulus values (G') higher than the loss modulus (G''), even after 98% water uptake. For instance, the G' of the PEH30-0.75 decreased from ~10^4 Pa to ~10 Pa by water uptake.

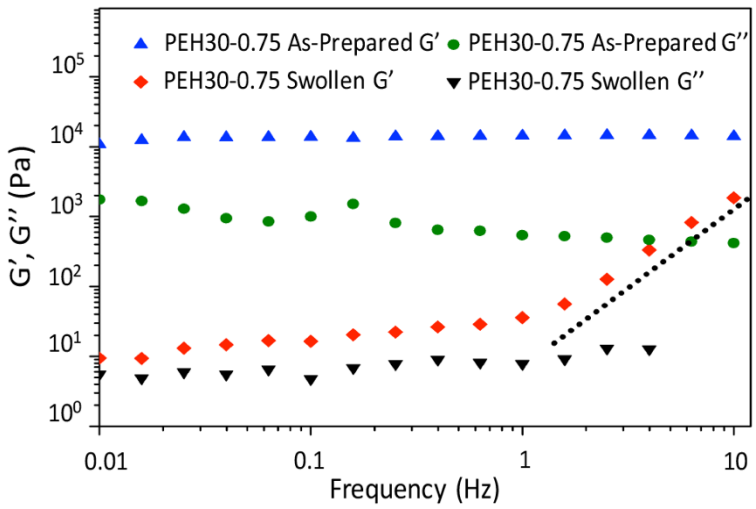

Figure 14. Frequency sweep comparison of as-prepared and swollen PEH30-0.75, shows swelling-induced clear change in G' profile.

Moreover, the swollen PEHs demonstrated an interesting increase in G' with frequency (Figure 14). Such increase was not observed in swollen covalently crosslinked AA-MBA. A sharp increase of G' was observed in swollen PEH after a critical frequency level (Figure 15a). All gels showed a similar profile, although the critical frequency slightly varied with the NG and monomer concentrations. The sharp increase of G' was detected at frequencies > 1Hz (Figure 15b). This stiffening of the gel with frequency can be interpreted on the basis of the dynamic and sliding nature of entanglement crosslinking. If the frequency of the external mechanical stimulus is higher than the time scale of the sliding mechanism, the entangled NGs would act as a non-movable crosslinking points, which leads to stiffening of hydrogels.

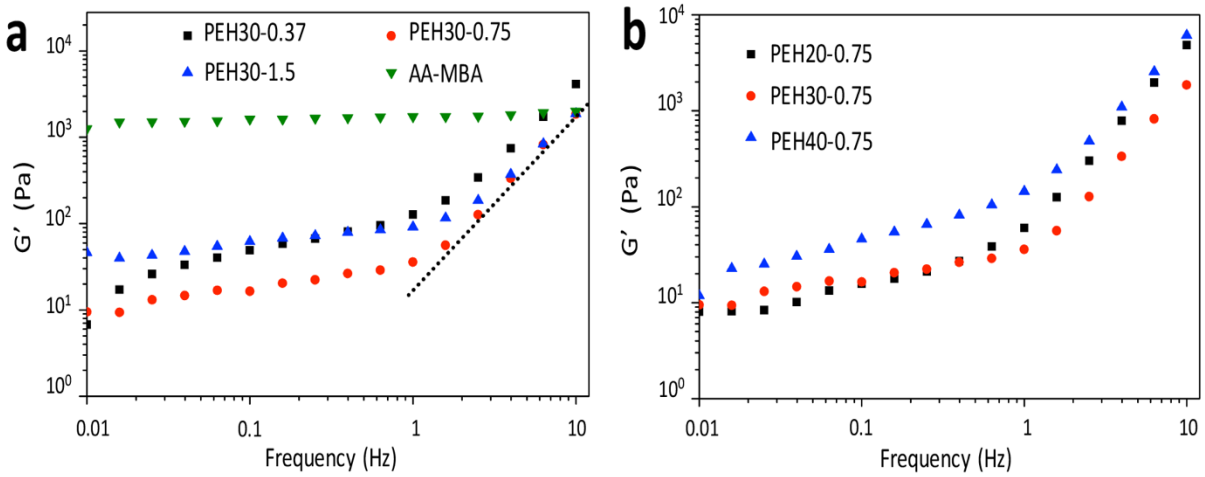

Figure 15. Frequency sweep of storage modulus, obtained from different swollen PEHs, Polymer fraction was set to 2 wt% before the measurements. a) Variance of NG amount and AA-MBA to indicate crosslinking effect b) Initial monomer feed influence of G' profile.

Strain sweep tests were also performed. PEHs and AA-MBA showed a strain thinning behaviour in the swollen state (Figure 16a, and 16b). When the strain reached a critical level, a decrease in G' values was observed, indicating a disruption and deformation of the hydrogel network. The required critical strain rate for deformation was lower in AA-MBA. This behavior is consequence of the non-dynamic nature of covalent crosslinking, which provides limited energy dissipation in the polymer network.

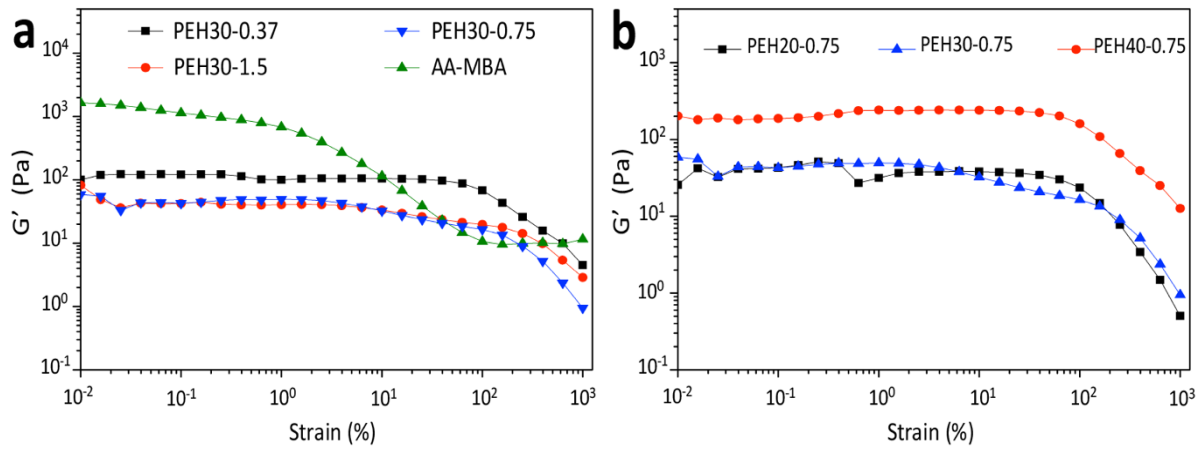

Figure 16. Strain sweep profile of hydrogels, in swollen state. a) NG concentration and covalent crosslinking dependency of strain-thinning nature. b) Alterations of G' by supply of different monomer concentrations.

In contrast, PEHs with sliding crosslinking were able to sustain the network unity up to higher rates. The data demonstrated that sliding entanglements can distribute the external forces in an efficient way, and prevent disruption of network at mild level of strains. On the other hand, critical strain to trigger deformation can be slightly varied by diversify the constituents, such as NG and initial monomer concentration.

For further investigation of mechanical properties, axial compression tests were performed to test toughness of PEH, and compared to AA-MBA control sample, as well (Figure 17, and 18). The compression test was performed for 2 min., and swollen hydrogels were used. In the exposed time range, limited compression of AA-MBA, with a maximal ~55% strain, was received, while PEHs were compressed up to 90% compressive strain without showing any fracture (Figure 17, and 18a). The compressive of modulus of control sample was ~100 kPa, which was greatly higher than modulus of PEHs (~1kPa). The rigid nature of MBA based on the covalent crosslinking had caused to observe such a high value of compressive modulus. Although crosslinking degree is undoubtedly low, AA-MBA hydrogel still exhibits a stiffer nature. In contrast, the weak interactions of physical entanglements facilitate to gather a softer hydrogel nature. Moreover, it should be denoted that hydrogels normally become brittle after absorbing such a great water content (98 wt%), but the designed entanglement crosslinking strategy overcomes this limitation of hydrogels.

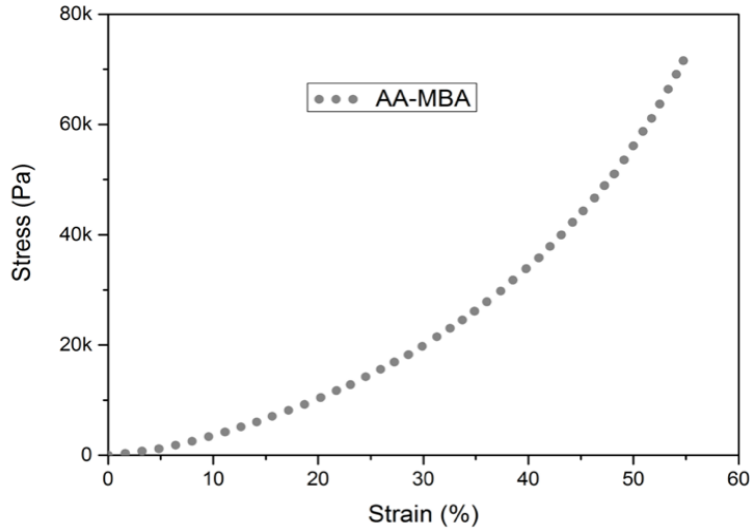

Figure 17. Compression graph of covalently crosslinked swollen AA-MBA hydrogel, which consist of 8 wt% polymer fraction).

In addition, the compression behavior of PEHs as function of feed monomer and NG concentrations was studied. Interestingly, PEH30-0.75 (modulus: ~1kPa) had shown a higher modulus than PEH20-0.75 (modulus: ~200 Pa), and PEH40-0.75 (modulus: ~500 Pa). It was attributed to the different swellability of hydrogels. PEH40-0.75 needs to be swollen for longer time (Figure 9) to reach 2 wt% polymer fraction, when compared to PEH30-0.75. In this case, loss of higher number of polymer chains is possible during the swelling. They could escape from the network, and cause to a softer mechanical property. The modulus of PEH20-0.75 is in agreement with this hypothesis. According to long term swelling data (Figure 9), PEH20-0.75 swells and loses the network unity faster, and 2 wt% set polymer fraction is very close to the critical dissolving point of it. As a result, the softest hydrogel nature was obtained in case of swollen PEH20-0.75 (Figure 18b).

No significant influence of NG, which act as crosslinker, on the compressive modulus was observed. PEH30-0.37, PEH30-0.75, and PEH30-1.5 showed similar values of the compression modulus (~1kPa). This result is controverse to most other hydrogel systems. Usually, changes in the crosslinker ratio lead to stiffennign or softening of the hydrogel. In PEHs the NG concentration did not affect the compression modulus (Figure 18b).

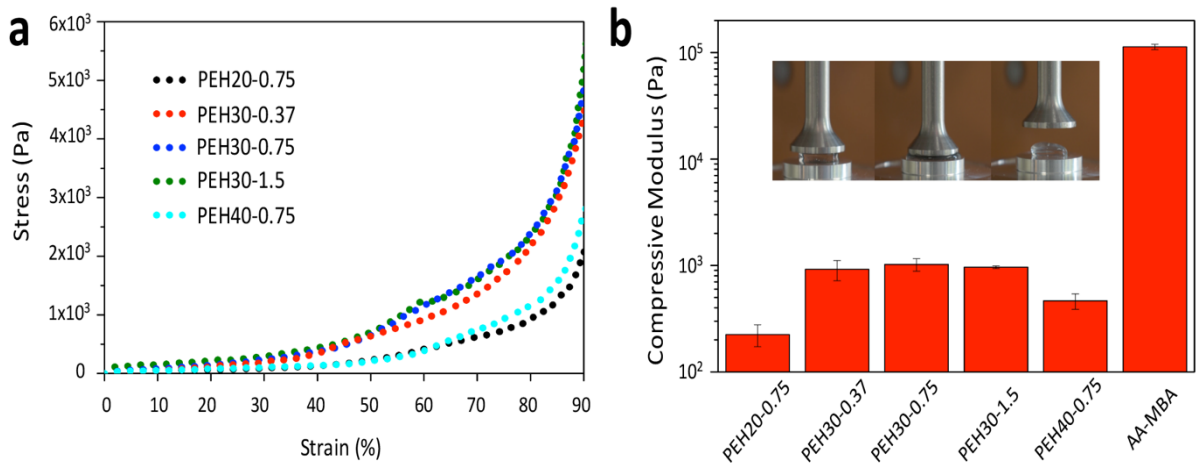

Figure 18. Compression graphs of swollen PEHs. Before test, PEH was swollen until reaching 2 wt% polymer fraction. AA-MBA with 8wt% polymer fraction was used, since its swelling capacity is limited. a) Compression graphs of PEH b) Average compressive modulus of each hydrogel.

2.2.5. Self Organization of PEH

Free sliding of entanglements suggested to provide an interesting feature, based on self-organization, to hydrogel. Lyophilization of hydrogels is relevant for pore formation inside bulky hydrogel matrix. The pore size and swelling ratio of hydrogel can be tuned by such a simple method. For this reason, it is utilized for several applications, including biomaterials, food and pharmaceutical industry etc. Lyophilization occurs in two steps: formation of ice crystals and sublimation. The ice crystals induce the creation of pores in the hydrogel structure (90, 91). However, lyophilization process leads to loss of mechanical properties in most covalent hydrogels. The growth of crystals stretches the constituent polymer chains and breaks the covalent crosslinks if the network has no dissipation or reorganization ability. When ice crystals destroy the polymer chains and the crosslinked network, the hydrogel becomes brittle, and eventually totally destroyed. Entanglement crosslinked hydrogels could offer some advantages for lyophilization due to their dynamic and sliding behavior (Figure 19). PEH was expected to permit the growth of ice crystals without undergoing any permanent damage in the polymeric network. To test this property, PEH samples were lyophilized and re-hydradited and their mechanical properties were tested.

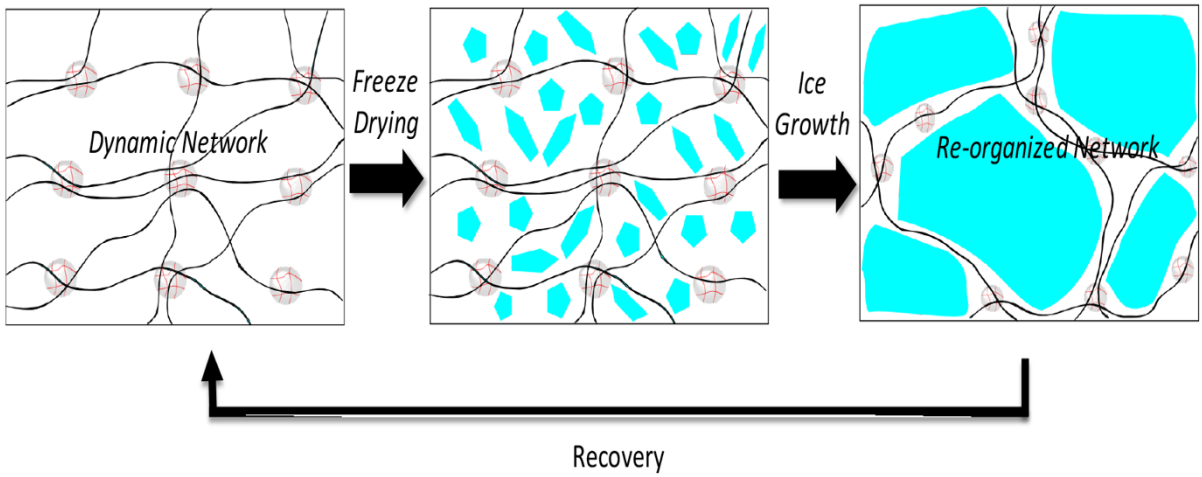

Figure 19. Schematical demonstration of suggested self-reorganization process concurrently with lyophilization process.

Rheology experiments by frequency sweep were performed (Figure 20, and 21). PEH hydrogels were lyophilized and then soaked in water for 24h. PEH gels not lyophilized and swollen for 24 hours were used as control samples. Covalently crosslinked AA-MBA hydrogels were also used to compare with the dynamic hydrogel samples. The shear modulus G' was measured within 0.01-10 Hz frequency range (Figure 20). A significant decrease of G' was observed in covalently crosslinked AA-MBA afterliophilization. This results confirm the loss in the mechanical properties due to the destroy of covalent crosslinking during crystal formation and growth. As a result of rigidly crosslinked polymer chains, hydrogels networks cannot reorganize and mechanical load cannot be dissipated. In contrast, G' did not change in PEH samples after liophilization. Entanglement crosslinking helps to obtain dynamic network and reorganization. It was attributed to free sliding ability of physical entanglements. The entanglements could move freely, when crystal growth is triggered. The location of NGs, which act as a crosslinker, can be re-organized to prevent break of polymer chains.

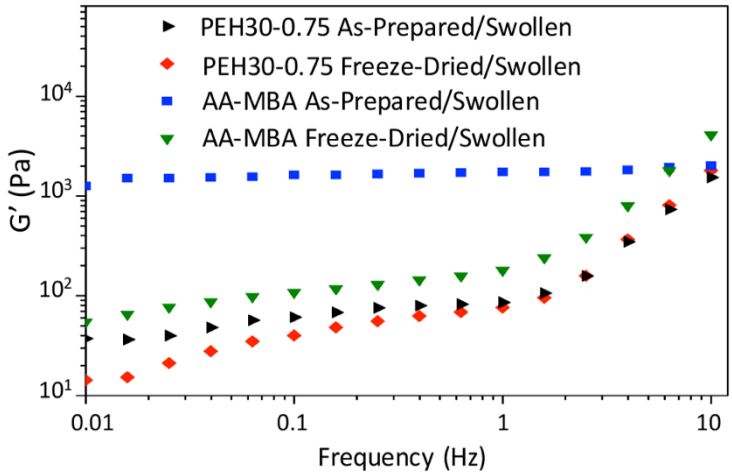

Figure 20. Storage modulus profiles of 24h swollen PEH30-0.75 and AA-MBA before and after lyophilization.

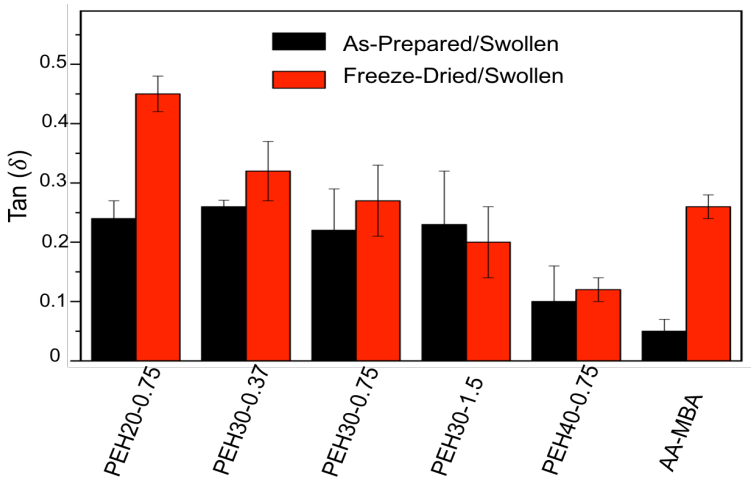

Figure 21. The tan(δ) (G"/G') at 1 Hz of all sample groups to investigate self-organization capability during freeze drying. 24h swollen hydrogels before and after lyophilization were compared.

The tan(δ) values were also collected for the evaluation of viscoelasticity change after the lyophilization process (Figure 21). Before the lyophilization, AA-MBA hydrogel had the lowest tan(δ), as expected from a crosslinked and stable network architecture. PEH showed higher tan(δ). The lyophilization process changed the viscoelasticity of both hydrogels. A significant increase in the tan(δ) (from ~0.05 to ~0.25) was observed in AA-MBA, indicating a loss in elasticity as consequence of the disrupted network and increase of G". In contrast to the covalent crosslinked network, the physical entangled PEH samples underwent a small change in tan(δ)

after lyophilization, except for PEH20-0.75. The tan(δ) value of PEH20-0.75 had an important boost, which was from ~0.25 to ~0.45. The increase in tan(δ) is attributed to entanglement presence in the network. In the case of PEH20-0.75, decrease in entangled polymer chains is expected, compared to PEH30-0.75, and PEH40-0.75. The less initial monomer concentration may lead to fewer entanglements, which cannot be efficient to sustain network unity during lyophilization process. Following that, viscosity is increased. The NG ratio also alters the viscoelasticity of polymer network. It was found that PEH30-1.5 had the lowest tan(δ) value, and its viscoelasticity is improved after liophilization-rehydration process. In contrast, PEH30-0.37 and PEH30-0.75 had demonstrated increase in tan(δ), which could be due to having not enough nanogel presence to regulate whole network. By increasing NG concentration, the network can re-organize more efficiently, and the decrease of tan(δ) can be observed.

2.3. Discussion

In overall, the designed strategy of entanglement crosslinking was a facile method to synthesis dynamic hydrogel networks using nanogels. Note that PEH were fundamental different from nanogel surface-polymer interaction based hydrogels, although nanogels behave as crosslinking points in both systems. Entanglement interaction was utilized in PEH, which was weaker and show a sliding nature, compared to other physical interactions that are used for nanogel surface interactions. For this reason, PEH would dissolve in water after swelling in water for several days, since entangled polymer chains slipped out from nanogels. In contrast, nanogel surface-polymer interaction should be stable in swelling such that stable hydrogels should present, even when physical self-assembly was used for crosslinking mechanism (11). It is also found free-sliding entanglement interaction led to nanogel fraction-independent swelling and mechanical properties in PEH. In case of nanogel surface-polymer interaction based hydrogels, swelling behavior and mechanical properties are dependent on the fraction of nanogels, since crosslinking interactions are enhanced by increase of nanogels. Therefore, stiffening behavior is commonly observed with enhancing nanogel fraction in such hydrogels (11) because the increase of nanogel fraction can lead to denser crosslinking degree with polymer-nanogel surface interaction.

PEH was able to form a polyrotaxane-like sliding crosslinking mechanism with reaching to very high water uptake ratio, and keep its good mechanical properties. Polyrotaxane hydrogels are formed with a small molecules (i.e. cyclodextrins) in angstrom level sizes. In contrast, PEH

is constructed by nanosize particles, which allow to form and control cluster of polymers inside. Ordinary, reaching to 98 wt% water uptake is very challenging for the most of the hydrogels, and polyrotaxane hydrogels, as well.Therefore, their mechanical properties are mainly lost even such level of water uptake is succeeded. Note that high polymer fractions, such as 10 wt%, are needed in case of the toughest hydrogel systems (24). In case of polyrotaxane hydrogels, the polymer fraction would be even higher more than 20 wt% (44). In terms of PEH, it can succeed to overcome such limitations. The hydrogel has demonstrated good toughness, resistance to cut and stretchability (~6 times) in 98 wt% swelling ratio. Considering these results, it can be concluded that physical entanglement strategy enables advantages in terms of network optimization to level up absorption and stress distribution. The stress distribution is contributed from polyrotaxane-like sliding crosslinking points and high molecular weight of polymers (up to 10^7 g/mol). In terms of typical covalently crosslinked hydrogels, reaching to such molecular weights is not possible, since crosslinkers would directly undergo copolymerization with the monomers, and block the long polymer chain growth. Therefore, polyrotaxane hydrogels require end-capping process that also limits the long chain polymer formation.

In addition, PEH shows a crosslinking-independent swelling behavior, which means that swelling ratio doesn't change by altering nanogel amount that behaves as crosslinking points. It is well-known, if crosslinking degree is increased, water uptake ability is limited in terms of typical hydrogels. The nature of PEH is controversy to this due to its moveable nanogel crosslinking points and dynamic entanglement free-sliding among long polymer chains. Constant value of swelling can be received, even though nanogel presence is altered. One of the interesting PEH behavior was frequency-dependent G' increase. G' value of PEH shows a sharp increase after a critical frequency value (~ 1 Hz). The dynamic nature of entanglement crosslinking triggers a very sharp stiffening effect by increase of frequency. Such a sharp increase is not contributed from nanogel presence in the network, it is directly contributed from physical entanglement crosslinking. The presence of nanoparticles would only trigger slight increases during frequency-sweep. Lastly, self-organization capability of PEH crosslinking was launched. With the help of this property, the mechanical properties of PEH can be recovered following the lyophilization-rehydration process. The dynamic crosslinking points can self-organize themselves in the polymer network during ice formation, and prevent damages in the crosslinked network. Following that, G' value doesn't demonstrate important changes. This property can be used in different fields to form porous hydrogels with keeping good mechanical properties at the same time.

2.4. Summary

In summary, a new design of physicaly crosslinked hydrogel was developed by exploiting polymer entanglements. PEH were fabricated by one-pot polymerization in the presence of nanogels. The NGs provide confined environments to absorb monomers and initiators, which were then in-situ polymerized to form a hydrogel. The newly-formed polymer chains can form entanglements with the polymer chains of NG, and pass through multiple NGs. Subsequently, a polymer network is constructed. Polyacrylamide-based PEHs with cluster entanglements are strong enough to keep well-defined hydrogel shapes. Moreover, it allows to free sliding of polymer chains, which contributes to dynamicity and good mechanical properties, even in highly swollen state. As a result, hydrogels with appealing properties were obtained. Firstly, soft and tough PEHs at very low polymer fractions (<2 wt%) were successfully realized. A crosslink-independent swelling ratio, up to 98 wt%, was gathered. In other words, when nanogel amount is increased, swelling ratio is not decreased as expected in conventional hydrogels. The shear modulus (G') of the hydrogels was regulated by the NG concentration. The reorganizable nature of physical entanglement crosslinking enabled resistance against mechanical property lose during lyophilization. With all these results considered, the cluster entanglement strategy represents a new approach for the design of stable high swollen hydrogels for various applications.

2.5. Materials and Methods

2.5.1. Materials

Acrylamide (⩾99%) (AA), ammonium persulfate (APS), N,N'-methylenebis(acrylamide) (MBA), dioctyl sulfosuccinate sodium salt (AOT), n-Hexane, and tetramethylethylenediamine (TEMED) were purchased from Sigma-Aldrich and used as received.

2.5.2. Synthesis of Polyacrylamide Nanogels

The synthesis of NGs succeeded by emulsion polymerization. Firstly, 1.59 g AOT surfactant was homogenously dissolved in 42 ml n-Hexane, and purged by N_2 for 10 min. Following that, 0.527 g acrylamide monomer and 0.15 g MBA crosslinker was mixed in 1.7 ml distilled water. The solution was supplied into main n-hexane phase to form the emulsion. Continuous stirring was conducted at room temperature (25 °C) for 30 minutes. To initiate the polymerization, 30µl of APS (100 mg/ml) solution, and 15µl TEMED were added into the emulsion. The polymerization was conducted for 2h with 900 rpm stirring (IKA RCT basic). Subsequently, excessive

n-hexane solvent was discarded via open-air evaporation. The remaining product was washed with ethanol, and centrifuged for 3 times to get rid of leftover surfactant and unreacted chemicals. Afterwards, the collected material was let to dry at room temperature before used in following procedures.

2.5.3. Preparation of Physical Entanglement Hydrogels

The fabrication of hydrogels was succeeded by using a simple free-radical polymerization. Previously synthesized NGs were provided into solution state to form crosslinking points with the help of polymer entanglements. In a typical process, 0.0023g NG (0.75 wt% of monomer) were supplied in 1 ml distilled water, and sonication was applied in ultrasonic bath (Bandelin Sonorex, 35 kHz, 80W) until NGs are totally dispersed. The dissolved O_2 was removed from the solution by N_2 purge for 5min. Following that, 0.009g of APS initiator was fed into solution and stirred for 30min at room temperature under N_2 environment in a sealed 10 ml glass vial (25 °C). In the last step, 0.3g acrylamide monomer was added into mixture, and kept at room temperature in a sealed vial for the gelation process.

As a control sample, covalently crosslinked acrylamide hydrogel, with consisting of long polymer chains, was synthesized. For the synthesis, 0.3g acrylamide, and 0.0001g MBA crosslinker dissolved in 1 ml distilled water. Before addition of the initiator, the solution was deoxygenated by N_2 flow for 5 min, and then 0.009g APS was supplied. The prepared solution was casted on a mold with 2 mm depth, and covered with a glass slide to avoid oxygen infusion. The gelation was accomplished at room temperature (25 °C).

2.5.4. Characterization of Nanogels

Following synthesis and washing steps of the NG, the chemical composition and existence of unsaturated residues of MBA crosslinker on the NG surface was inspected by ^{1}H NMR. Prior to analysis, the dried NGs were dispersed in methanol, and supplied into 5 mm NMR tubes. The ^{1}H NMR spectra was recorded on a Bruker 300 MHz (Rheinstetten, Germany) nuclear magnetic resonance equipment using methanol as the solvent. Chemical shifts were reported using the solvent as the reference, and the spectra was recorded at room temperature.

The average size of synthesized polyacrylamide NGs, and their size distribution were investigated by using dynamic light scattering (DLS). The dried NGs were dispersed in water at a

concentration of 1 mg/ml , and subsequently sonicated for 5 min in ultrasonic bath (Bandelin Sonorex, 35 kHz, 80W). Then, the NG solution was supplied into polystyrene cuvette, and the immediate analysis was performed. The measurement was studied with Malvern Zetasizer Nano ZS (Massachusetts, USA) equipped with a He-Ne light source (k=633 nm, 4 mW). The measurements were performed at a detection angle of 90°, and room temperature (25 °C). Size distribution of nanogels were gathered by considering number weighted analysis.

Morphological characterization of the NGs was performed with transmission electron microscope. TEM measurements were performed with a Jeol (Akishima, Tokyo, Japan) JEM-2100 microscope, including LaB6 cathode and operating at 200 kV. Ethanol was used as the solvent to disperse dried NGs by exposure of ultrasonication (Bandelin Sonorex, 35 kHz, 80W) for 5min. Prior to the imaging, 10 µl volume nanogel solution (1 mg/ml) was casted onto a copper TEM grid covered with a perforated carbon film. Following that, solution was evaporated at room temperature (25 °C). The average size of nanogels were calculated using ImageJ software.

2.5.5. Characterization of Hydrogels

Water-uptake capacity of all groups of the fabricated hydrogels were tested by considering weight change. As-prepared and freeze-dried hydrogels were soaked in distilled water, and their weights were measured after a certain timeframe (24h). All swelling assessments were performed at room temperature, and the swelling and polymer ratio were defined by following formula:

$$Swelling\ Ratio(\%) = \frac{Wswollen - Wdry}{Wdry} \times 100$$

$$Polymer\ fraction\ (\%) = \frac{Initial\ Monomer\ Amount(\%)}{W24h\ swollen(\%)} \times 100$$

The cross-sectional morphology of hydrogels was studied with employing scanning electron microscope (SEM, Quanta FEG 400, Thermo Scientific, Dreiech, Germany). Swollen and as-prepared bulky matrix formations of hydrogels were observed to realize porosity differences, induced by water absorption. The prepared hydrogels first immersed in a liquid nitrogen, and subsequently freeze-dried at −43 °C. 0.1 Pa vacuum power was exposed for 24h, during

freeze-drying. Before the imaging, the freeze-dried samples were coated with gold. The accelerating power of 30 kV and high vacuum mode was used to perform the imaging.

Rheological properties and compression tests of physical entanglement hydrogels were tested in a rheometer (TA Instruments, HR-3, USA), equipped with a temperature controlled Peltier plate. All measurements were performed at 25 °C, and controlled during the experiments. The upper plate of 12 mm was preferred, and as-prepared/swollen hydrogels were punched with 12 mm size. For rheological experiments, the gap distance was arranged at 2 mm. The dynamic frequency sweep was done between 1-10 Hz, and 0.1% strain rate. The strain sweep tests were performed between 0.01-1000% rate, with an application of certain frequency amplitude (1 Hz). To understand compressive behavior of hydrogels, time-dependent compression tests were performed. The 20 mm size upper plate was deployed and as-prepared and swollen hydrogels (2 wt% polymer ratio) were cut with 12 mm diameter puncher. The gap between plates was set to 2.5 mm, prior to compression. As a loading force, 10N was used and compression process had been conducted for 2 minutes. The compressive modulus of each hydrogel was gathered by considering stress value changes between 10-40% strain levels.

The molecular weight distributions of hydrogel constituent polyacrylamide chains were evaluated with gel permeation chromatography (GPC), performed on Agilent 1100 series (Palo Alto, USA) Series with RI-Detector. PSS-SUPREMA LUX Column with polystyrene standard was used as the reference. Before the measurement, hydrogels were immersed in distilled water for a long term swelling, and dissolved after a while. The concentration of dissolved product was set to 4 mg/ml by removing out the extensive water. The acquired polymer solutions were injected with 20 μl volume, with 1ml/min flow rate. Mobile phase of 0.1 M NaCl and 0.3 v/v% TFA were used for the GPC measurement. Moreover, nanogel molecular weights were evaluated by performing same measurement protocol.

Chapter 3: Manipulation of Entanglement-based Crosslinking via Temperature

3.1. Introduction

Stimulus-responsive polymeric hydrogels undergo changes in their physical and chemical properties in response to external stimuli. These kind of materials are advantageous for different applications, including controlled drug delivery, selective membranes, sensors, actuators, etc. (2, 92). The change of hydrogel property is principally based on collapse or expansion of the constituent polymer chains. The change in the polymer chain conformation causes alteration of physical properties, such as water uptake capacity and stiffness. Responsive hydrogel matrices are mostly non-dynamic polymeric networks. Thermoresponsive hydrogels allow dynamic manipulation of hydrogel stiffness triggered by water release or uptake upon temperature changes, which os accompanied by significant volume changes in the hydrogel sample. In this study, PEH designs will be exploited to design hydrogels able to stiffen in response to temperature, but without undergoing a size change.

Hydrogels can be synthesized to respond to the specific external stimuli, such as temperature, mechanical stress, pH, light, magnetic force, etc. (93, 94, 95). For this aim, the crosslinking of specific kinds of polymers, which are able to respond to either single or multiple stimuli, are used to build up hydrogels. Most of the responsive polymers, without any modification, can only change their conformation upon exposure to an individual stimulant. If the polymer chains are modified with extra functional groups, miscellaneous features could be incorporated into the hydrogels (96). The temperature responsiveness of hydrogels has been attained great attention in research, since it provides easy control of phase transition and dynamic response. Numerous examples of thermoresponsive polymer systems have been developed to construct hydrogels (97). The thermoresponsiveness of a polymer can be classified in two sub-groups: polymers with a lower critical solution temperature (LCST) and with an upper critical solution temperature (UCST). In case of heating/cooling exposure, these sub-groups response in a contrary way, since phase transitions of polymers are unlike. If a polymer becomes insoluble by heating to a certain temperature, it is characterized as LCST. In contrast, the solubility of UCST polymer in a solvent increase upon the heating (98). The phase transitions arise from the balance of hydrophilicity and hydrophobicity of polymer chains at existent conditions. In the LCST the hydration of polymer chains is enormously decreased by heating, and the balance shifts to the hydrophobic side. The most well-known and used thermoresponsive polymer with showing LCST behavior is poly(N-isopropylacrylamide) (PNIPAM) (99). The phase transition of

PNIPAM polymers occurs at around 32 °C. At this temperature, the hydrophilic nature of polymer chains turns into hydrophobic state, due to the significant coil-globule chain transformation.

Hydrogels constructed by crosslinked PNIPAM are also able to show LCST behavior, and a sharp phase transition can also be triggered at 32 °C. This property makes PNIPAM attractive for biological applications (e.g. drug delivery), since this polymer is biocompatible and its LCST is close to body temperature (100). The tuning of LCST is posible by simply copolymerization and substitution of alkyl groups of PNIPAM. Various copolymers of PNIPAM with tunable LCST have been presented in the literature. For instance, LCST values of poly(N-isopropylacrylamide-co-acrylic acid) P(NIPAM-co-AA) hydrogels undergo phase transition at 37.7 °C at pH 5., while the phase transition of PNIPAM at 32 °C at this pH (101). Larger shifts of LCST are also achievable. For instance, copolymers of PNIPAM and ionic liquids show higher LCST, i.e. PNIPAM-co-POMlmAc and PNIPAM-co-PHMImAc have LCSTs at 50 °C and 90 °C respectively (102). However, the incorporation of ionic liquid monomers containing hydrophobic side groups and counter anions leads to difficult phase transition. Alternatively. tunable LCST can be also be achieved by interpenetrating network designs. A tunable LCST Al-alginate/PNIPAM hydrogel had a transition between 22.5-32 °C, dependent on Al^{3+} cation concentration that regulates the crosslinking degree of alginate (103).

By considering temperature induced swelling and de-swelling feature, researchers have developed several hydrogels, which are able to change their stiffness, simultaneously. In principle, the water abundance in polymer network is altered with the conformational changes of polymer chains. In case of water release, the stiffening of hydrogel is received, while water uptake induces the softening. The water release out and stiffening relation can even be obtained by using simple hydrogel crosslinking chemistries, such as PNIPAM-PEGDA and PNIPAM-BIS (61). One of the best thermoresponsive stiffening hydrogel was developed by Xia *et al.,* by the incorporation of PNIPAM polymer network and NGs. The designed network shows a rapid response to temperature, and induces the enhancement of Young's moduli (~5 times). The improvement of mechanical property is succeeded after being shrunk ~10 times to the initial hydrogel size (62). Moreover, grafted PNIPAM hydrogels are also able to undergo such transformations. The covalently crosslinked PNIPAM and poly (N,N-dimethylacrylamide) hydrogel

can be stiffened, when heating is performed. The researchers have shown that mechanical property of such hydrogel was enhanced up to 7.7 times, if temperature is increased from 20 °C to 60 °C (104). However, it should be noted that hydrogel de-swelling is observed by increase of temperature. In addition to these, it was reported that semi-IPN hydrogels, which were built up from PNIPAM and polyacrylamide, were able to increase their stiffness (105). Above 32 °C, PNIPAM chains tend to collapse and trigger water releasing. Dependent on the PNIPAM fraction, the swelling ratio could be reduced up to ~20%, and induces hydrogel size changes. Subsequently, hydrogel stiffening, from ~100 kPa to ~120 kPa, was achieved.

Although inducing stiffening of hydrogels have been demonstrated by several researchers, all reported strategies involve dimensional changes, based on water uptake and release. In this case, the polymer fraction in the network is also altered. Responsive hydrogels that preserve the initial water existence and the size after the transition is challenging. Moreover, responsive behavior is mostly achieved in stimulus-responsive hydrogels with high polymer content. This chapter describes how PEH designs can achieve responsive behavior without dimensional changes. For this aim, a PNIPAM based PEHs were used, which incorporated sliding NG in an entangled polymer matrix. When the shrinkage of NGs was induced, the free sliding of entangled polymer chains would be blocked due to the restricted space in NGs network. 1 wt% of stimulus-responsive component is enough to observe a stiffening phenomenon. Therefore, it is supposed that significant water release would not be triggered, and the initial hydrogel size can be preserved.

3.2. Results

3.2.1. Synthesis of Thermoresponsive PEH

In this study, thermoresponsive PEH (TPEH) was synthesized by using the method described in Chapter 2. For this aim, thermoresponsive PNIPAM NGs without unsaturated vinyl group were incorporated, and polymer entanglement "cluster" was formed inside the NGs by using acrylamide monomer (Figure 22). The formed polyacrylamide chains pass through porous structure of NGs, and form inter-connective long chains to sustain hydrogel unity. Therefore, they are able to show free sliding behavior. By switching temperature, size of PNIPAM NGs can be tuned, due to its stimulus-responsive nature. In this case, the sliding of entangled polymer chains in PNIPAM NGs can be controlled, and the change in mechanical properties was aimed without changing swelling ratio of TPEH.

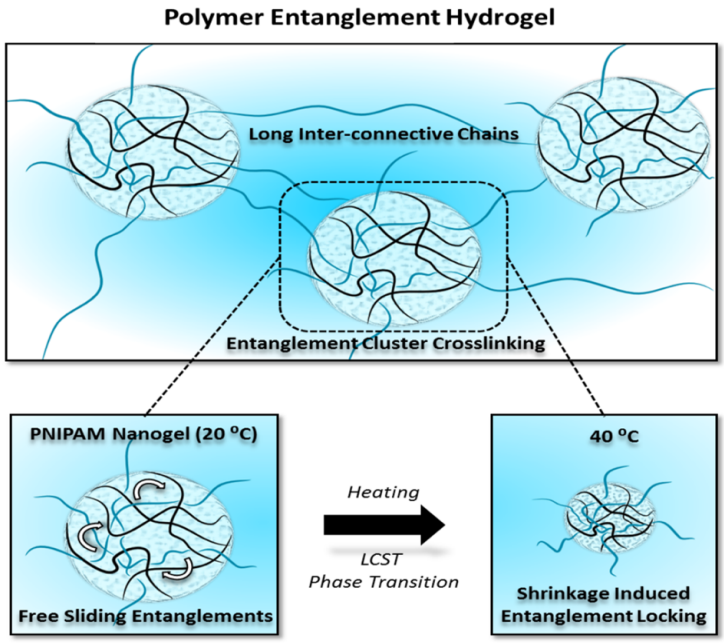

Figure 22. Schematical demonstration of physical entanglement crosslinking based hydrogel, and locking of entanglement sliding. When hydrogel is heated from 20 °C to 40 °C, PNIPAM NGs shrink and free movement entanglements are limited.

For studies, different ratios of monomers (20-40 wt%) and NGs (1-5 wt%) were supplied into the solution state for in-situ gelation, and thermoresponsive nature of each was investigated (Table 2). All concentration groups, except for 20 wt% monomer ratio, were successful to form the hydrogel.

Table 2. Chemical compositions of fabricated TPEHs

Sample Code	Monomer (Acrylamide)		PNIPAM NG		Initiator (APS)		Water
	Ratio/Amount		Ratio/Amount		Ratio/Amount		
TPEH20-1	20 wt%	0.2g	1 wt%	0.002g	3 wt%	0.009g	1ml
TPEH30-1	30 wt%	0.3g	1 wt%	0.003g	3 wt%	0.009g	1ml
TPEH30-2.5	30 wt%	0.3g	2.5 wt%	0.0075g	3 wt%	0.009g	1ml
TPEH30-5	30 wt%	0.3g	5 wt%	0.015g	3 wt%	0.009g	1ml
TPEH40-1	40 wt%	0.4g	1 wt%	0.004g	3 wt%	0.012g	1ml
AA-MBA	30 wt%	0.3g	0.03 wt% MBA	0.0001g MBA	3 wt%	0.009g	1ml

3.2.2. Characterization of PNIPAM Nanogels

The physical and chemical properties of the synthesized PNIPAM NGs were first characterized by several techniques. Firstly, the average size and size distribution of the NGs were investigated by DLS (Figure 23). Initially, the measurements were conducted at 20 °C, in an aqueous environment. The average size at this temperature was 133±74 nm. It should be noted that NGs are in fully swollen state under this condition. When the temperature was increased to 40 °C, a fast phase transition with significant size decrease was observed. The average size was sharply reduced to 46±22 nm.

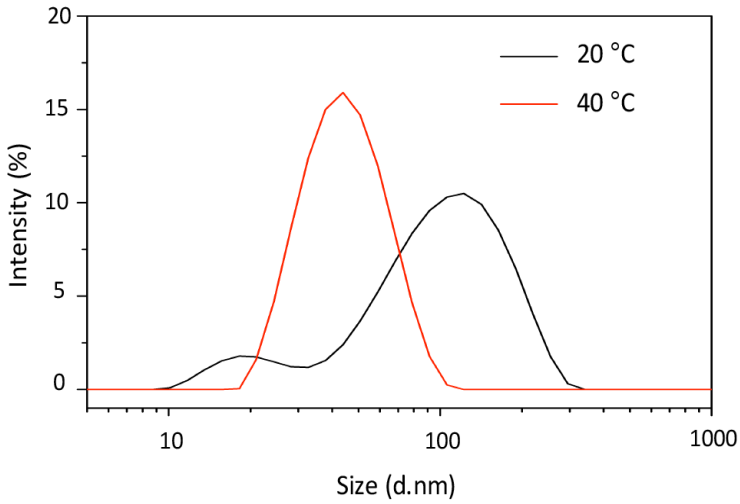

Figure 23. Size distribution of PNIPAM NG (w/ 2.5 crosslinking ratio) at different temperatures. The result was obtained from DLS measurement.

The chemical structure of the NGs was further characterized by ^{1}H NMR. As discussed in Section 1, the investigation of un-reacted vinyl groups (contributed from MBA crosslinker) presence is vital, due to their blocker behavior to entanglement formation. In the presence of un-reacted vinyl groups of MBA, the success of entanglement crosslinking is challenging, since acrylamide monomers and initiators are easily reacted by MBA radicals. In this case, they cannot penetrate inside the polymeric network of NG. Furthermore, they have tendency to conduct grafting polymerization on the NG surfaces. To understand the existence of such un-reacted vinyl groups residues, ^{1}H NMR was performed. According to ^{1}H NMR spectrum, remaining of vinyl groups were not detected in the region of 6.0-6.5 ppm (Figure 24). It demonstrates that all vinyl groups of MBA crosslinkers were consumed. In this case, the supplied acrylamide monomers and initiators can easily diffuse inside NGs to form the entangled structure, instead of forming surface grafting polymerization. In the ^{1}H NMR spectrum, -CH_3, -CH_2- and -CH- groups of PNIPAM are assigned to the peaks at 1.07 ppm, 1.5 ppm and 1.93 ppm, respectively. The peak at 3.81 ppm is contributed from -CH_2- group of MBA crosslinker. The solvent D_2O gives a signal at 4.7 ppm.

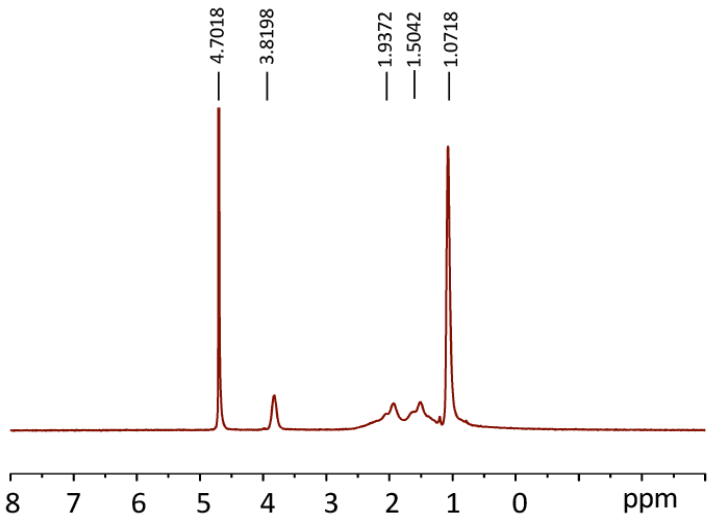

Figure 24. ^{1}H NMR spectrum of synthesized and freeze-dried PNIPAM NG after complete purification processes.

3.2.3. Characterization of Thermoresponsive PEH

PNIPAM NGs containing 2.5 wt% crosslinker were used to fabricate the hydrogels. Briefly, TPEH was prepared by using the principle of PEH. The NGs were firstly dispersed in water,

and degassed by using N_2 flow. After that, the addition of APS was performed and solution was mixed for 30 min. Subsequently, a certain amount of acrylamide monomer was added into solution. The solution was kept at room temperature for in-situ gelation. The samples are denoted as TPEHx-y, where x is the initial monomer ratio of acrylamide (wt%) and y is the percentage fraction of NG to monomer.

First of all, the temperature-dependent size change of TPEH was investigated at 20 °C and 40 °C (Figure 22a). To understand the temperature dependency and size change, as-prepared TPEH30-2.5 was directly immersed in a pre-heated 40 °C silicone oil, which prevents possible water evaporation during the heating. After immersing for 5 min, the hydrogel was taken out and the sizes of both states were measured for comparison. Normally, typical LCST thermoresponsive hydrogels undergo a huge shrinkage and size decrease, when high-temperature levels were applied. The reason is that huge amount of water is released out from the polymer network. In contrast, TPEH did not show a visible shrinkage. It was attributed to the low fraction of PNIPAM NG (2.5 wt%). In contrast to the size, the transmittance of the sample changes obviously when the temperature increases (Figure 25b). UV-Vis spectroscopy was used to characterize such change. At room temperature, as-prepared hydrogel is showing transmittance of ~40 %. The hydrogel becomes much opaque at 40 °C, showing transmittance of ~30 %.

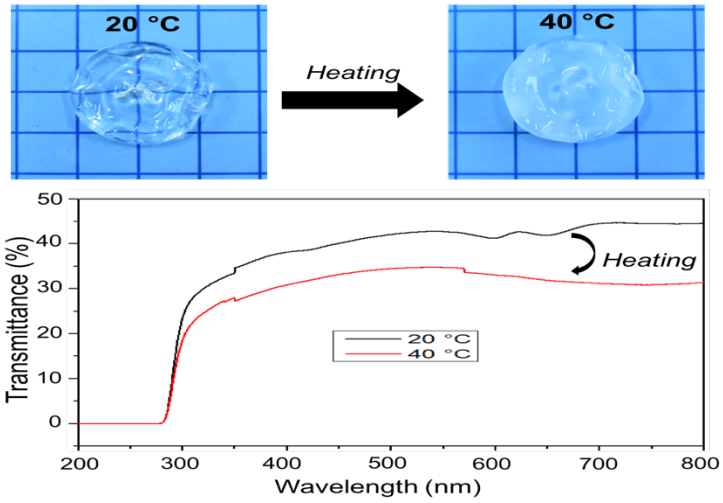

Figure 25. Temperature-dependent size and transmittance changes a) Initial size of TPEH at 20 °C and same hydrogel after being heated to 40 °C. The grids represent 1 cm scale b) UV-Vis transmission spectra of TPEH at two different temperature levels.

The temperature-dependent mechanical properties of TPEHs were investigated by dynamic rheology measurements. The frequency dependency tests were conducted at 20 °C and 40 °C, in

the range of 0.01-10 Hz frequencies. In a typical measurement, the as-prepared hydrogel was firstly tested at 20 °C, and the frequency profile was saved. Then, the sample was heated to 40 °C via a Peltier plate, and followed by 10 min soaking. Hydrogels with different monomer and NG ratio were used to study the structure-property relationship. The non-thermoresponsive covalently crosslinked AA-MBA hydrogels were preferred as the control group (Figure 26). The main polymeric network was constituted by non-responsive polyacrylamide chains and crosslinking regions, which were rigidly formed. The possible shifts in G' and G'' were monitored within frequency sweep at low and high temperatures. As expected, AA-MBA had almost similar G' and G'' profiles before and after the heating.

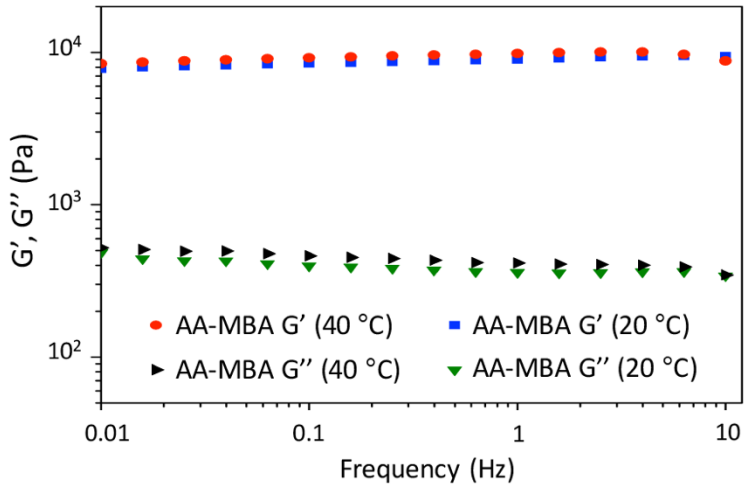

Figure 26. Frequency sweep of AA-MBA hydrogel, performed at 20 °C and 40 °C.

In terms of TPEH, first of all, the NG influence of thermoresponsiveness was checked by incorporation of 1%, 2.5%, and 5% PNIPAM NG ratio (Figure 27). At 20 °C, NGs were in swollen state and expected to allow free sliding of the entangled polymer chains. When the temperature was increased to 40 °C, the significant shifts of G' value in each concentration level was found. These results demonstrate stiffening of hydrogel by the NG shrinkage and entanglement locking. Interestingly, the amplitude of G' shift decreases at high frequencies, compared to low frequencies. The significant increase of G' at low frequency indicates the successful locking of inter-connective polymer chains by the polymeric network of PNIPAM NG.

At very high-frequency levels, the decrease in G' was observed at both 20 °C and 40 °C (Figure 27). In this level of frequency, the relaxation of polymer chains become impossible, and stay in a stretched conformation. It is supposed to lead to release of some polymer entanglements from

the NG network, and decreases relative crosslinking degree. When all sample groups were analyzed, it was found that only TPEH30-1 can sustain its G' without any decrease. By increase of NG presence above the critical level, the loss of G' was observed.

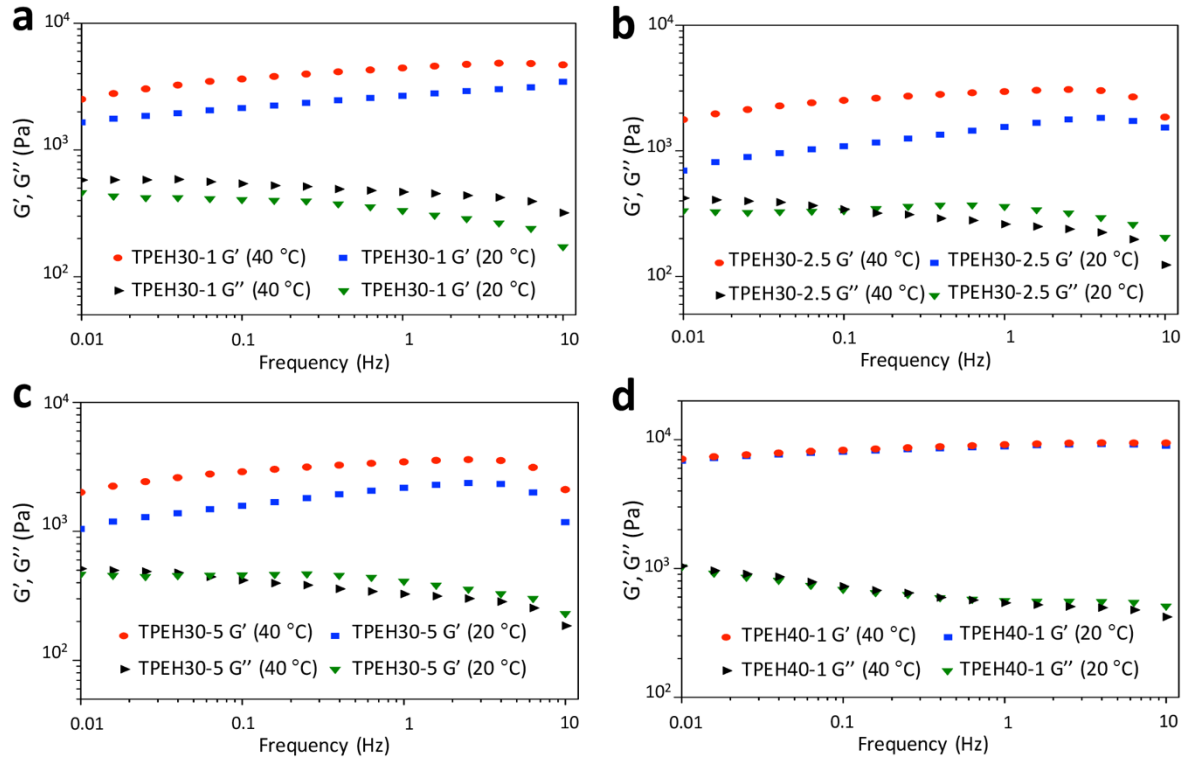

Figure 27. Frequency sweep of PEHs with different NG and monomer concentrations at 20 °C and 40 °C a) TPEH30-1 b) TPEH30-2.5 c)TPEH30-5 d) TPEH40-1.

Moreover, the influence of the initial monomer ratio was investigated. First of all, it should be noted that the solution with 20 wt% acrylamide fails to form a stable hydrogel, due to the inefficient entanglement formation. The TPEH30-1 was able to show thermo-responsiveness, and its G' increases with the temperature (Figure 27a). On the other hand, TPEH40-1 had shown nearly similar frequency profile at two different temperatures (Figure 27d). This behavior is unique, and allows regulating thermoresponsive feature only by altering the monomer concentration. It should be highlighted that conventional responsive hydrogels require change of responsive polymer fraction to manipulate the response. In case of TPEH, non-responsive constituent is also able to manipulate the hydrogel property, effectively.

To understand the changes in viscoelasticity, tan(δ) (G"/G') value was investigated in detail. For the comparison of sample groups, the G' and tan(δ) values were collected from 1 Hz frequency level (Figure 28a, and 28b). The investigation of tan(δ) is an effective approach to understand the crosslinking degree of hydrogel that has relevance to viscous and elastic responses. If the value is around 1, the behavior of hydrogel is called viscoelastic, which consists of viscous and elastic regions together. In case of lower values, the polymer network starts to demonstrate a dominant elastic behavior. Briefly, the lower tan(δ), the higher crosslinking degree. At 20 °C, as expected, the lowest tan(δ) value was obtained from AA-MBA. Due to the covalent crosslinking, which provides a permanent and consistent network, the constituent polymer chains are well stabilized. In contrast, TPEHs had shown higher values, since the physical crosslinking approach cannot provide a well-stabilized network. The dangled free polymer chains could increase the sample's viscosity. Only TPEH40-1 exhibited a tan(δ) value closer to the AA-MBA.

When the temperature is increased to 40 °C, the G' modulus of TPEH30-y significantly increased and their tan(δ) values decreased (Figure 28a, and 28b). The data indicated that the elastic feature of the sample enhanced due to the shrinkage of PNIPAM NG. With the shrinkage of NG, the sliding of entanglements was limited, and helped to observe increased crosslinking nature. This behavior is compelling, since crosslinking degree can be tuned without alteration of concentrations. Interestingly, the tan(δ) values of TPEH30-1, TPEH30-2.5, and TPEH30-5 are similar (around 0.1). Although the G' value is influenced by NG ratio, it could be concluded that the final degree of elasticity was not dependent on NG ratio after their shrinkage at 40 °C. In contrast, NG ratio played a vital role for the viscoelasticity at 20 °C, where the free sliding of entanglements was possible. As a result of sliding phenomenon, great differences of tan(δ) were observed before shrinkage of PNIPAM NGs. The tan(δ) had varied between ~0.1 and ~0.22 with the change of NG amount.

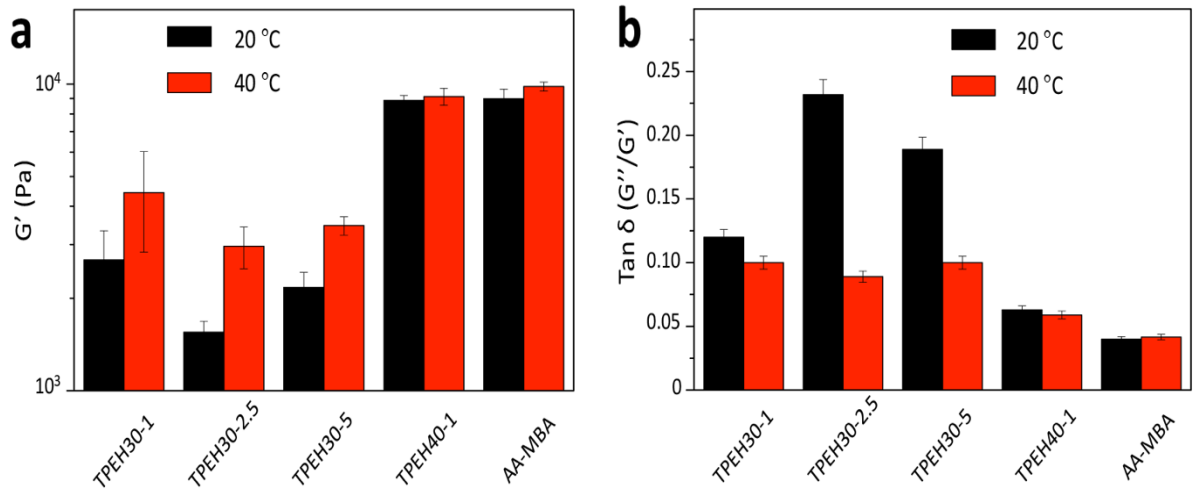

Figure 28. Rheological characterization of TPEHs at 20 °C and 40 °C. All data were collected from 1 Hz. a) G' values of each sample b) G"/G' ratio of TPEHs and AA-MBA to evaluate viscoelasticity change (All samples groups were repeated for 3 times).

The thermoresponsive performance of TPEH was also studied by time sweep rheology (Figure 29). Thermoresponsive TPEH30-2.5 and non-thermoresponsive AA-MBA samples were compared for better understanding. Both samples were exposed to the continuous 1 Hz frequency for 30 min at 20 °C, and then heated rapidly to 40 °C.

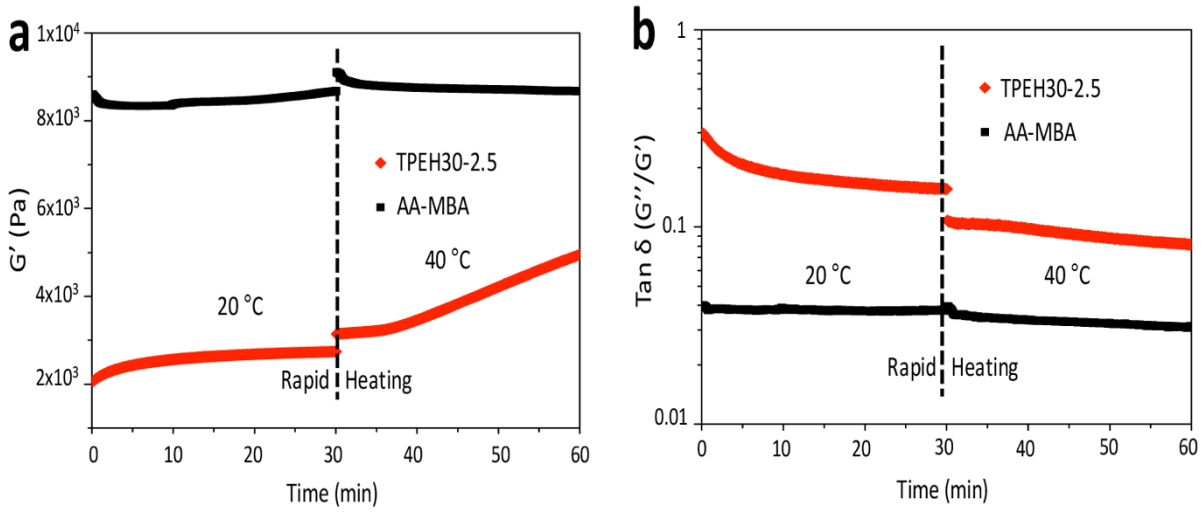

Figure 29. Time sweep rheology of TPEH30-2.5 and AA-MBA at 20 °C and 40 °C. a) Storage modulus profile among a certain time b) tan(δ) distribution of each sample.

As shown in Figure 29, with increasing the temperature, the G' of TPEH30-2.5 starts to undergo a sharp increase, while that of AA-MBA is constant. Furthermore, the tan(δ) of TPEH30-2.5

decreases from ~0.18 to ~0.1, after being heated to 40 °C. The AA-MBA hydrogel had shown a constant ~0.04 G"/G' value, although the temperature was increased.

3.2.4. Nanogel Size Influence on Thermoresponsiveness

To understand the possible influence of NG size to thermoresponsiveness, PNIPAM NGs made from 2.5 wt% and 7.5 wt% crosslinker, were selected to prepare TPEH. For the comparison, TPEH30-2.5 was fabricated by the incorporation of two NG species.

Firstly, the average size of NGs was compared before further characterizations (Figure 30). NG containing 2.5 wt% crosslinker shows an average size of 133±74 nm at 20 °C and 46±22 nm at 40 °C, respectively. The NG containing 7.5 wt% crosslinker shows smaller size, i.e. 78±43 nm at 20 °C and 41±20 nm at 40 °C. The sizes at 20 °C are important for the polymer network formation, since the gelation process takes in place at room temperature. Figure 29 shows the storage modulus and tan(δ) values of both samples, collected at 1 Hz. The G' of TPEH (7.5 wt% CR NG) was greatly higher than the TPEH (2.5 wt% CR NG) at 20 °C. It was attributed to small sizes of NGs, which could help to form stronger entanglement interactions between in-situ formed chains and polymer network of NG.

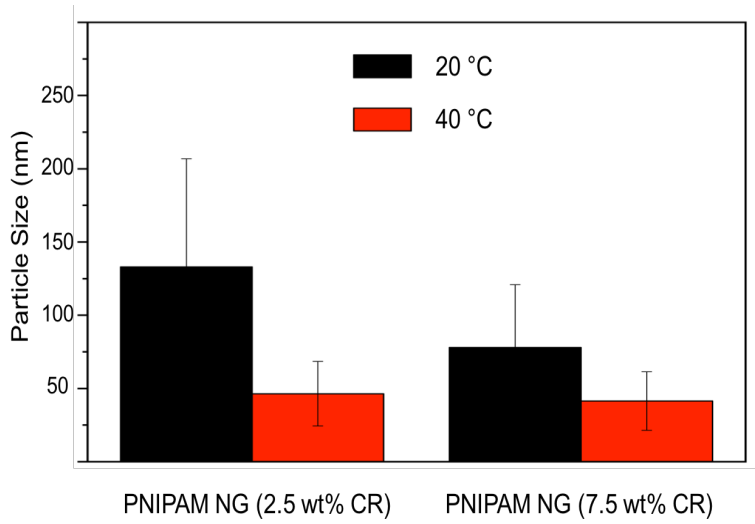

Figure 30. Average size distribution of PNIPAM NGs with varied crosslinking degree. The LCST induced shrinkage and size change was investigated at 20 °C and 40 °C.

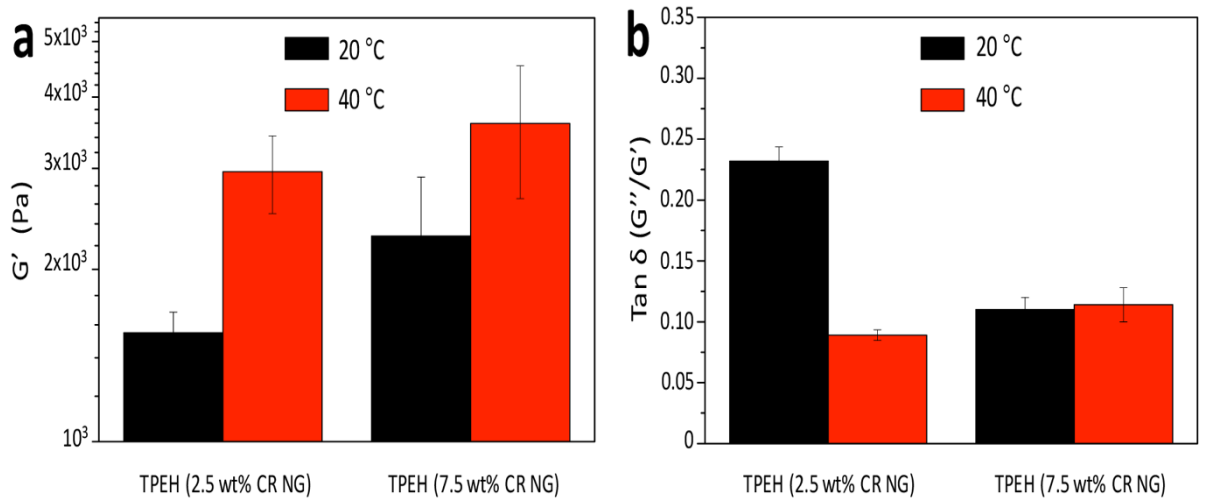

Figure 31. Rheological property change by alteration of temperature a) G' value of samples b) tan(δ) ratio of each sample at 20 °C and 40 °C, respectively.

In this case, the sliding nature of polymer chains is supposed to be limited, and the G' of TPEH enhanced. Moreover, by increasing the temperature and inducing NG shrinkage, the G' modulus was increased as observed in previous sample groups. The sliding behavior would become even harder after decreasing to ~40 nm NG sizes (Figure 31a). Following that, tan(δ) value characterization of hydrogels were conducted by considering the viscoelasticity (Figure 31b). At 20 °C, TPEH (7.5 wt% CR NG) had significantly lower rate (~0.1) with the demonstration of a high level of elasticity. This was attributed to denser entanglement crosslinking, due to the small NG size of NG. When the temperature was increased, TPEH (2.5 wt% CR NG) had displayed the reduction of tan(δ) from ~0.22 to less than 0.1. By the shrinkage of PNIPAM, the hydrogels become much elastic, and absorbed the applied energy. Furthermore, the viscous motions in the network, which favored in energy dissipation, were reduced. In contrast, in case of TPEH (7.5 wt% CR NG), the tan(δ) was not changed after being heated. Even though increase in network elasticity was triggered by NG shrinkage, the viscous motions were also increased.

3.3. Discussion

In this chapter, the developed PEH system was successfully modified to a thermoresponsive hydrogel. The universality of PEH strategy is also shown by differing the crosslinking nanogel component. It was demonstrated that responsive behavior can be gained by a simple change of incorporated nanogels (polyrotaxane-like crosslinking points). In such a hydrogel system, the big fraction of thermoresponsive components is not required. It was found that thermoresponsiveness was gained even with the supply of 1 wt% PNIPAM nanogels. The thermoresponsive property was supplied by controlling entanglement sliding inside polyrotaxane-like crosslinking. Typical polyrotaxane molecules are not able to undergo size change by stimulants, so that responsive hydrogel nature is supplied from main polymer matrix, not from the crosslinking regions. In contrast, PEH thermoresponsiveness is only triggered by crosslinking regions, and main polymer network does not demonstrate any responsive nature. At above LCST temperature, PNIPAM nanogels had shrunk almost three times, and sliding of polymer entanglements had become restricted. Following that, increase in G' were observed. Although stiffening was detected, no clear size change and water release from hydrogel were observed. Note that stiffening of hydrogels, including polyrotaxane systems, are mostly based on change in water amount and polymer fraction in literature. For this reason, it is common to observe 5-10 times shrinkage of hydrogels (44, 61, 62). In contrast, PEH strategy allows to receive stiffening phenomenon by keeping polymer fraction same.

Therefore, the viscoelasticity of the hydrogel can be regulated by controlling entanglement sliding.When entanglement sliding is limited, it contributes to elasticity of polymer network. Following that, the hydrogel starts to behave as possessing higher crosslinking degree. In addition, it was found that initial nanogel size could have impact on thermoresponsiveness. This behavior is also one interesting property that distinguish PEH strategy from polyrotaxane crosslinking. It demonstrates that cluster of polymer entanglements and their sliding would be altered. Note that such behavior is not possible in case polyrotaxane hydrogels, due to stable size and non-responsive nature of crosslinking molecules.Two different nanogels with 2.5 wt% and 7.5 wt% CR were used to investigate size change influence. At 40 °C, both nanogels had showed similar size after being shrunk. The data demonstrated that G' values increased for both cases. On the other hand, viscoelasticity of 7.5 wt% CR was kept almost stable with temperature increase, while nanogels with 2.5 wt% had a decrease. This result is attributed to smaller initial size of

nanogels. In that case, it could become difficult to form enough entanglements inside their polymeric network. If entanglements are not tight enough, viscous motions (G") would also increase by temperature apply. As a result, G"/G' ratio would stay stable, even increase in G' is detected. In overall, it can be concluded that responsiveness of TPEH is sensitive to monomer amount, nanogel ratio and nanogel size through in-situ formation.

3.4. Summary

Thermoresponsive PEH hydrogels have been prepared by using PNIPAM NGs as the sliding crosslinking points. The NGs allow the formation of physical entanglements that demonstrate a unique polymer chain sliding behavior. It was found that by shrinkage of NGs above LCST point, the sliding behavior of polymer chains can be tuned and limited. In case of shrunk NG conditions, the sliding of chains had become restricted and enhancement of G' and tan(δ) was succeeded.

Interestingly, no significant size or water release was observed after being heated. The gathered results are contrary to the conventional thermoresponsive hydrogels, which normally require release out of water for the stiffening effect. Moreover, it was realized that the thermoresponsiveness of PEH could be regulated by feeding non-responsive monomer concentration. If the initial acrylamide concentration is higher than a critical value, the thermoresponsive nature is lost, due to the dense entanglement interactions. Therefore, the crosslinking degree of supplied NG could play an important role to regulate the physical properties, since the size of NG at room temperature is altered. In this case, the presence and density of polymer entanglements inside NGs are altered during in-situ polymerization. It was found that the increase of NG crosslinking degree helped to enhance the G' by heating. On the other hand, the viscoelasticity of network is kept at same level.

3.5. Materials and Methods

3.5.1. Materials

Acrylamide (⩾99%) (AA), N-Isopropylacrylamide (NIPAM), ammonium persulfate (APS), N,N'-methylenebis(acrylamide) (MBA), sodium dodecyl sulfate (SDS), and tetramethylethylenediamine (TEMED) were purchased from Sigma-Aldrich and used as received.

3.5.2. Fabrication of Thermoresponsive PNIPAM Nanogels

The synthesis of NGs was conducted in an inert environment. First of all, 50 ml distilled water was added into 100 ml round-bottom flask, and continuously purged with N_2 for 5 min to remove out dissolved oxygen residues. In a typical example of the PNIPAM NG with 2.5 wt% crosslinking ratio, NIPAM monomer (1.13 g), MBA crosslinker (0.03 g), and APS initiator (0.027 g) were first dissolved in water phase, respectively. The mixture was stirred at room temperature (25 °C) until the clear solution was received. After the formation of clear solution, SDS surfactant (0.27 g) was supplied into the mixture to form micelles and emulsion. The stirring process was continuously conducted at 3000 rpm (IKA C-MAG HS7) in whole next synthesis steps. Before increase of the temperature, N_2 flow exposed to the inside air environment of round-bottom flask for 5 min, and then temperature was increased to 70 °C. The polymerization process was performed for 5h in a sealed environment. Afterward, the emulsion was inserted inside an ice bath to inhibit further polymerization, waited for until it is cooled down to room temperature. To purify the received solution, dialysis process was performed with the help of dialysis membrane (Spectra/Por 3, MWCO is 3.5 kD) for 3 days. The used MilliQ water was replaced in each day. For the synthesis of PNIPAM NG with 7.5 wt% crosslinking ratio, except for MBA crosslinker concentration, all conditions were kept same. Only the amount of supplied MBA was tripled during synthesis.

3.5.3. Fabrication of Thermoresponsive PEH

The thermoresponsive hydrogels were synthesized by performing introduced strategy of PEH. Thermoresponsive hydrogels were named as TPEHx-y, where x demonstrates wt% of acrylamide monomer, y is the weight percentage of the NG to the monomer. In a typical example of TPEH30-1, the freeze-dried PNIPAM NGs (0.003 g, 1 wt% of monomer) were dispersed in 1 ml of distilled water via ultrasonication. The obtained NG solution was then purged by N_2 for

5 min to remove oxygen. Following that, APS initiator (0.009g, 3 wt% of monomer) was supplied into the deoxygenated solution, and stirred for 30 min. After continuous stirring, the acrylamide monomer (0.3 g) was added to start polymerization/gelation process. All steps of the fabrication, including hydrogelation, were conducted at room temperature (25 °C). As control group in the following steps, AA-MBA hydrogel, with same composition that is detailed in Section 1, was used.

3.5.4. Characterization of Nanogels

The presence of unreacted vinyl groups in PNIPAM NG was investigated by ^{1}H NMR spectroscopy. Prior to the characterization, the freeze-dried PNIPAM NGs were dispersed in D_2O and treated by ultrasonication (Bandelin Sonorex, 35 kHz, 80 W) for 5 min, and subsequently transferred into 5 mm NMR tubes. The ^{1}H NMR spectra were obtained with Bruker 300 MHz (Rheinstetten, Germany) nuclear magnetic resonance equipment. Chemical shifts are reported using the solvent as the reference.The spectra was recorded at room temperature.

The average size of NGs were investigated via dynamic light scattering device (Malvern Zetasizer Nano ZS, Massachusetts, USA) equipped with He-Ne light source (k:633 nm, 4 mW) and temperature control. The PNIPAM NGs were dispersed in distilled water, and the mixture was ultrasonicated for 5 min in ultrasonic bath (Bandelin Sonorex, 35 kHz, 80 W). Following that, PNIPAM NG solution was injected into polystyrene cuvette, and immediate measurements of size distribution were conducted. Two different temperatures, such as 20 °C and 40 °C, were used to evaluate the LCST dependent size change during the measurements. Firstly, the measurement was performed at 20 °C, and followed by heating same sample to 40 °C.The soaking time was set as 5 min for heating in 40 °C, and then data was acquired.

3.5.5. Characterization of Thermoresponsive PEH

For the demonstration of size change by exposure of heating, photos of hydrogel were taken (Nikon D600), and compared with the initial as-prepared size. To prevent water evaporation, thermoresponsive hydrogels were immersed into the pre-heated silicone oil (10 cSt, 40 °C) for 5 min.

The temperature triggered transmittance change of TPEH was evaluated by conducting UV-Vis measurements performing Carry 4000 UV spectrophotometer (Santa Clara, USA). The spectrum of the as-prepared TPEH was first obtained at 20 °C, and followed by heating the sample to 40 °C with a step width of 5 °C. At every temperature, the sample was soaked for 10 min before measurement. The spectra was performed between 200-800 nm wavelengths.

The investigation of temperature dependency of stiffness was performed by dynamic rheology measurements, on TA Instruments HR-3 Rheometer (USA) equipped with a Peltier plate to control the temperature. The as-prepared hydrogels were tested with dynamic frequency and temperature sweeps. For the rheological characterization, as-prepared samples were punched into 8 mm diameter. The diameter of the upper plate was chosen as 8 mm, as well. The frequency sweeps were performed between 1-10 Hz with a constant 1% strain value. Two different temperature values (20 °C and 40 °C) were used to evaluate G' and G" changes by increase of temperature. In a typical measurement, the frequency sweep of hydrogel was performed at 20 °C. Subsequently, same hydrogel was heated to 40 °C, and soaked at this temperature for 10 min to obtain totally heated sample. After that, the second frequency sweep was conducted. Before the measurements, the hydrogel was covered with thin layer of silicone oil to prevent water evaporation. Time sweep of hydrogel was performed at constant 1 Hz and 1% strain values. First of all, the hydrogel was exposed to oscillation for 30 min at 20 °C. Then, rapid increase of temperature to 40 °C was provided into set-up, and continuous frequency-time sweep was performed.

Chapter 4: Fabrication of Organohydrogel with Anisotropic Properties

4.1. Introduction

Organohydrogels are soft materials, which consist of binary phases in their crosslinked network. In this case, hydrophilic and hydrophobic molecules can be combined in one gel system. As a result, soft material can show both hydrogel and organogel properties (106). The dominant properties would be tuned by the alteration of each phases' existence and chemical compositions. To fabricate such soft materials, emulsion method has been utilized (107). The binary phase and its possible modification provide great possible applications, such as sol-gel synthesis, bioactive molecule transportation, and molecular separation, etc. Therefore, improved mechanical properties (i.e. toughness, stretchability) can be obtained with the help of binary phase (108). Reported studies use rapid gelation kinetics, which do not allow to phase separation and dynamic re-organization during in-situ formation of the organohydrogel, and lead to isotropic systems. Herein the design of an organohydrogel is described that shows different characteristics, including surface and mechanical properties, in various regions.

The hydrophilic phase of organohydrogels is mostly created in water or water-miscible solvents, such as DMSO, ethylene glycol, glycerol, etc. (107). Silicone oil derivatives are the most preferred materials for hydrophobic phases. During phase formations, different types of monomers would be loaded in each phase. Subsequently, the crosslinked organohydrogel polymer network can be obtained via in-situ polymerization, which undergoes inside the phases and at the interface layer (109). In the literature, it has been shown that contribution of binary phases into one gel system is promising to obtain compelling features, such as freeze-tolerance (110, 62), shape memory and high stretching ability, etc. (63). For instance, researchers had reported a freeze-tolerance organohydrogel, constituted from hydrophilic N,N-dimethylacrylamide monomer (109). As oleophilic monomers, lauryl methyacrylate, butyl methacrylate with ethylene glycol dimethacrylate crosslinkers are supplied into the silicone oil phase. It has been clarified that continuous binary phase creation helped to prevent ice crystal formation during freezing process. On the other hand, continuous binary phase is not vital to obtain unique features of organohydrogels. The droplet formation of oleophilic constituents in water phase could help to improve mechanical properties and show interesting features. It was demonstrated that emulsion of hydrophilic monomer (N,N-dimethylacrylamide) and oleophilic monomers (lauryl methyacrylate, ethylene glycol dimethacrylate) can be stabilized with nanoclays to form organohydrogel (111). The monomers can undergo polymerization at the interface, and the gel network is succeeded. The organohydrogel was able to be stretched 6 times and had shown no

fracture after compression test. The applied stress can be dissipated via droplet deformation. The recovery of material is also possible, since the droplets are able to turn back to the initial state formations.

Emulsions are unique systems, which allow combining different properties and chemistries into a system. In principle, it can be obtained by a mixture of immiscible two solvent systems, and droplets of one phase are formed inside the second constituent phase (112). Even though the droplet formation is succeeded, two phases mostly tend to separate, again. To stabilize emulsion systems, surfactants and co-surfactants are required to be supplied into the solution state. Such chemicals consist of two different chemistries, like hydrophilic and lipophilic, and can be dissolved at the interface of two phases. In this case, the phase separation process can be prevented, and obtained structure can remain for a long duration. Although simple microemulsions are based on droplet formations in a continuous phase, various types of domain morphologies can also be obtained. The size and morphology of domains are dependent on the hydrophilic-lipophilic balance (HLB). By alteration of the balance in the system, water-in-oil (W/O), oil-in-water (O/W) and bicontinuous phases can be gathered (113). Slight modification of constituent ingredients could lead to striking changes in the morphology, due to the surface energy and entropy shifts of the system. The dynamicity and biphasic behavior of emulsion help to form different morphologies and phase separation. Therefore, polymerization can induce phase separation process. Polymerization-induced phase separation (PIPS) enables to achieve anisotropic properties, and gradient structures are provided during in-situ processes. During the formation of material, non-uniform kinetic processes generate long term continuous changes (114). The simultaneous spinodal decomposition process could be triggered by the polymerization of constituent monomers and solvents. Following that, instabilities in microemulsions are activated and phase separation is observed. The nature of PIPS is much complex than other types of phase separations. In case of PIPS, simultaneous phase separation and polymerization occur all at once. The reason for phase separation arises from enhanced immiscibility of the solvent, which is because of bigger polymer chain length formation. During the polymerization, molecular weight and branching of polymers are enormously increased, and continuous phase separation is observed (115, 116). The polymer branching could help to form crosslinking, as well. The phase-separated microemulsion morphology can be fixed with gelation via crosslinking process. In the gelled state, the movement of the phases is prohibited and stable gel structure is obtained.

The gelation and crosslinking in microemulsions can be achieved with the implementation of several strategies, such as the incorporation of micellar structures and colloidal droplets (117). Micellar systems are one of the most common strategies to obtain gel materials from microemulsions. Surfactants are provided into solution state to balance interface of each phase, due to their hydrophilic and hydrophobic tails. The incorporation of micellar structure is mostly used to form hydrogels, since the inner environment of micelles demonstrates relatively hydrophobic nature. Moreover, micelles allow dissolving and encapsulating monomers in a confined region. Some of the surfactants, such as SDS, F127 and CTAB, etc. that have been utilized as micellar crosslinking domains (118). For instance, SDS surfactant can be used to incorporate oleophilic C18 molecules in polymer networks. The micellar structure of SDS with performing hydrophobic nature is able to encapsulate long-chain C18 (33). In this case, hydrophobic tails of C18 form very strong interactions, and act as crosslinking mechanism. The polymer chains inside micelles are also able to undergo copolymerization with the hydrophilic monomer at the interface. The copolymerization capability enables to combine different phases together and form three-dimensional gel network. It has been shown that incorporation of micelles helps to obtain tough and stretchable hydrogels.

In this study, anisotropic organohydrogel was successfully fabricated, by phase separation principle. The microemulsion is mainly formed by binary water and silicone oil phases, with showing continuous phase separation, due to concentration changes and polymerization within time. As for the crosslinking mechanism, micelle strategy was chosen. During phase separation, the solution state was crosslinked with the help of hydrophobic interactions of long-chain C18 inside the micelles, and gel material was obtained. The organohydrogel shows variances in different parts, in terms of mechanical properties, surface chemistry and roughness, and self-healing ability.

4.2. Results

4.2.1. Synthesis of Organohydrogel

In organohydrogels two different phases coexist. For the synthsis of such a system, the micro-emulsion method with polymerization induced phase separation is used. Network formation and gelation was achieved via hydrophobic associations of long chain monomer.

The organohydrogel contains a water and a silicone oil phase. The hydrophilic phase contains hydrophilic acrylamide monomer, while the silicone oil phase has hydrophobic C18 monomer, with long alkyl side chain. As surfactants, SDS and 2-butanol were supplied to the mixture. SDS forms micellar structures in water phase, and allow copolymerization of hydrophilic/hydrophobic monomers. The continuous polymerization process induces simultaneous phase separation within time. As a result, materials with different properties can be achieved during phase separation. The fabricated organohydrogel is mainly crosslinked via hydrophobic interactions of C18. The concentration changes are supposed to result in crosslinking degree, and other properties alteration during in-situ gelation.

4.2.2. Phase Separation and Gelation

The fabrication of organohydrogel starts by mixing all components. A milky suspensionwas obtained and left at room temperature to observe phase separation and gelation process (Figure 32). Two phases formed in the first 30 min, and the bottom phase underwent phase separation again in ~4h, leading to the formation of three phases. A transparency change was observed during the phase separation. Gelation occurred when the three-phase structure was formed. The top solution, which mainly contained silicone oil, did not form a gel and was discarded. The middle and bottom phases were gelled. The gel state of each layer demonstrated that crosslinking with long-chain hydrophobic C18 was achieved. As reported previously, C18 molecules can form strong hydrophobic interactions inside SDS micelles, and behave as the crosslinker regions (33). The middle gelled solution was named “top gel/layer” to differ it from the bottom layer.

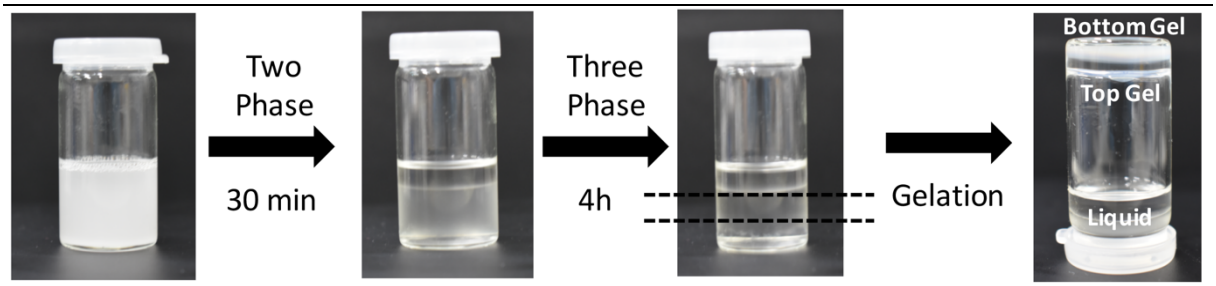

Figure 32. Phase separation process of microemulsion within time. The initial milky solution changes its morphology, continuously.

To understand morphological changes during the phase separation and gelation, confocal microscopy was used. The cross-section of organohydrogel was cut and investigated with the help of fluorescent dye, which labels the silicone oil phase (Figure 33). The top and bottom layers are fluid-like and gel-like, respectively. In terms of fluid-like top layer, intense presence of silicone oil is expected, since it would contribute to fluid nature. To understand the morphological differences, cross-section of gel was observed. First off all, regions close to top surface had bigger and denser silicone oil droplets. In contrast, the presence of silicone oil droplets were limited through the bottom side. Even close to bottom surface, mostly no clear droplet formation was detected. Therefore, the obtained image showed that a whole organohydrogel was obtained by gelation of O/W, in which the water phase is dominant, since oil droplets are barely found in whole gel network. The size and distribution of silicone oil droplets in the organohydrogel were inhomogeneous. In the following regions of organohydrogel, bigger silicone oil droplets (~100 μm) were incorporated into the bulky matrix. The inhomogenous oil droplet formation and distribution was attributed to polymerization induced phase separation and buoyancy of silicone oil. During phase separation, concentrations in solution state always change and molecules re-organize. Therefore, silicone oil tends to stay close to top surface part, due to its buoyancy. As a result, change in size and distribution in two layers are expected.

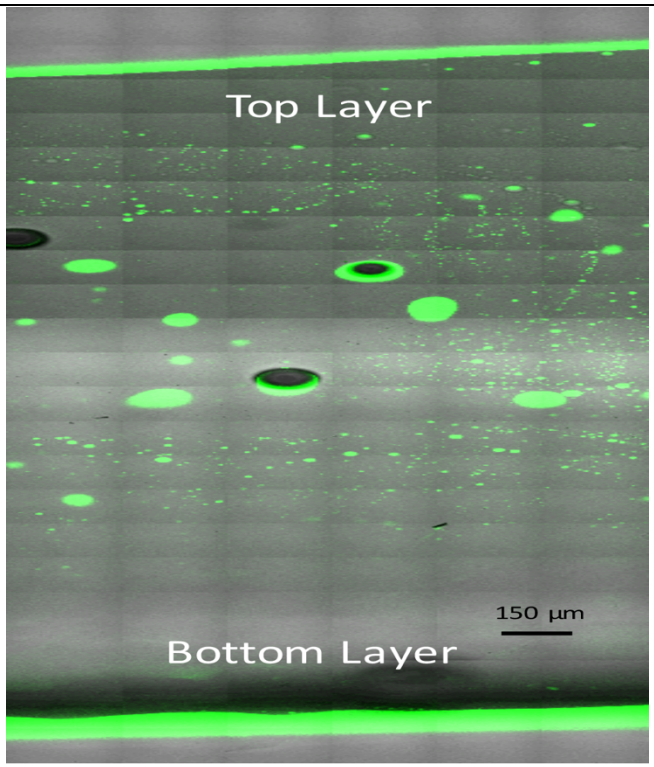

Figure 33. Confocal microscopy imaging of organohydrogel cross-section, gathered from bottom layer to top layer.

4.2.3. Characterization of HSurface Chemistry and Morphology

The chemical features of fabricated organohydrogel were investigated by FT-IR spectroscopy. During the phase separation process and in-situ polymerization, compositional changes in the monomer mixture are expected, since some portion of the chemicals are consumed and the system segregates in differnet phases. For this reason, the top and bottom surfaces were investigated by IR spectroscopy (Figure 34). Differences in the chemical composition across the thickness of the organohydrogel were detected. The IR spectrum of the top surface showed three peaks at the wavelength of 788.8 cm^{-1}, 1012.8 cm^{-1}, and 1254.4 cm^{-1}, characteristic vibrations of Si-O-Si, Si-C and Si-CH_3 bonds of the silicone oil, respectively. The intensity of these peaks increased towards the middle phase during phases separation and decreased again at the bottom phase. The signals at 2976 cm^{-1}, 2923 cm^{-1}, 2854 cm^{-1} were detected at the two phases and were associated to the vibrations of -CH_3, -CH_2-CH_2- and -CH_2-CH_3 bonds of the free alkyl chain groups of C18 and SDS molecules. These bands are more intense at the top phase. This is attributed to unconfined states, which could be result of losing crosslinking, and free presence of the alkyl chains.

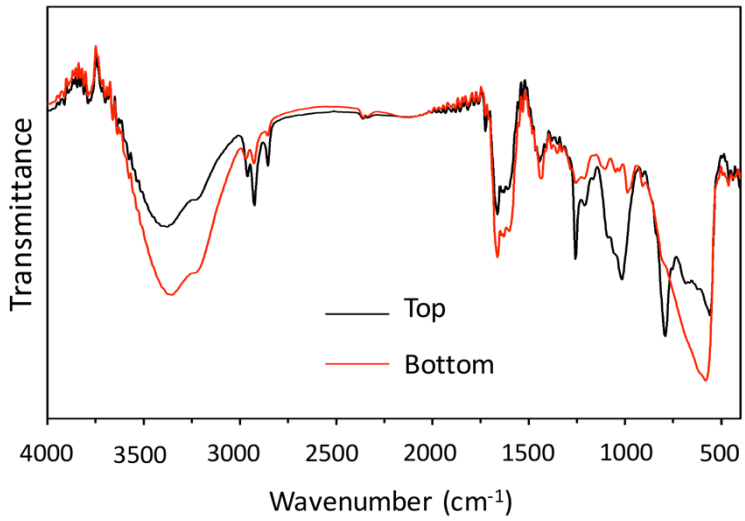

Figure 34. FT-IR transmittance spectrum of top and bottom organohydrogel surfaces.

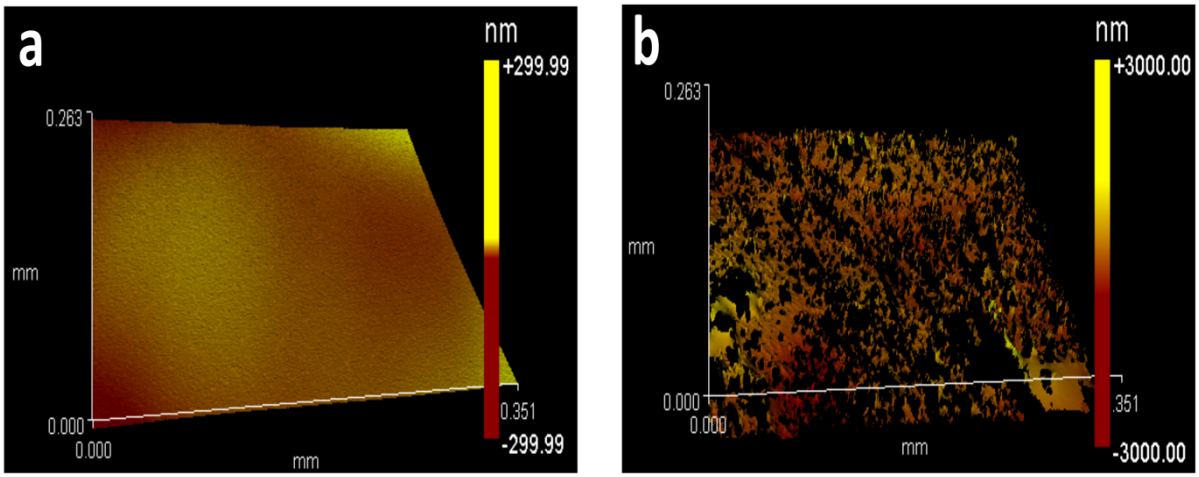

Figure 35. Roughness profile of organohydrogel surfaces as characterized by profilometer. a) Top surface b) Bottom surface.

In addition to the analysis of the chemical composition, the morphologies and roughness were characterized. The continuous phase separation, which occurs during polymerization and gelation, induced changes in the network structure of the organohydrogel. For instance, the crosslinking degree, existence of silicone oil, etc. is expected to be different in each section of the gel material. The roughness distribution profile of each surface was investigated by performing profilometer measurements (Figure 35). The presence of silicone oil helped to observe liquid-like gel at the top layer. The top layer was smooth, with an average roughness value (Ra) of 4 nm. In contrast, the nature of bottom layer, being a highly crosslinked gel material, showed

roughness in the micrometer scale. The surface had contained great morphological differences with depths and heights. The Ra value of the bottom surface was 0.2 μm.

4.2.4. Characterization of Mechanical Properties

Before the characterization, top and bottom layers were cut to 1.5 mm, separately.The mechanical of the organohydrogel parts were characterized by rheology within the frequency range from 0.01 to 10 Hz (Figure 36). At low frequencies, the G' and G" values of the top layer are very close. The tanδ value, which is around 1, also demonstrates that the gel is in viscoelastic state and close to nature of liquid-like gel. At higher frequencies, G' becomes greatly higher than G", which is an evidence of a well-crosslinked polymer network. At high frequency, such as 10 Hz, decrease in G' value was observed and the viscosity of the gel network went up. This behavior could be a result of loosely crosslinked nature of the gel. The unity of hydrophobic associations cannot be sustained anymore at high frequency, due to the inadequate C18 molecules as the crosslinking constituents.

In contrast, the bottom layer showed a constant and slight increase in G' during the frequency sweep experiment. It is attributed to a well-crosslinked network, in which C18 molecules were able to form a decisive conformation to form elastic gel network. The strongly formed hydrophobic crosslinking domains demonstrated limited re-organization with the increase of frequency amplitude. The tanδ value demonstrated that the bottom layer posseses very good elasticity, and the elasticity is slightly enhanced by increasing the frequency level. In general, the G' value of bottom layer (~10^4 Pa) was extremely higher than the top layer's (~10^2 Pa). It was attributed to dense cluster interactions of C18, and their consumption at bottom side during gelation. The strong hydrophobic interactions of C18 could lead to cluster formation, which increases the density and downfall. In this case, the immense presence of C18 at bottom side is expected. Therefore, these clusters, acting as the crosslinking regions, were incorporated into the bulky matrix during in-situ gelation. Moreover, the viscoelasticity of top layer was drastically higher than the bottom layer. These data had indicated the crosslinking difference, which is based on polymerization induced phase separation. When the G' and tanδ values are considered, it can be concluded that the top layer is loosely crosslinked, compared to the bottom layer. With the phase separation, the efficiency of crosslinking degree decreases.

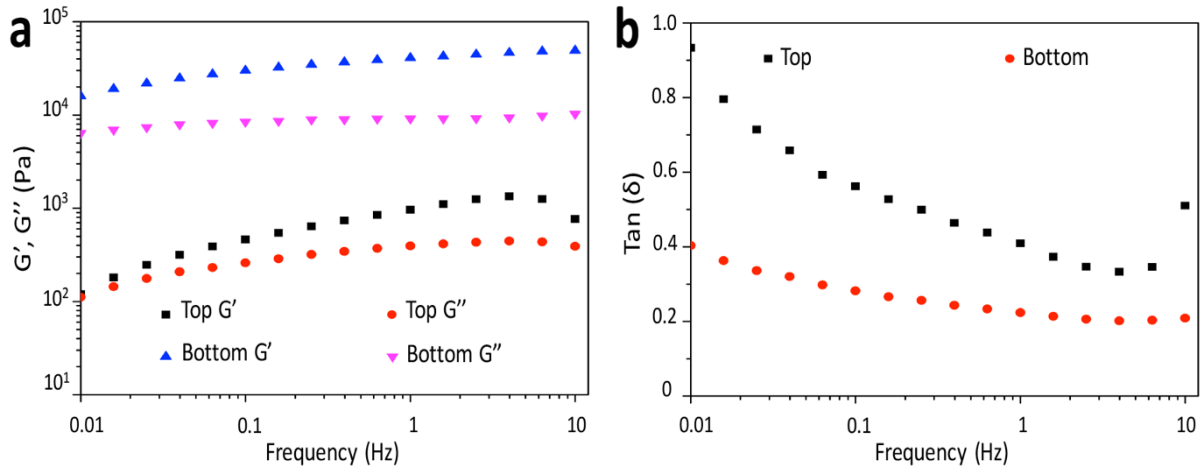

Figure 36. Rheological characterization of samples within dynamic frequency range (0.01-10 Hz). a) G' and G" values of each layer of organohydrogel. b) G"/G' ratio of top and bottom samples to evaluate viscoelasticity.

In addition to frequency-dependent characterization, strain sweep tests were performed within 10^{-2}-10^{3} (%) strain levels to understand network stability (Figure 37) (Table 3). According to obtained results, each bottom and top layer showed a strain thinning behavior, due to the physical crosslinking domains. The result indicates that physically crosslinked networks could be demolished, if a certain strain level is exceeded. It was attributed to physical crosslinking nature of long-chain C18 molecules, which form dynamic hydrophobic interactions. Even though hydrophobic interactions are able to form stable and strong associations to act as a crosslinker, the destroy of such physical crosslinking is possible with an appropriate stimulus. At low and moderate strain levels, the G' value of each sample was greater than the G", and the crosslinked elastic network is confirmed by G'>G" phenomenon. After reaching above a critical point, with the destroy of crosslinking domains, the G" becomes higher than the G' and viscous movements become dominant inside the network. For the bottom layer, which shows a well-crosslinked nature, its critical point was around 10^{2} (%) strain level. Moreover, the G">G' transition of loosely crosslinked top layer was received around ~$1.5x10^{2}$ (%). By considering the obtained data, loosely crosslinked top layer had G">G' transition slightly later than the bottom layer. It could be a result of easier dynamic movements of C18 molecules and abundance of silicone oil, which could contribute to the dynamicity with oleophilic nature. With the initial network dynamicity, C18 molecules can re-organize with strain exposure and form strong interactions. The elastic state of the top layer of organohydrogel can be kept much stable.

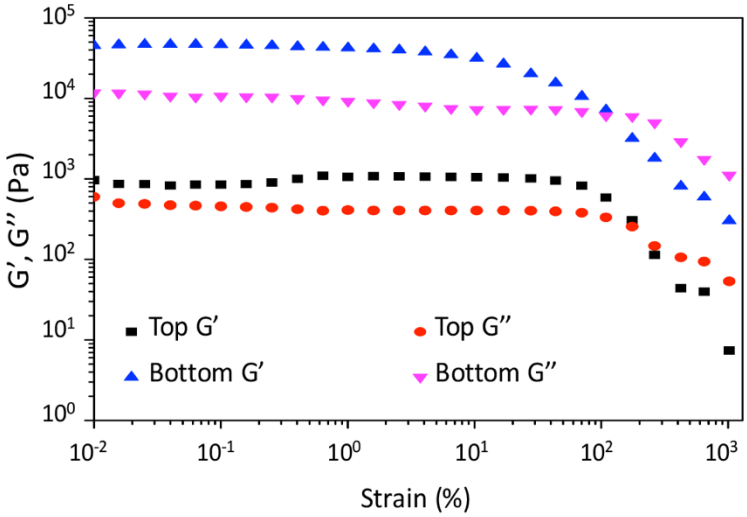

Figure 37. Strain sweeps of organohydrogel layers, performed between 10^{-2} and 10^{3} % strains.

Table 3. G' and G" of each layer at different strain levels.

Strain (%)	Top Layer	Bottom Layer
10^{-2}	G' > G"	G' > G"
10^{-1}	G' > G"	G' > G"
10^{0}	G' > G"	G' > G"
10^{1}	G' > G"	G' > G"
10^{2}	G' > G"	G' = G"
10^{3}	G" > G'	G" > G'

4.2.5. Self-Healing Ability of the Organohydrogel

C18 is constituted from long hydrophobic alkyl chains, and its self-healing ability was previously reported in hydrogels, which are constituted by micellar crosslinking. With contribution of C18 into hydrogel network, tough, stretchable and self-healing hydrogels can be obtained (33). Principally, self-healing in hydrogels is succeeded by demolishment of SDS micelles after being cut. By destroy of micellar structures, free hydrophobic constituents are presented inside the polymer network. When cut pieces of the gel are touched together, C18 molecules can re-form strong hydrophobic interactions at the interface, and self-healing is achieved.

In the organohydrogel synthesized in this chapter, the self-healing property is also expected to be observed for the top and bottom layers. Firstly, a tentative experiment of self-healing ability

was conducted. The organohydrogel was cut into two pieces, and merged together for a while. After being contacted, it was observed that two pieces come together and self-healing is succeeded. Even after stretching, the merged pieces do not lose the integrity and can be elongated. Moreover, self-healing was succeeded in terms of each layer (Figure 38a).

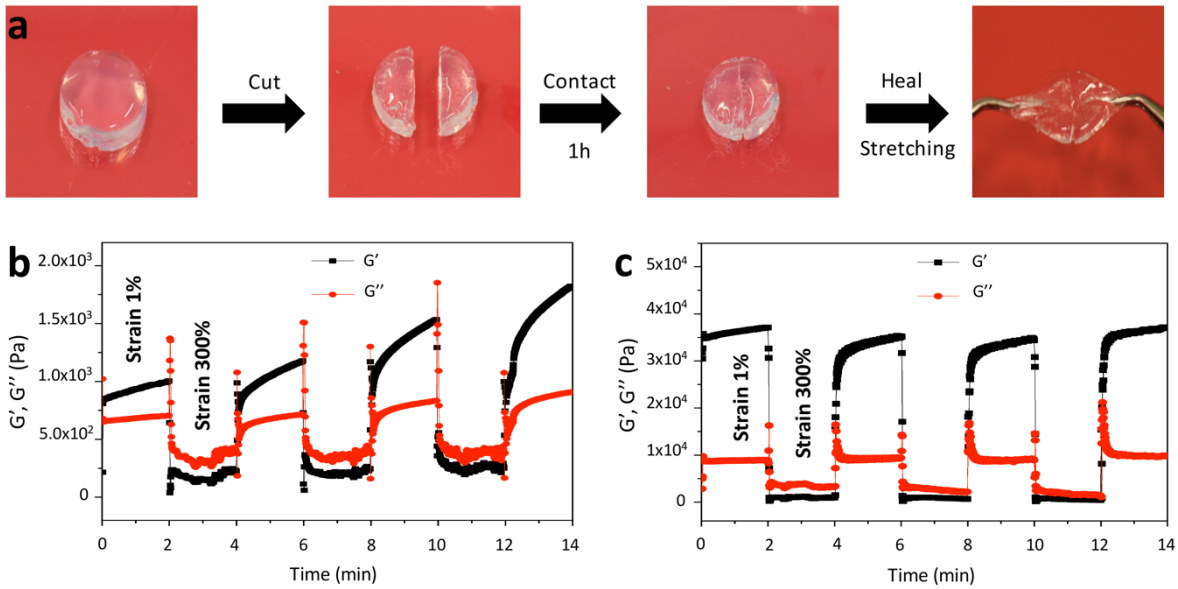

Figure 38. Investigation of self-healing feature of organohydrogel a) Demonstration of successful self-healing process. The radius of organohydrogel is 1 cm b) Rheological self-healing characterization of top layer c) Bottom layer characterization, by using 1% and 300% strain levels.

To evaluate the self-healing of each layer, cyclic time-dependent rheology test was performed, as well. The previous strain sweep test had demonstrated that after a certain strain level the crosslinked network is damaged. By considering these transitions, self-healing tests were conducted at two different strain levels, such as 1% and 300% (Figure 38b, and 38c). In terms of 1% strain, the crosslinked network should not show any destruction, since it is extremely low than the critical strain level. On the other hand, 300% strain induces loss of crosslinking, and different profile (G">G') should be obtained. The self-healing properties can be understood by continuously changing strain levels. For instance, the top and bottom layers of organohydrogel had shown an elastic state (G'>G") at 1% strain. With the trigger of crosslinking destruction at 300%, the behavior turned to G">G'. Although well-crosslinked elastic state is lost at high strain level, initial G'>G" characteristic can be received back, due to the self-healing nature. Following the high strain application, the 1% level was supplied and it was observed that G' becomes

dominant, again. The elastic state was re-gained, and this cycle was able to be repeated for several times. This unique self-healing feature was observed in the case of the top and bottom layers, as well. Interestingly, the differences in G' and G" were detected after each strain cycle. The top layer, which includes higher amount of silicone oil, had a continuous increase in G' within time. On the other hand, G' value of bottom layer was nearly constant, following self-healing repeats. This result demonstrated that the presence of higher silicone oil and loosely crosslinking of the top layer had provided to enhancement of rheological properties after self-healing process.

4.3. Discussion

In overall, organohydrogels combine two properties of hydrogels and organic gels inside their networks. Up to date, organohydrogels with isotropic macroscopic properties have been reported in literature (107, 111). In other words, the synthesized materials show same nature in case of whole network. Therefore, it is challenging to fabricate bilayer-like gel material with the previous report strategies, due to their fast gelation kinetics. The developed organohydrogel synthesis is based on using polymerization induced phase separation. Within time, the solution state undergoes three phases with changing compositions in each region. Following that, bi-layer-like organohydrogel, including loosely-crosslinked top layer (~10^2 Pa) and well-cross-linked bottom layer (~10^4 Pa), was obtained. The confocal imaging showed that loosely-cross-linked top layer had included intensified amount of silicone oil droplet, compared to bottom layer. Due to this, top layer had a fluid-like behavior, while bottom layer had a complete gel structure. In previous reports, combine of these two behaviors has not been reported, so far. The compositional changes were characterized by FT-IR, and confirmed that each layer had showed alterations of the peaks. Therefore, physical properties of top and bottom layer were differentiated during in-situ phase separation and gelation processes. For instance, surface of bottom part had showed a rougher nature, while top surface had almost a flat surface. It was attributed to loosely crosslinked nature and intense silicone oil presence in top layer. The silicone oil contributes fluidity into network, and a flatter surface can be received. As known from previous reports, hydrophobic interactions are useful to receive self-healing feature. Considering this, self-healing of synthesized organohydrogel was investigated. The top and bottom layers were characterized, separately. It was found that their self-healing capability is different than each others. The bilayer-like organohydrogel fabrication would allow to obtain layers with different

self-healing nature. Note that most of gel materials with self-healing do not possess such an anisotropic behavior. The self-healing behavior is contributed identically in whole network (33). The phase separation induced anisotropy contributes to a new property in the developed organohydrogel system. In overall, it can be concluded that this strategy helps to obtain distinctive physical (i.e. stiffness, roughness, self-healing) and chemical features in each layer of organohydrogel. It is believed that it can be modified to mimic anisotropy in natural systems, as well.

4.4. Summary

Herein, fabrication of binary phase consisting organohydrogel with anisotropic nature has been succeeded. Polymerization induced phase separation approach helped to receive three-phase systems in solution system. Subsequently, the incorporation of micellar structure with hydrophobic C18 molecules and continuous in-situ polymerization process had resulted in gelation, which was able to fix the separated phases into gel state. The layers of obtained organohydrogel show different nature, which is dissimilar to the previously reported organohydrogels in the literature. The compositional changes were confirmed by performing analytical techniques. The results demonstrated that the presence of silicone oil increases from bottom layer to top layer. Moreover, the crosslinking degree changes, induced by continuous phase separation, in organohydrogel was found. The lower value of G' and high viscoelasticity had been characterized at top layer. In addition, the fabricated organohydrogel is able to show self-healing capability, which is attributed to hydrophobic interactions. Interestingly, self-healing capacity of layers was also altered. The cyclic self-healing indicated that G' value of top layer was significantly increased within time, while bottom layer had almost similar elastic modulus. This difference was attributed loosely crosslinked network of top layer, which consists of immense silicone oil and leads to dynamicity of C18 molecules.

4.5. Materials and Methods

4.5.1. Materials

Acrylamide (⩾99%) (AA), stearyl methacrylate (C18), silicone oil (10 cST), 2-Butanol, sodium chloride (NaCl), ammonium persulfate (APS), (MBA) and sodium dodecyl sulfate (SDS) were purchased from Sigma-Aldrich and used as received.

4.5.2. Fabrication of Organohydrogel

The organohydrogel was fabricated by a typical microemulsion method, which consists of two phases of hydrophilic and oleophilic components. The hydrophilic phase was constructed by water and dissolving hydrophilic acrylamide monomers inside. On the other hand, the oleophilic phase was formed with silicone oil and long-chain hydrophobic C18 monomers. To build up organohydrogel polymer network, a certain amount of constituents, including distilled water (2 ml), silicone oil (1 ml), 2-Butanol (0.4 ml), SDS (0.32 g), NaCl (0.02g), acrylamide (0.8 g), and C18 (0.36 g) were added into glass vial to form microemulsion, respectively. In each adding step, vortex was performed to mix the supplied components. Before initiation of the polymerization, it was ensured that all components were completely dissolved. Afterward, APS initiator was supplied into the solution state to start polymerization process. Following that, an extra vortex was applied for 30 seconds to obtain homogenous solution. The obtained homogenous milky solution was left at room temperature for the phase separation and complete in-situ gelation.

4.5.3. Characterization of Organohydrogel

Chemical composition characterization of each surfaces were evaluated by performing Fourier Transform Infrared Spectroscopy (FT-IR) measurement. The measurements were conducted immediately after removing the sample from the glass vial, and conducted by using transmittance mode. FTIR spectra were obtained and recorded in the range of 400-4000 cm^{-1} using Bruker VERTEX 70C FT-IR spectrometer.

The morphologies of binary phases inside the organohydrogel were investigated via performing confocal microscopy imaging (Carl Zeiss LSM 880, New York, USA). For the imaging process, PDI-conjugated silicone oil was used to form organohydrogels. The received organohydrogel was cut to observe the cross-sectional view before the imaging. Subsequently, the cross-section

was monitored with implementation of 40X objective. The imaging process had been conducted in the region between the top and bottom layers, and obtained images were stacked together.

Mechanical properties of the top and bottom layers were characterized by using rheometer, equipped with a temperature controlled Peltier plate (TA Instruments, HR-3, USA). All measurements were performed at 25 °C, and controlled during the experiments. Prior to performing the tests, each layers of organohydrogel was cut to 1.5 mm thickness, and punched with 8 mm size. For rheological experiments, the upper plate of 8 mm was preferred. The dynamic frequency sweep was performed between 1-10 Hz, and 1% strain rate. The strain sweep tests were performed between 0.01-1000% rate, with an application of certain frequency amplitude (1 Hz).

To evaluate the self-healing ability of the layers, rheological experiments were conducted. Two different strain levels, which were 1% and 300% at a constant 1 Hz frequency, had been used for the tests. Firstly, 1% strain rate was applied for 2 min, and followed by 300% strain exposure at same time exposure. Moreover, the cycle test was duplicated for 5 times to understand repetitive nature of self-healing. All measurements were performed at 25 °C, with a sample of 1.5 mm thickness and 8 mm diameter.

Surface roughness values of the top and bottom layers were characterized by using Zygo 3D optical surface profiler device (USA). The measurement of each layer's roughness was conducted approximately 15 min after the removal of the sample from the vial. For the characterization, the images were gathered with 10X magnification and 100 μm depth of field for scan.

Chapter 5: Conclusion and Outlook

In this thesis new supramolecular crosslinking methods to construct dynamic hydrogels were developed. Non-covalent interactions were exploited to crosslink the polymer chains, which not only endows the system with dynamic nature but also provide an energy-dissipation mechanism for toughening the hydrogel. On one hand, the cluster effect of weak interactions, i.e. applying multiple weak interactions, rather than using a single strong bond, to form a crosslinking point, was used. Multiple weak interactions are strong enough in sum to stabilize the hydrated system and also allow for reversible association to dissipate energy. On other hand, I exploited physical entanglement as extremely weak supramolecular interaction to construct a crosslinked structure of hydrogels by itself. This thesis proofs that the cluster effect to sum the weak physical entanglement interactions can be used to prepare hydrogels.

The main conclusions of this thesis presented as follows:

- Progress in our understanding of entanglement-based on crosslinking interaction. PEH developed in this thesis indicates that clustering polymer physical entanglement interaction can stabilize network structure for gelation. The hydrogel also demonstrates some new properties that are not found in previous systems, including the extremely low polymer fractions (<2 wt%) for maintaining a hydrogel, crosslinking independent swelling ability, recoverability in a dehydration-rehydration cycle, which broadened the understanding of dynamic hydrogels.
- Based on PEH, this thesis also contributes to developing a novel strategy to stiffen hydrogels without compromising the swelling ability, i.e. enhancing the crosslinking strength. This stiffening strategy is fundamentally different from previous methods such as changing the crosslinking degree of polymer chains, self-assembled state of building blocks, or alternating the solubility of the polymer chains. This strategy might inspire new methods to design responsive hydrogel materials.
- Polymerization-induced phase separation (PIPS) was utilized to prepare the asymmetrical bilayer organohydrogels. Although PIPS is well-known, it was the first time to exploit it in the preparation of supramolecular organohydrogel.

Although we have established the novel system of physical entanglement hydrogels and bilayer-like organohydrogel, many issues should be addressed in further research. The main outlook presented as follows:

- Is the rotaxane-like structure is thermodynamically stable? The stable mechanical properties of the swollen hydrogel implied that it was energy-favor. However, the rotaxane-like structure limits the mobility of the linear polymer strand, suggesting an energy-unfavorable state. Further studies should be conducted to address this debate. Also, self-crosslinking reaction might occur during polymerization, which might introduce covalent crosslinking structures into the network structure. Although the results of the water-dissolving experiment suggested the absence of such a self-crosslinking phenomenon, the conclusion was not strong enough since the swelling process could induce bond scission. Therefore, the process of how polymer chains escape from the nanogel during swelling could be an interesting topic for future research.

- Although the stiffening of TPEH is possible by temperature increase, it did not show full reversibility to gain the initial stiffening value after the temperature drops back. To optimize the reversibility, further research should be conducted to understand the system in more detail, such as interactions between nanogels and polymer entanglement clusters. On the other hand, the stiffening effect is not obvious enough in many applications. Further molecular design is needed to improve the restricting effect of the sliding behavior of the crosslinking clusters.

- Current results have indicated that PIPS is a powerful method to prepare asymmetrical materials but the potential of this method has not been fully exploited yet. Future research should be performed to understand the phase separation kinetics and thus develop reliable methods to control the structure and the properties of the organohydrogels.

Bibliography

1. Hines, L., Petersen, K., Lum, G. Z., & Sitti, M. (2017). Soft actuators for small-scale robotics. *Adv. Mater.*, *29*(13), 1603483.

2. Ionov, L. (2014). Hydrogel-based actuators: possibilities and limitations. *Mater. Today*, *17*(10), 494-503.

3. Lin, S., Yuk, H., Zhang, T., Parada, G. A., Koo, H., Yu, C., & Zhao, X. (2016). Stretchable hydrogel electronics and devices. *Adv. Mater.*, *28*(22), 4497-4505.

4. Li, J., & Mooney, D. J. (2016). Designing hydrogels for controlled drug delivery. *Nat. Revi. Mater.*, *1*(12), 16071.

5. Hoare, T. R., & Kohane, D. S. (2008). Hydrogels in drug delivery: Progress and challenges. *Polymer*, *49*(8), 1993-2007.

6. Wang, H., & Heilshorn, S. C. (2015). Adaptable hydrogel networks with reversible linkages for tissue engineering. *Adv. Mater.*, *27*(25), 3717-3736.

7. Drury, J. L., & Mooney, D. J. (2003). Hydrogels for tissue engineering: scaffold design variables and applications. *Biomaterials*, *24*(24), 4337-4351.

8. Cipriano, B. H., Banik, S. J., Sharma, R., Rumore, D., Hwang, W., Briber, R. M., & Raghavan, S. R. (2014). Superabsorbent hydrogels that are robust and highly stretchable. *Macromolecules*, *47*(13), 4445-4452.

9. Wang, W., Zhang, Y., & Liu, W. (2017). Bioinspired fabrication of high strength hydrogels from non-covalent interactions. *Prog. in Polym. Sci.*, *71*, 1-25.

10. Zhao, X. (2014). Multi-scale multi-mechanism design of tough hydrogels: building dissipation into stretchy networks. *Soft matter*, *10*(5), 672-687.

11. Appel, E. A., Tibbitt, M.W., Webber M.J., Mattix, B. A., Veiseh, O., & Langer, R. (2015). Self-assembled hydrogels utilizing polymer-nanoparticle interactions. *Nat. Comm., 6(1),* 1-0.

12. Dai, X., Zhang, Y., Gao, L., Bai, T., Wang, W., Cui, Y., & Liu, W. (2015). A Mechanically Strong, Highly Stable, Thermoplastic, and self-healable supramolecular polymer hydrogel. *Adv. Mater.*, *27*(23), 3566-3571.

13. Maitra, J., & Shukla, V. K. (2014). Cross-linking in hydrogels-a review. *Am. J. Polym. Sci.*, *4*(2), 25-31.

14. Liu, S. Q., Tay, R., Khan, M., Ee, P. L. R., Hedrick, J. L., & Yang, Y. Y. (2010). Synthetic hydrogels for controlled stem cell differentiation. *Soft Matter*, *6*(1), 67-81.

15. Patenaude, M., Smeets, N. M., & Hoare, T. (2014). Designing Injectable, Covalently Cross-Linked Hydrogels for Biomedical Applications. *Macromol. Rapid Commun.*, *35*(6), 598-617.

16. Liu, S., Kang, M., Li, K., Yao, F., Oderinde, O., Fu, G., & Xu, L. (2018). Polysaccharide-templated preparation of mechanically-tough, conductive and self-healing hydrogels. *Chem. Eng. J.*, *334*, 2222-2230.

17. Nguyen, Q. V., Park, J. H., & Lee, D. S. (2015). Injectable polymeric hydrogels for the delivery of therapeutic agents: A review. *Eur. Polym. J.*, *72*, 602-619.

18. Xin, Y., & Yuan, J. (2012). Schiff's base as a stimuli-responsive linker in polymer chemistry. *Polym. Chem.*, *3*(11), 3045-3055.

19. Patenaude, M., Smeets, N. M., & Hoare, T. (2014). Designing Injectable, Covalently Cross-Linked Hydrogels for Biomedical Applications. *Macromol. Rapid Commun.*, *35*(6), 598-617.

20. Singhal, R., & Gupta, K. (2016). A review: tailor-made hydrogel structures (classifications and synthesis parameters). *Polym. Plast. Technol. and Eng.*, *55*(1), 54-70.

21. Sui, X., van Ingen, L., Hempenius, M. A., & Vancso, G. J. (2010). Preparation of a Rapidly Forming Poly (ferrocenylsilane)-Poly (ethylene glycol)-based Hydrogel by a Thiol-Michael Addition Click Reaction. *Macromol. Rapid Commun.*, *31*(23), 2059-2063.

22. Devine, D. M., & Higginbotham, C. L. (2003). The synthesis of a physically crosslinked NVP based hydrogel. *Polymer*, *44*(26), 7851-7860.

23. Parhi, R. (2017). Cross-Linked Hydrogel for Pharmaceutical Applications: A Review. *Adv. Pharm. Bull.*, *7*(4), 515-530.

24. Gong, J. P. (2010). Why are double network hydrogels so tough?. *Soft Matter*, *6*(12), 2583-2590.

25. Perrin, C. L., & Nielson, J. B. (1997). “Strong” hydrogen bonds in chemistry and biology. *Annu. Rev. Phys. Chem.*, *48*(1), 511-544.

26. Neal, J. A., Mozhdehi, D., & Guan, Z. (2015). Enhancing mechanical performance of a covalent self-healing material by sacrificial noncovalent bonds. *J. Am. Chem. Soc.*, *137*(14), 4846-4850.

27. Song, G., Zhang, L., He, C., Fang, D. C., Whitten, P. G., & Wang, H. (2013). Facile fabrication of tough hydrogels physically cross-linked by strong cooperative hydrogen bonding. *Macromolecules*, *46*(18), 7423-7435.

28. Yang, Y., & Urban, M. W. (2013). Self-healing polymeric materials. *Chem. Soc. Rev.*, *42*(17), 7446-7467.

29. Cui, J., & del Campo, A. (2012). Multivalent H-bonds for self-healing hydrogels. *Chem. Commun.*, *48*(74), 9302-9304.

30. Jiang, G., Liu, C., Liu, X., Chen, Q., Zhang, G., Yang, M., & Liu, F. (2010). Network structure and compositional effects on tensile mechanical properties of hydrophobic association hydrogels with high mechanical strength. *Polymer*, *51*(6), 1507-1515.

31. Jeon, I., Cui, J., Illeperuma, W. R., Aizenberg, J., & Vlassak, J. J. (2016). Extremely stretchable and fast self-healing hydrogels. *Adv. Mater.*, *28*(23), 4678-4683.

32. Jiang, H., Duan, L., Ren, X., & Gao, G. (2019). Hydrophobic association hydrogels with excellent mechanical and self-healing properties. *Eur. Polym. J.*, *112*, 660-669.

33. Tuncaboylu, D. C., Sari, M., Oppermann, W., & Okay, O. (2011). Tough and self-healing hydrogels formed via hydrophobic interactions. *Macromolecules*, *44*(12), 4997-5005.

34. Can, V., Kochovski, Z., Reiter, V., Severin, N., Siebenbürger, M., Kent, B., ... & Okay, O. (2016). Nanostructural evolution and self-healing mechanism of micellar hydrogels. *Macromolecules*, *49*(6), 2281-2287.

35. Hu, W., Wang, Z., Xiao, Y., Zhang, S., & Wang, J. (2019). Advances in crosslinking strategies of biomedical hydrogels. *Biomater. Sci.*, *7*(3), 843-855.

36. Lee, K. Y., & Mooney, D. J. (2012). Alginate: properties and biomedical applications. *Prog. Polym. Sci.*, *37*(1), 106-126.

37. Berger, J., Reist, M., Mayer, J. M., Felt, O., & Gurny, R. (2004). Structure and interactions in chitosan hydrogels formed by complexation or aggregation for biomedical applications. *Eur. J. Pharm. Biopharm.*, *57*(1), 35-52.

38. Sun, T. L., Kurokawa, T., Kuroda, S., Ihsan, A. B., Akasaki, T., Sato, K., ... & Gong, J. P. (2013). Physical hydrogels composed of polyampholytes demonstrate high toughness and viscoelasticity. *Nat. Mater.*, *12*(10), 932.

39. Luo, F., Sun, T. L., Nakajima, T., Kurokawa, T., Zhao, Y., Sato, K., ... & Gong, J. P. (2015). Oppositely charged polyelectrolytes form tough, self-healing, and rebuildable hydrogels. *Adv. Mater.*, *27*(17), 2722-2727.

40. Noda, Y., Hayashi, Y., & Ito, K. (2014). From topological gels to slide-ring materials. *J. Appl. Polym. Sci.*, *131*(15).

41. Mantooth, S. M., Munoz-Robles, B. G., & Webber, M. J. (2019). Dynamic hydrogels from host–guest supramolecular interactions. *Macromol. Biosci.*, *19*(1), 1800281.

42. Li, J., Li, X., Zhou, Z., Ni, X., & Leong, K. W. (2001). Formation of supramolecular hydrogels induced by inclusion complexation between pluronics and α-cyclodextrin. *Macromolecules*, *34*(21), 7236-7237.

43. Okumura, Y., & Ito, K. (2001). The polyrotaxane gel: A topological gel by figure-of-eight cross-links. *Adv. Mater.*, *13*(7), 485-487.

44. Imran, A. B., Esaki, K., Gotoh, H., Seki, T., Ito, K., Sakai, Y., & Takeoka, Y. (2014). Extremely stretchable thermosensitive hydrogels by introducing slide-ring polyrotaxane cross-linkers and ionic groups into the polymer network. *Nat. Commun.*, *5*, 5124.

45. Costa, A. M., & Mano, J. F. (2015). Extremely strong and tough hydrogels as prospective candidates for tissue repair–A review. *Eur. Polym. J.*, *72*, 344-364.

46. Furukawa, H., Horie, K., Nozaki, R., & Okada, M. (2003). Swelling-induced modulation of static and dynamic fluctuations in polyacrylamide gels observed by scanning microscopic light scattering. *Phys. Rev. E.*, *68*(3), 031406.

47. Hsu, T. P., Ma, D. S., & Cohen, C. (1983). Effects of inhomogeneities in polyacrylamide gels on thermodynamic and transport properties. *Polymer*, *24*(10), 1273-1278.

48. Xu, B., Liu, Y., Wang, L., Ge, X., Fu, M., Wang, P., & Wang, Q. (2018). High-Strength Nanocomposite Hydrogels with Swelling-Resistant and Anti-Dehydration Properties. *Polymers*, *10*(9), 1025.

49. Cui, K., Sun, T. L., Liang, X., Nakajima, K., Ye, Y. N., Chen, L., ... & Gong, J. P. (2018). Multiscale energy dissipation mechanism in tough and self-healing hydrogels. *Phys. Rev. Lett.*, *121*(18), 185501.

50. Zhao, X. (2014). Multi-scale multi-mechanism design of tough hydrogels: building dissipation into stretchy networks. *Soft matter*, *10*(5), 672-687.

51. Sun, J. Y., Zhao, X., Illeperuma, W. R., Chaudhuri, O., Oh, K. H., Mooney, D. J., ... & Suo, Z. (2012). Highly stretchable and tough hydrogels. *Nature*, *489*(7414), 133.

52. Matsuda, T., Kawakami, R., Namba, R., Nakajima, T., & Gong, J. P. (2019). Mechanoresponsive self-growing hydrogels inspired by muscle training. *Science*, *363*(6426), 504-508.

53. Bai, Z., Dan, W., Yu, G., Wang, Y., Chen, Y., Huang, Y., ... & Dan, N. (2018). Tough and tissue-adhesive polyacrylamide/collagen hydrogel with dopamine-grafted oxidized sodium alginate as crosslinker for cutaneous wound healing. *RSC Adv.*, *8*(73), 42123-42132.

54. Wang, C., Stewart, R. J., & KopeČek, J. (1999). Hybrid hydrogels assembled from synthetic polymers and coiled-coil protein domains. *Nature*, *397*(6718), 417.

55. Agrawal, A., Rahbar, N., & Calvert, P. D. (2013). Strong fiber-reinforced hydrogel. *Acta Biomater.*, *9*(2), 5313-5318.

56. Chen, Q., Chen, H., Zhu, L., & Zheng, J. (2015). Fundamentals of double network hydrogels. *J. Mater. Chem. B*, *3*(18), 3654-3676.

57. Caló, E., & Khutoryanskiy, V. V. (2015). Biomedical applications of hydrogels: A review of patents and commercial products. *Eur. Polym. J.*, *65*, 252-267.

58. Sannino, A., Demitri, C., & Madaghiele, M. (2009). Biodegradable cellulose-based hydrogels: design and applications. *Materials*, *2*(2), 353-373.

59. Shi, Q., Liu, H., Tang, D., Li, Y., Li, X., & Xu, F. (2019). Bioactuators based on stimulus-responsive hydrogels and their emerging biomedical applications. *NPG Asia Mater.*, *11*(1), 1-21.

60. Zheng, J., Xiao, P., Le, X., Lu, W., Théato, P., Ma, C., ... & Chen, T. (2018). Mimosa inspired bilayer hydrogel actuator functioning in multi-environments. *J. Mater. Chem. C*, *6*(6), 1320-1327.

61. Lehmann, M., Krause, P., Miruchna, V., & von Klitzing, R. (2019). Tailoring PNIPAM hydrogels for large temperature-triggered changes in mechanical properties. *Colloid Polym. Sci.*, *297*(4), 633-640.

62. Xia, L. W., Xie, R., Ju, X. J., Wang, W., Chen, Q., & Chu, L. Y. (2013). Nano-structured smart hydrogels with rapid response and high elasticity. *Nat. Commun.*, *4*, 2226

63. Rong, Q., Lei, W., Chen, L., Yin, Y., Zhou, J., & Liu, M. (2017). Anti-freezing, Conductive Self-healing Organohydrogels with Stable Strain-Sensitivity at Subzero Temperatures. *Angew. Chem. Int. Ed.*, *56*(45), 14159-14163.

64. Zhao, Z., Zhang, K., Liu, Y., Zhou, J., & Liu, M. (2017). Highly Stretchable, Shape Memory Organohydrogels Using Phase-Transition Microinclusions. *Adv. Mater.*, *29*(33), 1701695.

65. Porter, R. S., & Johnson, J. F. (1966). The entanglement concept in polymer systems. *Chem. Rev.*, *66*(1), 1-27.

66. Busse, W. F. (1967). Mechanical structures in polymer melts. II. Roles of entanglements in viscosity and elastic turbulence. *Journal of Polymer Science Part A-2: Polymer Physics*, *5*(6), 1261-1281.

67. Edwards, S. F. (1967). The statistical mechanics of polymerized material. *Proc. Phys. Soc.*, *92*(1), 9.

68. de Gennes, P. G. (1971). Reptation of a polymer chain in the presence of fixed obstacles. *J. Chem. Phys.*, *55*(2), 572-579.

69. Graessley, W. W. (1974). The entanglement concept in polymer rheology. In *The entanglement concept in polymer rheology* (pp. 1-179). Springer, Berlin, Heidelberg.

70. Xiang, S., Li, T., Wang, Y., Ma, P., Chen, M., & Dong, W. (2016). Long-chain branching hydrogel with ultrahigh tensibility and high strength by grafting via photo-induced polymerization. *New J. Chem.*, *40*(10), 8650-8657.

71. Devotta, I., Ambeskar, V. D., Mandhare, A. B., & Mashelkar, R. A. (1994). The life time of a dissolving polymeric particle. *Chem. Eng. Sci.*, *49*(5), 645-654.

72. Narasimhan, B., & Peppas, N. A. (1996). Disentanglement and reptation during dissolution of rubbery polymers. *J. Polym. Sci. Part B: Polym. Phys.*, *34*(5), 947-961.

73. Zhu, J., & Luo, J. (2018). Effects of entanglements and finite extensibility of polymer chains on the mechanical behavior of hydrogels. *Acta Mech.*, *229*(4), 1703-1719.

74. Yang, Q. S., Ma, L. H., & Shang, J. J. (2013). The chemo-mechanical coupling behavior of hydrogels incorporating entanglements of polymer chains. *Int. J. Solids Struct.*, *50*(14-15), 2437-2448.

75. Yasuda, K., Kitamura, N., Gong, J. P., Arakaki, K., Kwon, H. J., Onodera, S., ... & Osada, Y. (2009). A novel double-network hydrogel induces spontaneous articular cartilage regeneration in vivo in a large osteochondral defect. *Macromol. Biosci.*, *9*(4), 307-316.

76. Gong, J. P., Katsuyama, Y., Kurokawa, T., & Osada, Y. (2003). Double‐network hydrogels with extremely high mechanical strength. *Adv. Mater.*, *15*(14), 1155-1158.

77. Na, Y. H., Tanaka, Y., Kawauchi, Y., Furukawa, H., Sumiyoshi, T., Gong, J. P., & Osada, Y. (2006). Necking phenomenon of double-network gels. *Macromolecules*, *39*(14), 4641-4645.

78. Huang, M., Furukawa, H., Tanaka, Y., Nakajima, T., Osada, Y., & Gong, J. P. (2007). Importance of entanglement between first and second components in high-strength double network gels. *Macromolecules*, *40*(18), 6658-6664.

79. Chimene, D., Peak, C. W., Gentry, J. L., Carrow, J. K., Cross, L. M., Mondragon, E., ... & Gaharwar, A. K. (2018). Nanoengineered ionic–covalent entanglement (NICE) bioinks for 3D bioprinting. *ACS Appl. Mater. Interfaces*, *10*(12), 9957-9968.

80. Myung, D., Koh, W., Ko, J., Hu, Y., Carrasco, M., Noolandi, J., ... & Frank, C. W. (2007). Biomimetic strain hardening in interpenetrating polymer network hydrogels. *Polymer*, *48*(18), 5376-5387.

81. Stevens, L., Calvert, P., & Wallace, G. G. (2013). Ionic-covalent entanglement hydrogels from gellan gum, carrageenan and an epoxy-amine. *Soft Matter*, *9*(11), 3009-3012.

82. Huang, T., Xu, H. G., Jiao, K. X., Zhu, L. P., Brown, H. R., & Wang, H. L. (2007). A novel hydrogel with high mechanical strength: a macromolecular microsphere composite hydrogel. *Adv. Mater.*, *19*(12), 1622-1626.

83. Yang, J., Wang, X. P., & Xie, X. M. (2012). In situ synthesis of poly (acrylic acid) physical hydrogels from silica nanoparticles. *Soft Matter*, *8*(4), 1058-1063.

84. Carlsson, L., Rose, S., Hourdet, D., & Marcellan, A. (2010). Nano-hybrid self-crosslinked PDMA/silica hydrogels. *Soft Matter*, *6*(15), 3619-3631.

85. Jiang, F., Huang, T., He, C., Brown, H. R., & Wang, H. (2013). Interactions affecting the mechanical properties of macromolecular microsphere composite hydrogels. *J. Phys. Chem. B*, *117*(43), 13679-13687.

86. Meid, J., Dierkes, F., Cui, J., Messing, R., Crosby, A. J., Schmidt, A., & Richtering, W. (2012). Mechanical properties of temperature sensitive microgel/polyacrylamide composite hydrogels—from soft to hard fillers. *Soft Matter*, *8*(15), 4254-4263.

87. Ianchis, R., Ninciuleanu, C., Gifu, I., Alexandrescu, E., Somoghi, R., Gabor, A., ... & Icriverzi, M. (2017). Novel hydrogel-advanced modified clay nanocomposites as possible vehicles for drug delivery and controlled release. *Nanomaterials*, *7*(12), 443.

88. Kokabi, M., Sirousazar, M., & Hassan, Z. M. (2007). PVA–clay nanocomposite hydrogels for wound dressing. *Eur.Polym. J.*, *43*(3), 773-781.

89. Haraguchi, K., & Li, H. J. (2006). Mechanical properties and structure of polymer− clay nanocomposite gels with high clay content. *Macromolecules*, *39*(5), 1898-1905.

90. Annabi, N., Nichol, J. W., Zhong, X., Ji, C., Koshy, S., Khademhosseini, A., & Dehghani, F. (2010). Controlling the porosity and microarchitecture of hydrogels for tissue engineering. *Tissue Eng. Part B: Rev.*, *16*(4), 371-383.

91. Shams Es-haghi, S., Mayfield, M. B., & Weiss, R. A. (2018). Effect of Freeze/Thaw Process on Mechanical Behavior of Double-Network Hydrogels in Finite Tensile Deformation. *Macromolecules*, *51*(3), 1052-1057.

92. Koetting, M. C., Peters, J. T., Steichen, S. D., & Peppas, N. A. (2015). Stimulus-responsive hydrogels: Theory, modern advances, and applications. *Mater. Sci. Eng. R Rep.*, *93*, 1-49.

93. Wei, M., Gao, Y., Li, X., & Serpe, M. J. (2017). Stimuli-responsive polymers and their applications. *Polym. Chem.*, *8*(1), 127-143.

94. Guragain, S., Bastakoti, B. P., Malgras, V., Nakashima, K., & Yamauchi, Y. (2015). Multi-stimuli-responsive polymeric materials. *Chem. Eur. J.*, *21*(38), 13164-13174.

95. Li, L., Scheiger, J. M., & Levkin, P. A. (2019). Design and Applications of Photoresponsive Hydrogels. *Adv. Mater.*, *31*(26), 1807333.

96. Liu, F., & Urban, M. W. (2010). Recent advances and challenges in designing stimuli-responsive polymers. *Prog. Polym. Sci.*, *35*(1-2), 3-23.

97. Koetting, M. C., Peters, J. T., Steichen, S. D., & Peppas, N. A. (2015). Stimulus-responsive hydrogels: Theory, modern advances, and applications. *Mater. Sci. Eng. R Rep.*, *93*, 1-49.

98. Cheng, C. C., Fan, W. L., Wu, C. Y., & Chang, Y. H. (2019). Supramolecular Polymer Network-Mediated Structural Phase Transitions within Polymeric Micelles in Aliphatic Alcohols. *ACS Macro Lett.*, *8*, 1541-1545.

99. De las Heras Alarcón, C., Pennadam, S., & Alexander, C. (2005). Stimuli responsive polymers for biomedical applications. *Chem. Soc. Rev.*, *34*(3), 276-285.

100. Shen, T., Kan, J., Benet, E., & Vernerey, F. J. (2019). On the blistering of thermo-sensitive hydrogel: the volume phase transition and mechanical instability. *Soft matter*, *15*(29), 5842-5853.

101. Gao, X., Cao, Y., Song, X., Zhang, Z., Xiao, C., He, C., & Chen, X. (2013). pH-and thermo-responsive poly (N-isopropylacrylamide-co-acrylic acid derivative) copolymers and

hydrogels with LCST dependent on pH and alkyl side groups. *J. Mater. Chem. B*, *1*(41), 5578-5587.

102. Jain, K., Vedarajan, R., Watanabe, M., Ishikiriyama, M., & Matsumi, N. (2015). Tunable LCST behavior of poly (N-isopropylacrylamide/ionic liquid) copolymers. *Polym. Chem.*, *6*(38), 6819-6825.

103. Zheng, W. J., An, N., Yang, J. H., Zhou, J., & Chen, Y. M. (2015). Tough Al-alginate/poly (N-isopropylacrylamide) hydrogel with tunable LCST for soft robotics. *ACS Appl. Mater. Interfaces*, *7*(3), 1758-1764.

104. Mussault, C., Guo, H., Sanson, N., Hourdet, D., & Marcellan, A. (2019). Effect of responsive graft length on mechanical toughening and transparency in microphase-separated hydrogels. *Soft matter*, *15*(43), 8653-8666.

105. Muniz, E. C., & Geuskens, G. (2001). Compressive elastic modulus of polyacrylamide hydrogels and semi-IPNs with poly (N-isopropylacrylamide). *Macromolecules*, *34*(13), 4480-4484.

106. Hanay, S. B., O'Dwyer, J., Kimmins, S. D., de Oliveira, F. C., Haugh, M. G., O'Brien, F. J., ... & Heise, A. (2018). Facile Approach to Covalent Copolypeptide Hydrogels and Hybrid Organohydrogels. *ACS Macro Lett.*, *7*(8), 944-949.

107. Helgeson, M. E., Moran, S. E., An, H. Z., & Doyle, P. S. (2012). Mesoporous organohydrogels from thermogelling photocrosslinkable nanoemulsions. *Nat. Mater.*, *11*(4), 344.

108. Lou, D., Wang, C., He, Z., Sun, X., Luo, J., & Li, J. (2019). Robust organohydrogel with flexibility and conductivity across freezing and boiling temperature of water. *Chem. Comm.*

109. Gao, H., Zhao, Z., Cai, Y., Zhou, J., Hua, W., Chen, L., ... & Jiang, L. (2017). Adaptive and freeze-tolerant heteronetwork organohydrogels with enhanced mechanical stability over a wide temperature range. *Nat. Comm.*, *8*, 15911.

110. Chen, F., Zhou, D., Wang, J., Li, T., Zhou, X., Gan, T., ... & Zhou, X. (2018). Rational Fabrication of Anti-Freezing, Non-Drying Tough Organohydrogels by One-Pot Solvent Displacement. *Angew. Chem. Int. Ed.*, *57*(22), 6568-6571.

111. Zhao, Z., Zhang, K., Liu, Y., Zhou, J., & Liu, M. (2017). Highly Stretchable, Shape Memory Organohydrogels Using Phase-Transition Microinclusions. *Adv. Mater.*, *29*(33), 1701695.

112. Menon, V. B., & Wasan, D. T. (1988). A review of the factors affecting the stability of solids-stabilized emulsions. *Sep. Sci. Technol.*, *23*(12-13), 2131-2142.

113. Sajjadi, S., Jahanzad, F., Yianneskis, M., & Brooks, B. W. (2003). Phase Inversion in Abnormal O/W/O Emulsions. 2. Effect of Surfactant Hydrophilic− Lipophilic Balance. *Ind. Eng. Chem. Res.*, *42*(15), 3571-3577.

114. Hirose, A., Shimada, K., Hayashi, C., Nakanishi, H., Norisuye, T., & Tran-Cong-Miyata, Q. (2016). Polymer networks with bicontinuous gradient morphologies resulting from the

competition between phase separation and photopolymerization. *Soft matter*, *12*(6), 1820-1829.

115. Chan, P. K., & Rey, A. D. (1996). Polymerization-induced phase separation. 1. Droplet size selection mechanism. *Macromolecules*, *29*(27), 8934-8941.

116. Chan, P. K., & Rey, A. D. (1997). Polymerization-induced phase separation. 2. Morphological analysis. *Macromolecules*, *30*(7), 2135-2143.

117. Liang, R., Wang, L., Yu, H., Khan, A., Amin, B. U., & Khan, R. U. (2019). Molecular design, synthesis and biomedical applications of stimuli-responsive shape memory hydrogels. *Eur. Polym. J.l.*

118. Fu, J. (2018). Strong and tough hydrogels crosslinked by multi-functional polymer colloids. *J. Polym. Sci. Part B: Polym. Phys.*, *56*(19), 1336-1350.